ADDIS ABABA UNIVERSITY
ADDIS ABABA INSTITUTE OF TECHNOLOGY
SCHOOL OF CIVIL AND ENVIRONMENTAL ENGINEERING

A Comparative Study of Beams on Elastic Foundations Using Available Subgrade Models

By:
Beza Tesfu

2018
ADDIS ABABA, ETHIOPIA

ADDIS ABABA UNIVERSITY
ADDIS ABABA INSTITUTE OF TECHNOLOGY
SCHOOL OF CIVIL AND ENVIRONMENTAL ENGINEERING

A Comparative Study of Beams on Elastic Foundations Using Available Subgrade Models

By:

Beza Tesfu

Advisor: Asrat Worku(Dr.-Ing)

A Thesis submitted at Addis Ababa Institute of Technology in partial fulfillment of the requirements for the Degree of Master of Science in Geotechnical Engineering

2018
Addis Ababa

The undersigned have examined the thesis entitled **'A Comparative Study of Beams on Elastic Foundations Using Available Subgrade Models'** presented by **Beza Tesfu Bekele,** a candidate for the degree of Master of Science and hereby certify that it is worthy of acceptance.

_____	_____	_____
Advisor	Signature	Date
_____	_____	_____
External Examiner	Signature	Date
_____	_____	_____
Internal Examiner	Signature	Date
_____	_____	_____
Chairman	Signature	Date

UNDERTAKING

I certify that the research work titled **"A Comparative Study of Beams on Elastic Foundations Using Available Subgrade Models"** is my own work. The work has not been presented elsewhere for assessment. Where material has been used from other sources, it has been properly acknowledged /referred.

Name: Beza Tesfu

signature:_____

Advisor:Asrat Worku(Dr-Ing)

signature:_____

Acknowledgment

First of all, I would like to give my thanks to the Ethiopian Roads Authority (ERA) Scholarship Program for granting me scholarship to pursue the Master's Program in Addis Ababa Institute of Technology. Secondly, I would like to pay owed gratitude to my advisor, Dr-Ing. Asrat Worku for his endless patience. Beside my advisor, I would like to thank all friends of Geotechnical Engineering chair student for their assistance and encouragement throughout my work. Last but not least, I would like to thank my family for their great support during my study.

TABLE OF CONTENTS

List of Figures

List of Tables

LIST OF SYMBOLS AND ABBREVIATION

AAU: Addis Ababa University
B: Beam width
D: Flexural rigidity of a plate
DE: Differential equation
E: Modulus of elasticity of a beam
Es: Modulus of elasticity of a soil
FE: Finite element
G: Shear modulus of an elastic medium
G_k: Kerr's shear layer constant with units of force
$\overline{G}_k$: Kerr's shear layer constant with units of kN/m
G_p: Pasternak's shear layer constant with units of kN
$\overline{G}_p$: Pasternak's shear layer constant with units of kN/m
H: Thickness of a stratum
I: Moment of inertia of a beam
K_e: Equivalent spring stiffness with units of kN/m2
$\overline{K}_e$: Equivalent spring stiffness with units of kN/m3
K_l: Kerr's lower spring layer constant with units of kN/m2
$\overline{K}_l$: Kerr's lower spring layer constant with units of kN/m3
K_u : Kerr's upper spring layer constant with units of kN/m2
$\overline{K}_u$: Kerr's upper spring layer constant with units of kN/m3
K_s : Modulus of subgrade reaction with units of kN/m2
$\overline{K}_s$: Modulus of subgrade reaction with units of kN/m3
K_{sc}: Horvath's equivalent modulus of subgrade reaction
K_0: Lateral earth-pressure coefficient for at rest condition
M: Moment
M_0: concentrated moment
ODE : Ordinary differential equation
P: Applied concentrated vertical/horizontal load
p: Load intensity at an interface the foundation members
PDE : partial differential equation
PTSC: Pasternak-type simplified continuum
q: Applied vertical/horizontal surface pressure
SWTM : Simplified Winkler-type model
T: Applied tension force on a Filonenko-Borodich model
u: Displacement in the x-direction
V: Shear force
v: Displacement in the y-direction

w: Displacement in the z-direction

W_1 : Deflection of Kerr's upper spring layer

W_2 : Deflection of Kerr's lower spring layer

WTSC: Winkler-type simplified continuum

σ: Normal stress

τ : Shear stress

ϵ : Strain

θ: Slope

χ: Calibration factor

ABSTRACT

Soil-structure interaction (SSI) is present in every problem, wherein a structural element is in contact with soil. A concrete beam supported directly by the soil continuum is a very common construction form. The response of the beam when it carries external load is influenced by the soil, and the response of the soil is also influenced by the action of the beam under the load. Thus, developing a subgrade model for soil-structure interaction problem is essential in order to predict the response of both components of the system and arrive at an optimum design. The simplest subgrade model is the single parameter Winkler mechanical model which represents the foundation soil by a series of independent springs. Winkler model is widely used and practiced in spite of its deficiency in depicting the continuous behavior of real soils. Later, many advanced mechanical subgrade models have been proposed in order to improve on the inherent lack of shear interaction among the individual springs. Moreover, these models still have shortcomings with the nature of simplifying assumptions they make to ease the mathematical relationships and not suggesting ways of estimating the model parameters. With the objective to improve on such drawbacks, a generalized continuum-based model has been recently proposed by Worku. This generalized subgrade model satisfies the fundamental elastic laws and all the boundary conditions because it is derived by considering all stress, strain and displacement components. The main objective of this work is to make a comparative study between existing single and two parameter selected subgrade models. Microsoft Excel programs are written for the computation of deflection, moment and shear force. Finite Element based Plaxis 2D is used as a tool to determine the calibration factor for generalized models. Lastly, numerical illustration is provided using these models in comparison with the Plaxis 2D model and other simplified models for finite and infinite beam subjected to selected symmetrical loading conditions. The results of the comparison show that the generalized models especially the two-parameter model, are in very good agreement with the FE Plaxis 2D outputs.

Chapter 1

Introduction

1.1 Background

Soil-structure interaction has been one of the challenging problems in geotechnical engineering because of the complexity of soil behavior. In geotechnical and structural engineering practices, soil-structure interaction is neglected to offer analytical simplicity. As a result, the superstructure and the substructure are analyzed independently. Neglecting soil-structure interaction without considering its effects is not realistic and can lead to the unsatisfactory performance of the designs.

Regular use of beams on elastic foundation in civil or mechanical engineering works initiated the development of analytical methods for the analysis of foundations interacting with soils. The key issue in the analysis is modeling the contact between the beam and the soil bed which is a soil-structure interaction (SSI) problem. Finite-Element (FE) based software is often used by geotechnical engineers to solve such problems. But to find FE software, which model both the superstructure and the foundation soil as a unit is mostly unaffordable, especially in routine designs. In addition, most static analysis software use the simplified Winkler's foundation model to account for the SSI effect, which represents the subgrade using a mechanical assemblage of uniformly spaced elastic springs.Thus, there is a need for closing the gap between the FE modeling and the use of highly simplified analytical foundation models such as that of Winkler, by developing simple and yet sound analytical models that optimize accuracy and effort. Both continuum and mechanical modeling approaches are available for this purpose (Worku, 2013).

The mechanical approach simulates the subgrade behavior by using a few mechanical elements like springs, elements in pure bending, in pure shear or similar other arrangements. To this effect, some models introduced additional mechanical elements of one type or another to interconnect Winkler's springs (Filonenko-Borodich, 1950; Hetenyi, 1950; Pasternak, 1954; Kerr, 1964). The elastic continuum approach, in contrast, idealizes the subgrade as an elastic layer overlying a rigid base characterized by the elastic parameters of elastic modulus, Poisson's ratio and the layer thickness. Continuum models have the advantage that the elastic constants can be established from tests but suffer from a common shortcoming that they are difficult to apply directly. While in mechanical models, the higher order models were devised with the intention of improving on the drawbacks of the simplest and long-enduring Winkler single spring bed model by introducing additional elements to ensure shear interaction among the springs that is missing in Winkler's model. However, mechanical models suffer in general from a major common drawback of not suggesting ways of estimating the model parameters. Synthesis of

the two approaches has the benefit of using the strengths of both methods. Also, it provides a means of quantifying the mechanical model parameters in terms of the known parameters of the continuum model (Horvath,2002; Worku,2010).

Recently, by considering all stress, strain and displacement components, Worku (2010) proposed a generalized continuum-based subgrade model. The proposed model can have a range of applications including in the analysis of beams and plates on elastic foundations. Based on this model, this paper tries to calibrate the model parameters and to compare the results with the classical models and FE based Plaxis 2D software.

1.2 Objective of The Study

The main objective of this work is to make a comparative study between existing single and two parameter selected subgrade models. Furthermore, evaluations of shear, moment and deflection of beams are conducted through analytical solutions obtained in the excel spreadsheet program. The response of both finite and infinite beams subjected to common loadings, such as a uniformly distributed load, concentrated force and concentrated moment on soils with different rigidity are studied.

1.3 Scope of The Work

The scope of this work is limited to the comparison of the response of finite and infinite beams on an elastic foundation by using single and two parameter subgrade models. It includes only beams with constant cross-sections, which are subjected to selected symmetrical loadings and rest on homogeneous strata. The analysis of prismatic beams, unsymmetrical loadings, and non-homogeneous strata is not included in this work. Analysis of the beams on the Kerr-type subgrade model is not covered due to its relative complexity for analytical treatment, and also for the reason that Worku (2014), showed that it can be replaced by an equivalent two-parameter Pasternak-type model with no loss of accuracy.

1.4 Methodology

The research is conducted per the methodology outlined below to achieve the objectives:

Literature Review

Both existing mechanical and continuum subgrade models are reviewed. The synthesis of mechanical and continuum models, which have the same order of differential equations, is provided.

Analytical Work and Programming

The governing differential equations and solutions are presented. An excel spreadsheet program is coded for the determination of deflection, bending moment and shear force based for the closed-form solutions of the ordinary differential equation.

Comparison and Evaluation

A comparison of the results was made between the synthesized advanced/rigorous analytical models, conventional models and Plaxis 2D foundation software.

1.5 Applications of The Research Result

Despite the growth in technology, there are still many applications in routine practice where the use of subgrade models is still preferred. Subgrade models are not as such complete constitutive models as they attempt to replicate only certain aspects of soil behavior using analytical relations. The Winkler model is the most commonly used subgrade model which is a poor representation of subgrade behavior as it does not consider the important behavioral mechanism of the stresses that occur within an actual subgrade, especially of the shear continuity.
Different mechanical models were later proposed to introduce shear interaction among Winkler springs, but they do not suggest means of quantifying model parameters. In continuum models, the elastic constants can be established from tests. The synthesis that relates the two sets of parameters enables the determination of the mechanical model parameters indirectly.

1.6 Organizations of The Thesis

The thesis is organized in five chapters. The first chapter is a brief description of the background of the study, its objective, scope, and methodology. In the second chapter, a review of both mechanical and continuum models and their synthesis is made. In the third chapter, analysis of both finite and infinite beams on elastic foundations subjected to some common loading cases is conducted, and the formulation of the differential equations and their solutions using single and two parameter subgrade models are presented. In the fourth chapter, calibration of the rigorous continuum model with Plaxis 2D is undertaken. Also, a comparison of results between the calibrated model and Plaxis 2D is made. In the last chapter, conclusions are drawn and some recommendations made.

Chapter 2

Literature Review

2.1 Review of Subgrade Models

2.1.1 General

The problem of beams resting on elastic foundations is very often encountered in the analysis foundations of buildings, geotechnical, highway, and railway structures. These problems require a material model for the ground that can be expressed mathematically. Such Subgrade models represent a unique type of constitutive models in geotechnical engineering, because such models are not intended to be general or complete material models. Rather, the intent of a subgrade model is to strike a balance between theoretical accuracy and ease of use in routine geotechnical engineering practice when solving a particular soil-structure interaction application. These procedures demand the modeling of (a) the mechanical behavior of the beam (b) the mechanical behavior of the soil and (c) the form of interaction between the beam and the soil.

Assuming a linear elastic, homogeneous and isotropic behavior of the soil two major approaches of subgrade modeling have been suggested in the past. Mechanical models proposed in the past have varying degrees of mathematical complexity and different numbers of model parameters. These models range from the classical single-parameter model to the multi-parameter models. In contrast, continuum-based subgrade models proposed in the past are relatively few in number and highly simplified in most cases.

2.1.2 Mechanical Models

Mechanical subgrade models are assemblages of mechanical elements like springs, elements in pure bending or in pure shear in various arrangements to simulate the subgrade behavior. Such models are conceptually simple and easy to use. The models range from the simplest single-parameter model to the more complex ones depending on the number of parameters involves. Mechanical models may accordingly be of single-parameter, two-parameter, and three-parameter (Worku, 2010).

2.1.2.1 Single Parameter Models

2.1.2.1.1 Winkler Single Parameter Model

The model was suggested by Winkler (1867), who assumed that the base is represented by a bed of closely spaced, independent linear springs. The model is a highly simplified single

parameter subgrade model, which uses the coefficient of subgrade reaction k_s to describe the foundation behavior. Winkler assumed that the deflection,$w(x, y)$, of the soil medium at any point on the surface is directly proportional to the stress $p(x, y)$, applied at the same point, and thus independent of stresses applied at other locations, i.e.

$$p(x, y) = k_s w(x, y) \tag{2.1}$$

where $p(x, y)$ is an applied vertical surface pressure,k_s is coefficient or modulus of subgrade reaction with units of force per length cubed, $w(x, y)$ is the vertical surface deflection.
For two dimensional (2-D) problems, like beams, Equation(2.1) reduces to

$$p(x) = k_s w(x) \tag{2.2}$$

This analogy is a discrete model, which may be represented by an assemblage of equally spaced independent mechanical elements (springs). The response at one point is not dependent on the response at any other point. In other words, there is no shear coupling or interaction among the springs, whereas there is a definite load spreading by vertical shear within the actual soil mass. Furthermore, for both types of loading shown in Figure (2.1c) and (2.1b), the displacements are zero outside the loaded region. However, in reality for soils,the displacements of the foundation surface are as shown in Figure (2.1a), in which the portion beyond the edges of the foundation is also deformed due to the inherent continuity.

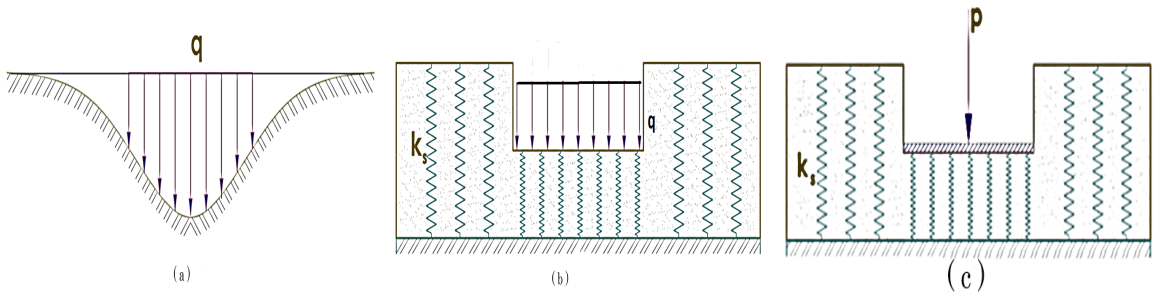

Figure 2.1: a)actual deformation b) surface displacement on a flexible foundation Winkler model due to a uniform load c)surface displacement on a rigid foundation Winkler model due to a concentrated load

In addition to the discontinuity behavior of the model, k_s is not unique, and it depends on various properties of the beam and the soil. The verity is as a result of the fact that the simple linear relationship of Equation (2.1) does not represent the more complex soil-structure interaction problem. A variety of approaches have been suggested over the years. Terzaghi (1955), presented tables of recommended values of k_s, showing that the modulus of subgrade reaction depends upon the dimensions of the area acted upon by the subgrade reaction, and size effects has been incorporated in the equations.
In an attempt to develop a more realistic method to determine k_s , Biot (1937) solved the

problem of an infinite beam with a concentrated load resting on a three-dimensional subgrade by evaluating the maximum bending moment in the beam. Biot found that a good correlation can be obtained with the Winkler model for maximum moment case by setting k_s as follows (Straughan, 1990).

$$k_s = \frac{0.95E_s}{B(1-\upsilon^2)}\left[\frac{E_s B^4}{EI(1-\upsilon^2)}\right]^{0.108} \tag{2.3}$$

where E_s and E are elasticity modulus of the soil and the beam,respectively; I is the moment of inertia of the beam, and υ is the Poisson's ratio of the soil.
Vesic (1961), confirmed that k_s depends up on both the stiffness of the soil, as well as the stiffness of the structure, so that similar size structures of different stiffness's will yield different values of k_s for the same applied load. He found the continuum solution correlated with the Winkler model where all terms were previously defined (Straughan,1990).

$$k_s = \frac{0.65E_s}{B(1-\upsilon^2)}\sqrt[12]{\frac{E_s B^4}{EI}} \tag{2.4}$$

Note that such relations have an empirical nature and are available with varying forms.

2.1.2.2 Two-Parameter Models

Two parameter models where proposed to account for the continuity of the elastic foundation by introducing a second parameter that effects interaction among the individual springs.Two-parameter models (Filonenko-Borodich, 1950; Hetenyi, 1950; Pasternak, 1954) ensure the continuity of the soil medium by adding a second element which interacts with the spring elements. These elements bring about another parameter to the subgrade model in addition to the coefficient of subgrade reaction and result a higher order relationship of the general form:

$$p(x,y) = C_1 w(x,y) + C_2 \nabla^2 w(x,y) \tag{2.5}$$

where C_1 and C_2 are model parameters.
Not that the complexity of Equation (2.5) compared to Equation (2.1) despite the addition of just one more element.

2.1.2.2.1 Filonenko-Borodich Model

The model proposed by Filonenko-Borodich (1945), achieves continuity between the individual spring elements in the Winkler model by interconnecting them by a thin elastic membrane under a horizontal constant tension T (Figure 2.2).

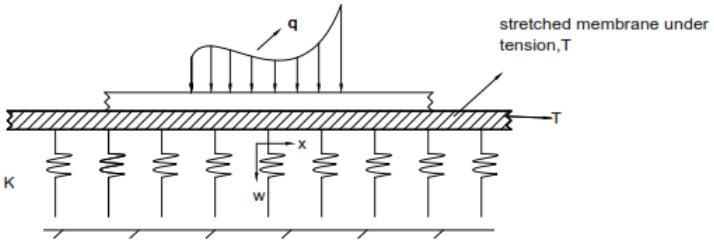

Figure 2.2: Filonenko-Borodich Model

Selvadurai (1979), derived the surface deflection due to the pressure q by considering the equilibrium of the membrane-spring system

$$p(x,y) = k_s w(x,y) - T\nabla^2 w(x,y) \tag{2.6}$$

where $\nabla^2 = \frac{\partial^2}{\partial x^2} + \frac{\partial^2}{\partial y^2}$
For two dimensional (2-D) problems, like beams, Equation(2.6) reduces to

$$p(x) = k_s w(x) - T\frac{d^2 w(x)}{dx^2} \tag{2.7}$$

The two elastic constants necessary to characterize the model are k_s and T. From the above equations, it can be seen that the shear interaction of the spring elements is effected by the tension field T in the membrane (Selvadurai, 1979).

2.1.2.2.2 Hetenyi's Model

Hetenyi (1946), proposed a model incorporating a pure flexural elastic plate in the case of three-dimensional problems or an elastic beam in the case of two-dimensional problems to introduce the interaction between the independent, linear spring elements.The response function of the three-dimensional case is given by;

$$p(x,y) = k_s w(x,y) - D\nabla^4 w(x,y) \tag{2.8}$$

where $\nabla^4 = \frac{\partial^4}{\partial x^4} + \frac{\partial^4}{\partial y^4}$

D is the flexural rigidity of the elastic plate

For two dimensional (2-D) problems, like beams, Equation(2.8) reduces to

$$p(x) = k_s w(x) - EI\frac{d^4 w(x)}{dx^4} \tag{2.9}$$

Where EI is the flexural rigidity of the beam (Selvadurai,1979). This model is not commonly used because the missing connection is shear interaction, not flexure, which is less relevant in

soils.

2.1.2.2.3 Pasternak's Model

This model was proposed by Pasternak (1954), to model the soil behavior by including the shear interaction among the spring through connecting the spring elements to a layer of incompressible vertical elements which deform in transverse pure shear (Figure 2.3).

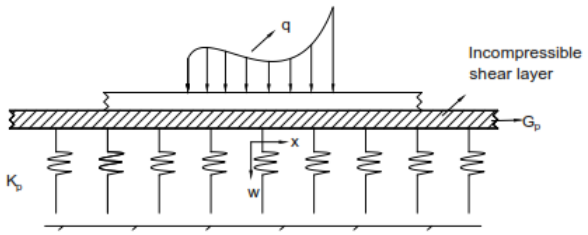

Figure 2.3: Pasternak Model

The governing partial differential equation for this model is:

$$p(x,y) = k_s w(x,y) - G_p \nabla^2 w(x,y) \tag{2.10}$$

Where G_p is the shear parameter of the layer and $w(x,y)$ is the deflection. It can be seen that Equation (2.10) becomes identical to Equation (2.8) when G_p is replaced by T. For two dimensional (2-D) problems, like beams, Equation (2.10) reduces to

$$p(x,y) = k_s w(x) - G_p \frac{d^2 w(x)}{dx^2} \tag{2.11}$$

With the two-parameter models considered so far, the Winkler case can be recovered when T, D, and G_p tend to zero (Selvadurai,1979).

2.1.2.3 Three-Parameter Models

The three-parameter models constitute a generalization of two-parameter models; the third parameter has been introduced with the intention of making them more realistic. One of the basic features of the three-parameter models is the flexibility and convenience that they offer in the determination of the level of continuity of the vertical displacements at the boundaries between the loaded and the unloaded surfaces of the soil but at the cost of mathematical complexity. Among all the three parameter model, the Kerr model is the most widely known.

2.1.2.3.1 The Kerr or Modified Pasternak Model

Because of the occurrence of concentrated reaction along free edges of a structure when the

Pasternak model is used, Kerr proposed a generalization of the Pasternak model by adding a spring layer on top of the shearing layer as shown in Figure 2.4. Kerr model consists of two layers of springs separated by a shear layer.

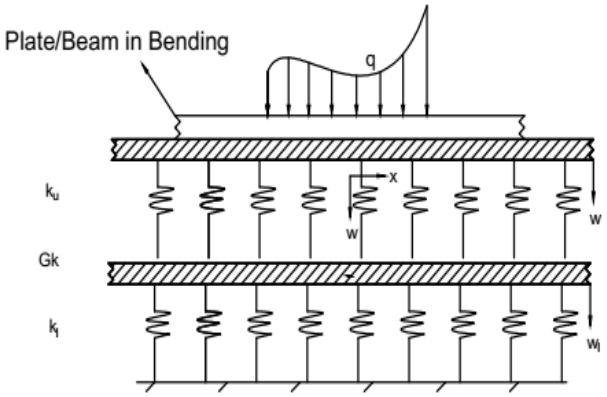

Figure 2.4: Beam Resting on Kerr Pasternak-Type Elastic Subgrade Mechanical Model

The beam equation is derived by considering the beam deflection consisting of two parts due to the contraction or extension of the upper spring layer w_u and due to the rest of foundation w_l (Worku and Degu, 2010).

$$w = w_u + w_l \tag{2.12}$$

where w is the surface deflection.
According to (Figure 2.4) and for the equilibrium of the upper spring.

$$\sum F_y = 0 = k_u dx(w - w_l) = pdx \tag{2.13}$$

$$w_l = w - \frac{p}{k_u} \tag{2.14}$$

The lower part is identical to Pasternak's model except w is replaced by w_l.Thus,

$$p(x) = k_l w_l - G_k \nabla^2 w_l \tag{2.15}$$

Inserting the Equation (2.12) into Equation (2.14) and rearranging one obtains the relation between the interface pressure and deflection of the plate as:

$$(1 + \frac{k_l}{k_u})p(x,y) - \frac{G_k}{k_u}\nabla^2 p(x,y) = k_l w(x,y) - G_k \nabla^2 w(x,y) \tag{2.16}$$

Where k_u and k_l, stiffness per unit area of the upper and lower spring beds, respectively; G_k

coefficient of the shear element in Kerr's model with the dimension of force per unit length. The corresponding 2-D equivalent of Equation (2.16) is given by

$$(1+\frac{k_l}{k_u})p(x)-\frac{G_k}{k_u}\frac{d^2p(x)}{dx^2}=k_lw(x)-G_k\frac{d^2w(x)}{dx^2} \tag{2.17}$$

2.1.2.3.2 The Modified Filonenko-Borodich Model

This model is identical to the modified Pasternak model with the mere replacement of G_k by T the three parameters involved are: k_u, k_l, and T.

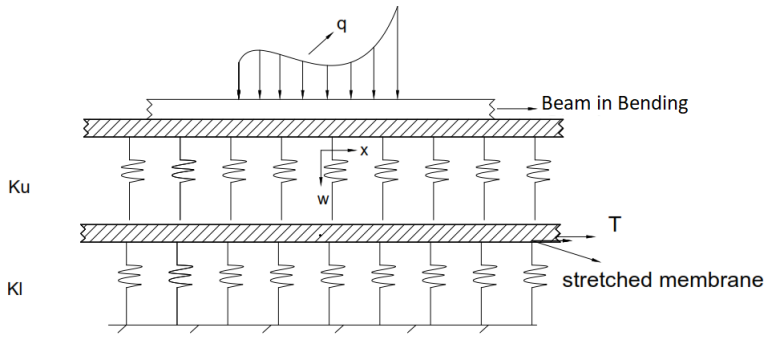

Figure 2.5: Modified Filonenko-Borodich Mechanical Subgrade Model

The relation between the interface pressure and deflection of the plate given by;

$$(1+\frac{k_l}{k_u})p(x,y)-\frac{T}{k_u}\nabla^2p(x,y)=k_lw(x,y)-T\nabla^2w(x,y) \tag{2.18}$$

The corresponding 2-D equivalent of Equation (2.18) is given by

$$(1+\frac{k_l}{k_u})p(x)-\frac{T}{k_u}\frac{d^2p(x)}{dx^2}=k_lw(x)-T\frac{d^2w(x)}{dx^2} \tag{2.19}$$

2.1.2.4 Higher-Order Models

2.1.2.4.1 Kerr and Rhines Models

Kerr and Rhines (1967) thought that any level of accuracy could be achieved by subsequent modification of these models through the addition of more spring beds and shear elements in various combinations. This is, however, more an academic exercise than is a realistic and practical approach.

2.1.3 Continuum Subgrade Models

In soil media, surface deflection is not only occurring immediately under the loaded region but also within certain limited zones beyond the loaded region. Elastic continuum models typically

idealize the subgrade as a layer overlying a rigid base with the elastic modulus, Poisson's ratio, and layer thickness as parameters. In the past, certain assumptions are made concerning selected stress, strain, and displacement components as well as compatibility conditions to produce a material with behavioral approximations built into it.
This category includes models developed by (Reissner, 1958; Vlasov and Leont'ev, 1966; Horvath, 2002; Worku, 2009). All continuum models make certain assumptions to ease the mathematical work involved; the rigor of a given model depends on how realistic are the simplifying assumptions.

2.1.3.1 Reissner's Simplified Model

Reissner (1958), proposed a subgrade model by introducing displacement and stress constraints and making certain simplifying assumptions concerning the stress developed within an isotropic, homogeneous, linear-elastic continuum of finite thickness as a result of applied surface stress (Figure 2.6).

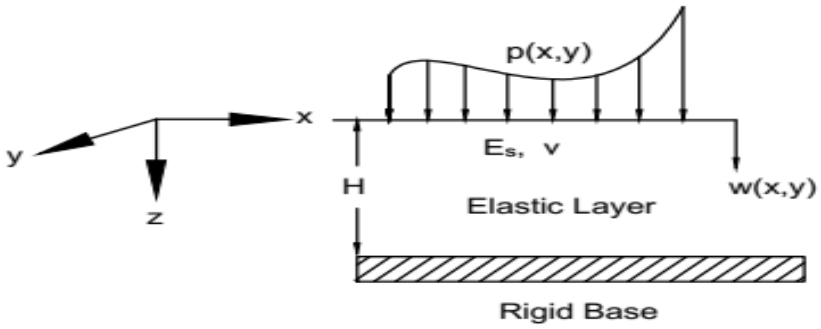

Figure 2.6: Reissner Simplified Elastic Continuum Model

Reissner specifically assumed that the in-plane stresses in the x-y plane throughout a soil layer of thickness H are negligibly small; i.e $\sigma_x = \sigma_y = \tau_{xy} = 0$.
The remaining stress components satisfy the well-known equilibrium differential equations.

$$\begin{aligned} \frac{\partial \tau_{xz}}{\partial z} &= 0 \\ \frac{\partial \tau_{yz}}{\partial z} &= 0 \\ \frac{\partial \tau_{xz}}{\partial x} + \frac{\partial \tau_{yz}}{\partial y} + \frac{\partial \tau_z}{\partial z} &= 0 \end{aligned} \tag{2.20}$$

The strain-stress and strain-displacement relations are

$$\begin{aligned} \frac{\partial w}{\partial z} &= \frac{\sigma}{E_s} \\ \frac{\partial u}{\partial z} + \frac{\partial w}{\partial x} &= \frac{\tau_{xz}}{G} \\ \frac{\partial v}{\partial z} + \frac{\partial w}{\partial y} &= \frac{\tau_{yz}}{G} \end{aligned} \tag{2.21}$$

Where u, v and w are the displacement in x,y,z direction respectively.To solve Equation (2.20) and Equation (2.21) the prevailing boundary conditions are required. At the base of the foundation, the conditions are:

$$Z = H; u = v = w = 0 \tag{2.22}$$

While at the surface of the foundation

$$Z = 0; v = u = 0, \sigma = p \tag{2.23}$$

Applying the displacement boundary conditions at the bottom and at the surface the resulting differential equation is

$$w - \frac{GH^2}{3E_s}\nabla^2 w = \frac{H}{E_s}\left(p - \frac{GH^2}{12E_s}\nabla^2 p\right) \tag{2.24}$$

Where G is the shear modulus of the elastic continuum, E_s is Young's modulus of the subgrade, p is the load intensity at the interface and H is the subgrade thickness (Reissner,1958).

2.1.3.2 Vlasov's Model

Vlasov (1966), proposed a model of soil response which is a type of two-parameter elastic model derived by introducing displacement constraints that simplify the basic equations for linear elastic isotropic continuum . In addition to neglecting the horizontal deformations u and v, this model further imposes a deformation mode shape, $\phi(z)$, which is determined by applying the principle of minimum potential energy in the foundation-soil system as shown in Figure 2.7 (Vlasov and Leont'ev, 1966).

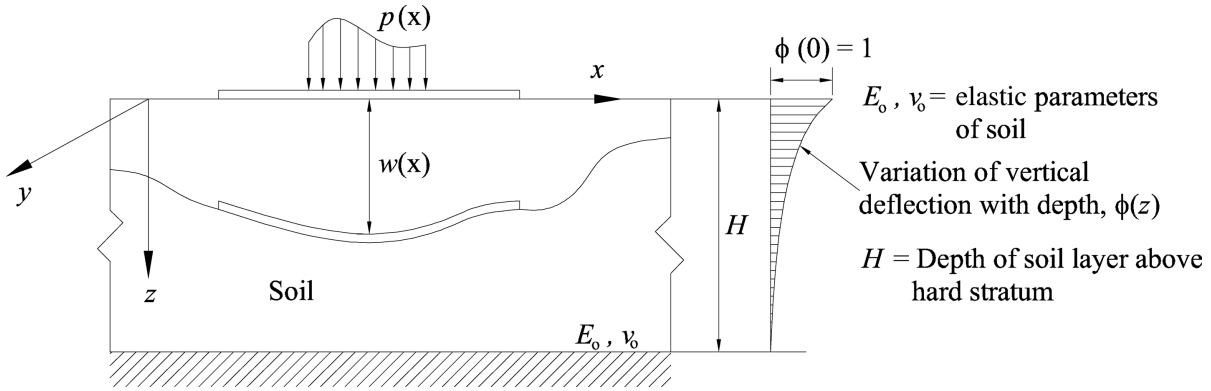

Figure 2.7: Vlasov Subgrade Model

The strain in the foundation layer is assumed to be such that the displacement components are;

$$u(x,y) = v(x,y) = 0; w(x,z) = w(x)\phi(z) \tag{2.25}$$

Where u and w are the displacements in the x and z directions,respectively, and the function $\phi(z)$ describes the variation of the displacement $w(x,y)$ in the z-direction.Several displacement variations have been proposed by Vlasov and Leontiev (1966), including a linear one.The values of $\phi(z)$ are stipulated such that $\phi(0) = 1.0$ and $\phi(H) = 0$.
The resulting differential equation is given by;

$$p(x) = k_v w(x) - G_v \frac{d^2 w(x)}{dx^2} \tag{2.26}$$

where

$$\begin{aligned} k_v &= \overline{E} \int_0^H \phi^2 dz \\ G_v &= G \int_0^H \phi^2 dz \end{aligned} \tag{2.27}$$

$$\begin{aligned} \overline{E} &= \frac{1-\upsilon}{(1+\upsilon)(1-2\upsilon)} E \\ G &= \frac{E_s}{2(1+\upsilon)} \end{aligned} \tag{2.28}$$

Where G is the shear modulus of the elastic continuum, E_s is Young's modulus of the subgrade, p is the load intensity at the interface and H is the subgrade thickness.
The vertical deformation mode shape, $\phi(z)$, as determined by applying variational principles is

given by

$$\phi(z) = \frac{sinh\gamma(1-\frac{Z}{H})}{sinh\gamma} \tag{2.29}$$

Where γ is a dimensionless parameter.
The parameter γ is given by the following expression:

$$\left(\frac{\gamma}{H}\right)^2 = \frac{G}{E}\frac{\int_{-\infty}^{+\infty}\int_{-\infty}^{+\infty}(\nabla w)^2 dxdy}{\int_{-\infty}^{+\infty}\int_{-\infty}^{+\infty} w^2 dxdy} \tag{2.30}$$

A more general expression of γ for plates on elastic foundations, which was used by Straughan (1990), is

$$\left(\frac{\gamma}{H}\right)^2 = \frac{(1-2\upsilon)}{2(1-\upsilon)}\frac{\int_{-\infty}^{\infty}\int_{-\infty}^{\infty}(\nabla w)^2 dxdy}{\int_{-\infty}^{\infty}\int_{-\infty}^{\infty} w^2 dxdy} \tag{2.31}$$

Substituting Equation (2.28) and Equation (2.29) into Equation (2.27),one obtains

$$k_v = \frac{E}{H}\frac{(1-\upsilon)}{(1+\upsilon)(1-2\upsilon)}\frac{\gamma(\sinh\gamma\cosh\gamma+\gamma)}{2\sinh^2\gamma} \tag{2.32}$$

$$G_v = \frac{GH(\sinh\gamma\cosh\gamma-\gamma)}{2\gamma\sinh^2\gamma} \tag{2.33}$$

As could be noted, Vlasov's model parameters, k_v and G_v, are dependent upon the vertical deformation mode shape and the layer thickness. The mode shape in turn depends on the surface deformation through the parameter,γ. The general trend of Vlasov's model parameters is that the vertical stiffness increases and the shear parameter decreases with increasing values of γ. The shear parameter is independent of the Poisson's ratio, whereas the vertical stiffness increases with increasing values of Poisson's ratio υ (Worku 2014).

Note that for $\gamma = 0$, the deformation mode shape, $\phi(z)$, in Equation (2.29) becomes indeterminate. It can, however, be shown using L'Hospital's rule that with the limit of γ approaching zero, the mode shape assumes a linear shape given by:

$$\phi(z) = 1 - \frac{Z}{H} \tag{2.34}$$

2.1.3.3 Horvath's Winkler-Type Model

Horvath (2002),came up with a highly simplified form of Reissner's model by using the same physical model,but,assuming that all stress and strain components except the vertical normal stress (σ_z), and strain (ϵ_z), were equal to zero.Horvath solved the following cases:
$E_s = A$(constant with depth)
$E_s = A + Bz$
$E_s = A + Bz^{0.5}$
Where: E_s -Young's modulus of the subgrade
A - Young's modulus value directly beneath the loaded area
B– the rate of change of Young's modulus with depth, z.
By making use of the equation of equilibrium, the stress-strain and strain–displacement relations he derived the following Winkler-type simplified continuum model for the respective cases mentioned above.

$$p = k_{sc}w \tag{2.35}$$

Where : k_{sc} equivalent modulus of subgrade reaction for simplified continuum

$$\begin{aligned} k_{sc} &= \frac{A}{H}(forE_s = A) \\ k_{sc} &= \frac{A}{In(A+BH) - In(A)}(forE_s = A + Bz) \\ k_{sc} &= \frac{B^2}{2\left[(A+BH^{0.5}) - AIn(A+BH^{0.5}) - A + AIn(A)\right]}(forE_s = A + Bz^{0.5}) \end{aligned} \tag{2.36}$$

Where H is the thickness of the stratum.Equation (2.35) is a highly simplified Winker-type simplified continuum model (WTSC).

2.1.3.4 Horvath's Pasternak-Type model

Horvath also came up with a two-parameter model by modifying Reissner's concept by making the assumption that the horizontal displacements are zero in addition to the in-plane stresses. Horvath obtained the following Pasternak-type simplified continuum model (PLSC) for a constant young modulus,E_s with depth.

$$p = \frac{E_s}{H}w - \frac{GH}{2}\nabla^2 w \tag{2.37}$$

Equation (2.37) has the same order as the Pasternak model in Equation (2.11). Again, it is to be noted that Equation (2.37) represents another simplified version of Reissner model given by Equation (2.24). Hence, both Equation (2.35) and Equation (2.37) may not be considered as independent models.

2.1.3.5 The Generalized Subgrade Model

According to Worku (2009), the subgrade is idealized as a homogeneous, isotropic elastic layer of thickness H overlying a firm stratum (Figure 2.8) in the same way as Reissner's idealization.

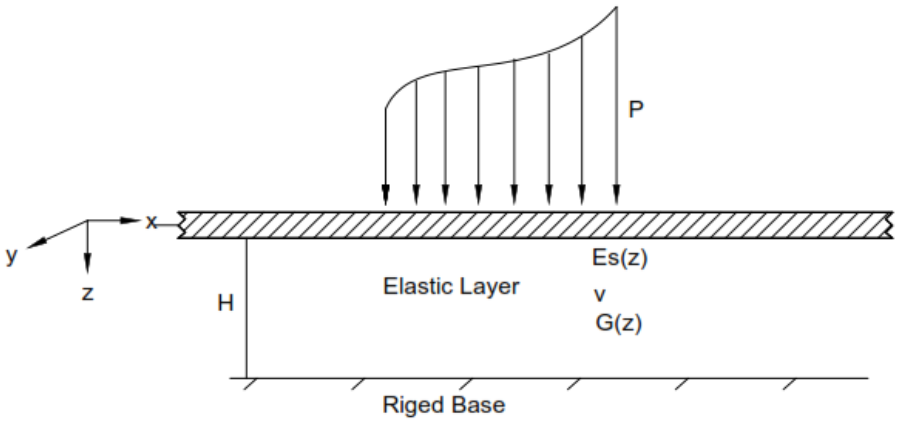

Figure 2.8: Worku Elastic Continuum Subgrade Model

Worku assumed that the elasticity modulus, Es, and the shear modulus, G, varies with depth. Since his model is less sensitive to Poisson's ratio, the Poisson's ration is considered constant. Unlike Reissner's model, he didn't neglect any of the stress, strain or displacement components. According to this model the depth wise variation of the vertical shear stress components, horizontal to vertical normal stress ratios and all components of the stress tensor in the subgrade are regarded.
Lateral normal stresses are expressed in terms of the vertical normal stress:

$$\begin{aligned} \sigma_x(x,y,z) &= g_x(z)\sigma_z(x,y,z) \\ \sigma_y(x,y,z) &= g_y(z)\sigma_z(x,y,z) \end{aligned} \tag{2.38}$$

Where g_x and g_y are functions of z.
Whereas the vertical shear stress components are expressed as

$$\begin{aligned} \tau_{zx}(x,y,z) &= I_{zx}(z)\overline{\tau}_{zx}(x,y) \\ \tau_{zy}(x,y,z) &= I_{zy}(z)\overline{\tau}_{zy}(x,y) \end{aligned} \tag{2.39}$$

In which I_{zx} and I_{zy} are functions of z only, whereas $\overline{\tau}_{zx}$ and $\overline{\tau}_{zy}$ are functions of x and y. The equilibrium equation in z-direction without body forces is given by

$$\sigma_{z,z} + \overline{\tau}_{zx,z} + \overline{\tau}_{zy,z} = 0 \tag{2.40}$$

Necessary boundary conditions and stress-strain, strain-displacement relationships,which the model uses for the formulation are;

a) Boundary conditions:

$$\begin{aligned}
&\sigma_z(x,y,0) = -p \\
&u(x,y,0) = v(x,y,0) = 0 \\
&w(x,y,0) = w_0 \\
&u(x,y,H) = v(x,y,H) = w(x,y,H) = 0
\end{aligned} \tag{2.41}$$

b)Stress-strain and strain-displacement relationships:

$$\begin{aligned}
&\frac{\partial w}{\partial z} = \frac{1}{E_s(z)}[\sigma_z - \upsilon(\sigma_x + \sigma_y)] \\
&\frac{\partial u}{\partial z} + \frac{\partial w}{\partial x} = \frac{\tau_{zx}}{G} \\
&\frac{\partial v}{\partial z} + \frac{\partial w}{\partial y} = \frac{\tau_{zy}}{G}
\end{aligned} \tag{2.42}$$

Worku after a lengthy mathematical work, came up with the following differential equation for his model

$$p(x,y) - \frac{G}{E_s K_I}\left(L_{gI} - \frac{K_{gI}L_g}{K_g}\right)\nabla^2 P(x,y) = \frac{E_s}{K_g}w_0(x,y) - \frac{GL_{gI}}{K_g K_I}\nabla^2 w_0(x,y) \tag{2.43}$$

In which the terms in the coefficients are definite integrals given by

$$
\begin{aligned}
&K_g = \int_0^H g(z)dz; \quad K_I = \int_0^H I_z(z)dz; \quad K_{gI} = \int_0^H g(z)I(\tilde{z})_z dz \\
&L_g = \int_0^H \left[\int g(z)dz - \left(\int g(z)dz\right)_{Z=H}\right] dz \\
&L_{gI} = \int_0^H \left[\int g(z)\tilde{I}_z(z)dz - \left(\int g(z)\tilde{I}_z(z)dz\right)_{Z=H}\right] dz \\
&g(z) = 1 - \upsilon\left[g_x(z) - g_y(z)\right]; \;\; \tilde{I}_z(z) = \left[\int I_z(z)dz\right]_{z=0} - \int I_z(z)dz \\
&g_x(z) = \frac{\sigma_x(z)}{\sigma_z(z)}; \;\; g_y(z) = \frac{\sigma_y(z)}{\sigma_z(z)}; \;\; I_z(z) = \frac{\tau_{xz}(x,y,z)}{\overline{\tau}_{xz}(x,y)} = \frac{\tau_{yz}(x,y,z)}{\overline{\tau}_{yz}(x,y)}
\end{aligned}
\tag{2.44}
$$

Equation (2.43) is the mathematical model for generalized case of an elastic subgrade, the elastic and shear moduli of which may vary with depth, and in which no simplifying assumption has been made with respect to stress, strains or displacements. This formulation shows that the maximum order of the governing differential equation of the non-homogeneous, isotropic elastic subgrade is two.

The equation has the same order and form to that of Kerr's mechanical model Equation (2.16). For this reason,it is referred to as Kerr-type generalized continuum model. Based on this generalized model, Worku noted that a number of model variants can be obtained by introducing different simplifying assumption on the lateral deformations, the vertical shear stress, and the depth-wise variation of the functions $g_x(z)$, $g_y(z)$ and $I(z)$. Some of these model variants are presented in the following sections.

2.1.3.5.1 Winkler-Type Continuum Model

According to Worku (2013),the generalized continuum model reduces to Winkler-type models,if the vertical shear stress alone are zero;i.e the necessary condition is.

$$\tau_{xz} = \tau_{yz} = 0 \tag{2.45}$$

Not any additional simplifying assumptions are made regarding the normal stress components or the shear stress τ_{xy}.With the assumptions made in Equation (2.45), the equilibrium equation for the vertical direction becomes

$$\sigma_{z,z} = 0 \tag{2.46}$$

Equation (2.46) implies that σ_z is constant with respect to depth.This constant is determined from the boundary condition in Equation (2.41) so that

$$\sigma_z(x,y) = -p(x,y) \tag{2.47}$$

Substituting Equation (2.38) into Equation (2.42), integrating the resulting equation and applying the boundary condition, the following Winkler-type model is obtained:

$$p(x,y) = k_s w_0(x,y) \tag{2.48}$$

Where, k_s, the coefficient of subgrade reaction is given by

$$k_s = \frac{1}{\int_0^H \frac{g(z)}{E_s(z)} dz} \tag{2.49}$$

and

$$g(z) = 1 - \upsilon[g_x(z) + g_y(z)] \tag{2.50}$$

Equation (2.48) is similar to Winkler model given by the Equation (2.1) and it is referred to as the generalized Winkler-type continuum model.This result shows that disregarding the vertical shear stress components alone suffices to arrive at a Winkler-type subgrade model without the need to omit the lateral normal stresses unlike what was done by Horvath (1983) in Equation (2.35).
Equation (2.50) can also be obtained directly from Equation (2.43) provided that L_{gI} and K_{gI} vanish which again require that I_z is zero. Thus, the type of model sought is obtained with k_w given by $\frac{1}{k_g}$.This yields

$$p(x,y) = \frac{E_s}{k_g} w_0(x,y) \tag{2.51}$$

Where K_g is a definite integral as defined in Equation (2.44).

2.1.3.5.2 Pasternak-Type Continuum Model

Worku(2010), has also shown that a Pasternak-type or(FB-type) continuum model can be obtained from the generalized approach presented in Equation (2.43) when the lateral displacements $u(x,y)$ and $v(x,y)$ alone are neglected. The model variant obtained in this manner is thus referred to as the generalized Pasternak type (generalized FB-type) continuum model.

$$u = v = 0 \tag{2.52}$$

Because of this assumption, the relationship between the horizontal and vertical normal stresses becomes

$$\sigma_x = \sigma_y = \frac{\upsilon}{1-\upsilon}\sigma_z = k_0 \sigma_z \tag{2.53}$$

Where k_0 is the lateral earth-pressure coefficient for at-rest condition.
It has to be noted that the assumption in Equation (2.52) is not identical to assuming at

rest condition, because this assumption is not limited to merely mean$\epsilon_{xx} = \epsilon_{yy} = 0$,but goes beyond this and affects all the shear strain components.The vertical shear stress components are represented by Equation (2.39).

The pertinent combined stress-strain and strain-displacement relationships are simplifies to

$$\begin{aligned} \frac{\partial w}{\partial z} &= \frac{\alpha_0}{E_s}\sigma_z \\ \frac{\partial w}{\partial x} &= \frac{\tau_{zx}}{G} \\ \frac{\partial w}{\partial y} &= \frac{\tau_{zy}}{G} \end{aligned} \tag{2.54}$$

where, $\alpha_0 = \frac{1-\upsilon-2\upsilon^2}{1-\upsilon}$

By employing these relationship into the equilibrium Equation (2.40) and later introducing the boundary conditions, Worku came up with the model.

$$p = \frac{1}{L_E}\left[\frac{1}{\alpha_0}w_0 + L_x w_{0,xx} + L_y w_{0,yy}\right] \tag{2.55}$$

Where,

$$\begin{aligned} L_x &= \int_0^H \frac{\tilde{I}_{zx}}{E_s I_{zx}} G dz; \quad L_y = \int_0^H \frac{\tilde{I}_{zy}}{E_s I_{zy}} G dz; \quad L_E = \frac{H}{E_s} \\ \tilde{I}_{zx}(z) &= \left(\int I_{zx} dz\right)_{z=0} - \int I_{zx} dz \\ \tilde{I}_{zy}(z) &= \left(\int I_{zy} dz\right)_{z=0} - \int I_{zy} dz \end{aligned} \tag{2.56}$$

If further, the assumption $I_{zx} = I_{zy} = I_z$ is made, Equation (2.56) becomes

$$p = \frac{1}{L_E}\left[\frac{1}{\alpha_0}w_0 + L\nabla^2 w_0\right] \tag{2.57}$$

In which,

$$L = L_x = L_y = \int_0^H \frac{\tilde{I}_z G}{E_s I_z} dz \tag{2.58}$$

Equation (2.57) is referred to as the generalized Pasternak-type continuum model which has a similar form and order to the mechanical model of Pasternak given by Equation (2.11).

In the case of a homogeneous subgrade, $E_s$and G are constant with depth so that Equation (2.57) simplifies to;

$$p = \frac{E_s}{H\alpha_0}w_0 - \frac{GH}{2}\nabla^2 w_0 \tag{2.59}$$

For the particular case of zero Poisson's ratio α_0 , Equation (2.59) reduces to the form

$$p = \frac{E_s}{H} w_0 - \frac{GH}{2} \nabla^2 w_0 \tag{2.60}$$

$$p = K_p w_0 - G_p \nabla^2 w_0 \tag{2.61}$$

This is identical to Equation (2.37) showing that Horvath's version of model is highly simplified.

2.1.3.5.3 Kerr-Type Continuum Model

For homogenous elastic stratum of thickness H overlaying a rigid half space a generalized mathematical relationship as obtained by Worku, (2010) given by Equation (2.43) is .

$$p - \frac{G_k}{E_s k_{kI}} \left(L_{gI} - \frac{k_{gI} L_g}{k_g} \right) \nabla^2 p = \frac{E_s}{k_g} w - \frac{G k_{gI}}{k_g k_I} \nabla^2 w \tag{2.62}$$

The approach of this model does not neglect any stress, strain or displacement in advance. The differential equation is similar in form and order to Kerr's mechanical model.Thus this equation is referred to as the generalized Kerr-type continuum model(Worku,2010). It clearly shows that this is the maximum order and form of differential equation that represents the physical model of Figure (2.8).

2.1.4 Synthesis of Mechanical and Continuum Models

The approach and origins of mechanical model and simplified continuum models are different. However, there is similarity in their governing differential equations. This similarity can be utilized to synthesize corresponding models of the two categories so that the mechanical model parameters can be quantified in terms of the continuum parameters. Thus, Synthesis of the two approaches has the benefit of using the strengths of both models (Worku, 2013).

2.1.4.1 Synthesis of Single-Parameter Mechanical and Continuum Models

2.1.4.1.1 Synthesis of Winkler's Mechanical Model with Horvath's Continuum Model

Winkler's mechanical model Equation (2.2) and Equation (2.35) of Horvath's Winkler-type model have the same linear form of $p = \overline{k}_s w$, which implies that

$$\overline{k} = k_{sc} \tag{2.63}$$

Where

$$k_{sc} = \frac{E_s}{H} \tag{2.64}$$

2.1.4.1.2 Synthesis of Winkler's Mechanical Model with Worku's Simplified Winkler- Type Continuum Model

The synthesis can similarly be made between Winkler's mechanical model Equation (2.2) and the Winkler-type generalized Equation (2.51). This results in

$$\overline{K}_s = \frac{E_s}{k_g} \tag{2.65}$$

This equation is a generalized form of expression in terms of the continuum parameter. The definite integrals involved in this expression and defined in Equation (2.44) are evaluated once the functions$g_x(z), g_y(z)$ and $I_z(z)$ are specified.

Worku (2010, 2014), stated that the variation for the ratio of the lateral-to-vertical normal stress components with depth $\frac{\sigma_x}{\sigma_z}$, and $\frac{\sigma_y}{\sigma_z}$, under circular and rectangular regions subjected to uniformly distributed loads can be represented by an exponentially decaying function. Similarly,the distribution of the vertical shear stresses can be expressed using a bilinear function. Hence based on curve fitting to plotted data, relations for g and I_z are obtained as;

$$\begin{aligned} g(z) &= 1 - \upsilon\left[g_x(z) + g_y(z)\right] = 1 - \upsilon e^{-(3.96\frac{z}{H})} \\ I_z(z) &= \begin{cases} \frac{5z}{3H}, 0 \leq \frac{z}{H} \leq 0.6 \\ 2.35 - \frac{2.25z}{H}, 0.6 \leq \frac{z}{H} \leq 1 \end{cases} \end{aligned} \tag{2.66}$$

Substituting Equation (2.66) into Equation (2.44) and evaluating the pertinent definite integrals,Equation (2.65) takes the following form:

$$\overline{K}_w = \frac{E_s}{(1 - 0.4\upsilon)H} \tag{2.67}$$

The layer thickness H in the above equation is eliminated by using the substitution $\chi_w = \frac{H}{B}$, which yields;

$$\overline{K}_w = \frac{E_s}{(1 - 0.4\upsilon)B\chi_w} \tag{2.68}$$

Where χ_w is used as a calibration factor for Winkler's model.

2.1.4.2 Synthesis of Two-Parameter Mechanical and Continuum Models

2.1.4.2.1 Synthesis of Pasternak's Mechanical Model with Vlasov's Continuum Model

Synthesis of Pasternak's mechanical model, Equation (2.11), and Vlasov's continuum model, Equation (2.26), can be made by comparing the model coefficients.

$$k_v = \frac{E}{H}\frac{(1-\upsilon)}{(1+\upsilon)(1-2\upsilon)}\frac{\gamma(\sinh\gamma\cosh\gamma+\gamma)}{2\sinh^2\gamma} \tag{2.69}$$

$$G_v = \frac{GH(\sinh\gamma\cosh\gamma-\gamma)}{2\gamma\sinh^2\gamma} \tag{2.70}$$

2.1.4.2.2 Synthesis of Pasternak's Mechanical Model with Horvath's Continuum Model

Equation (2.11) of Pasternak's mechanical model and Equation (2.37) of Horvath's Pasternak-type model have the same order of differential equation but, different in the determination of elastic constants. When we compare the two models,one obtains the following equations for the unknown coefficients.

$$k_p = \frac{E_s}{H} \quad G_p = \frac{GH}{2} \tag{2.71}$$

2.1.4.2.3 Synthesis of Pasternak's Mechanical Model with Worku's Simplified Pasternak-Type Generalized Continuum Model

The synthesis can be made between Pasternak's mechanical model, Equation (2.11), and the Pasternak-type generalized Equation (2.59) of Worku's model.This yields

$$\begin{aligned} k_p &= \frac{E_s}{H\alpha_0} \\ G_p &= \frac{GH}{2} \end{aligned} \tag{2.72}$$

For the special case of $\upsilon = 0, \alpha_0$ becomes 1 so that,

$$\begin{aligned} k_p &= \frac{E_s}{H} \\ G_p &= \frac{GH}{2} \end{aligned} \tag{2.73}$$

Worku (2014) pointed out that because of the neglected lateral deformations, the generalized Pasternak-type model is obviously less accurate than the generalized Kerr-type model. For this reason, better expressions for the Pasternak model parameters are presented in section 2.4.4

that give results comparable with his rigorous model.

2.1.4.3 Synthesis of Three-Parameter Mechanical and Continuum Models

2.1.4.3.1 Synthesis of Kerr Mechanical Model with Reissner Continuum Model

Comparison of the coefficients in Kerr mechanical model, Equation (2.17) with Equation (2.24) of Reissner's continuum model, which has the same order of differential equation, gives the following expressions

$$\begin{aligned} k_u &= \frac{4E_s}{H} \\ k_l &= \frac{4E_s}{3H} \\ k_k &= \frac{4GH}{9} \end{aligned} \tag{2.74}$$

2.1.4.3.2 Synthesis of Kerr Mechanical Model with Worku's Generalized Continuum Model

Equating the corresponding terms in Equation (2.17) and Equation (2.43) one obtains the following expressions for Kerr's model parameters (Worku, 2014);

$$\begin{aligned} k_u &= \frac{L_{gI}H}{(k_g L_{gI} - k_{gI} L_g)} \frac{E_s}{H} \\ k_l &= \frac{L_{gI}H}{(L_g k_{gI})} \frac{E_s}{H} \\ G_k &= \frac{{L_{gI}}^2}{(k_I L_g k_{gI} H)} GH \end{aligned} \tag{2.75}$$

Similarly, substituting Equation (2.66) into Equation (2.44) and evaluating the definite integrals, Equation (2.75) takes the following form.

$$\begin{aligned} k_u &= \frac{E_s}{0.46 - 0.18\upsilon} H \\ k_l &= \frac{E_s}{0.54 - 0.26\upsilon} H \\ G_k &= \left(\frac{0.33 - 0.15\upsilon}{0.14 - 0.11\upsilon} \right) GH \end{aligned} \tag{2.76}$$

In the above equations the stratum thickness H is eliminated by using the substitution of $\chi_k = \frac{H}{B}$ as above where B is the width of the beam and χ_k is the calibration factor for Kerr's model (Worku, 2013).

2.1.4.4 The new Kerr-Equivalent Pasternak model

Two-parameter Pasternak model is more convenient for practical applications than the three-parameter Kerr model.According to Worku (2014), Kerr-equivalent Pasternak parameters can be established by seeking equivalence of performance to the calibrated Kerr model parameters stated in Equation (2.76). For the two mechanical models shown in (Figure 2.9), with the corresponding relations in Equation (2.11) and Equation (2.17) to yield equivalent results, it may be required that they have to exhibit identical shear interaction (i.e. G_k must be equal to G_p) and their surface deflection under the action of the same system of loading. This impels

$$w_0 = w_u + w_l \tag{2.77}$$

Where w_0 is the surface deflection in both models, and w_u and w_l are the deflection in the upper and lower spring beds, respectively, of the Kerr model.

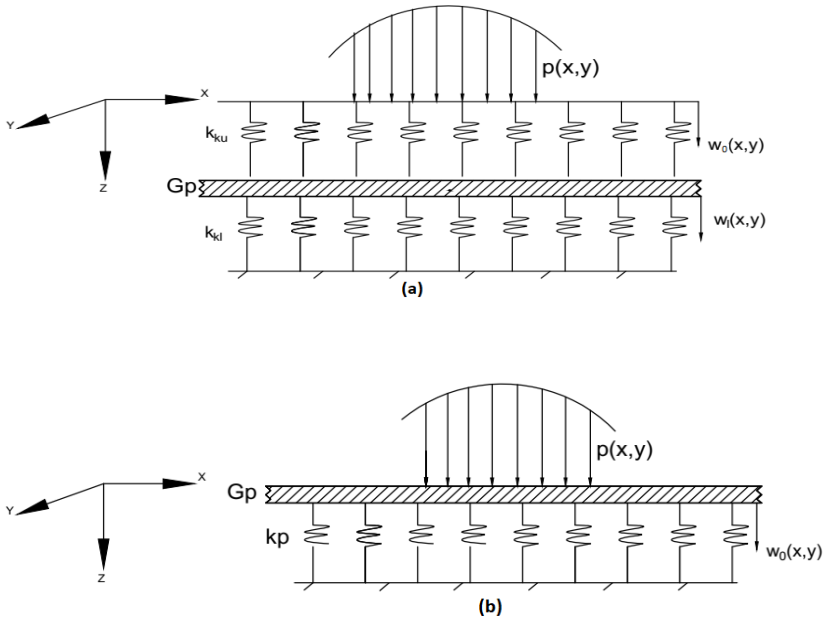

Figure 2.9: (a) Kerr model; (b) Kerr-equivalent Pasternak model

The surface pressure in Equation (2.61) can be expressed as:

$$p = p_p + p_{sl} \tag{2.78}$$

Where p_{sl} is the pressure attributed to the shear layer and p_p is the surface pressure shared by the Pasternak spring bed as shown in Figure (2.9b).

Similarly, the pressure sharing in the Kerr model of Figure (2.9a) can be written as

$$p = p_l + p_{sl} \tag{2.79}$$

Where p_{sl} is the pressure attributed to the shear layer and p_l is the pressure carried by the lower spring bed of Kerr's model.Since the upper spring layer of Kerr's model directly transfers the entire contact pressure to the shear layer and the lower spring bed, the pressure shared by this layer is identical to p. i.e.

$$p_u = p \tag{2.80}$$

Substituting Equation (2.78) and Equation (2.79) into Equation (2.77) together with the definition of a linear spring, the following expression is obtained:

$$\frac{p - p_{sl}}{k_p} = \frac{p}{k_u} + \frac{p - p_{sl}}{k_l} \tag{2.81}$$

Dividing Equation (2.81) by p and rearranging, one obtains:

$$k_p = \frac{k_u k_l}{k_u + \eta k_l} \tag{2.82}$$

Where
$\eta = \frac{1}{1-\left(\frac{p_{sl}}{p}\right)}$
To obtain the normalized equivalent Pasternak spring coefficient, the expressions of k_u and k_l in Equation (2.75) are inserted into Equation (2.82) giving;

$$\bar{k}_p = \frac{k_p}{\left(\frac{E_s}{H}\right)} = \frac{{L_{gI}}^2 H}{k_{gI} L_g L_{gI} + \eta(k_g {L_{gI}}^2 - k_{gI} L_g L_{gI})} \tag{2.83}$$

Similarly, the normalized shear parameter for the replacement Pasternak model in Equation (2.75) can be written as:

$$\bar{G}_p = \frac{G_p}{(GH)} = \frac{{L_{gI}}^2 H}{k_{gI} L_g k_I H} \tag{2.84}$$

For most actual cases the value of η may be expected to be close to unity.
For $\eta = 1$, Equation (2.83) simplifies to:

$$\bar{k}_p = \frac{k_p}{\left(\frac{E_s}{H}\right)} = \frac{H}{k_g} \tag{2.85}$$

Thus, the replacement Pasternak model is fully established with the two Pasternak parameters,

$\bar{k}_p$ and $\bar{G}_p$,found as in Equation (2.83) and Equation (2.84).
The plot of the normalized spring stiffness of the Kerr-equivalent Pasternak model against Poisson's ratio shows for that the stiffness is sensitive to Poisson's ratio (Worku, 2014). With the introduction of the evaluated definite integrals defined in Equation (2.44) and additional observations from the plots of the respective normalized forms, linear relationships are fitted. This, together with the introduction of the calibration factor, leads to the Kerr-equivalent Pasternak model parameters:

$$k_p = \frac{(0.4\upsilon + 0.67)E_s}{\chi_p B}$$
$$G_p = (1.36\upsilon + 2.28)GB\chi_p \tag{2.86}$$

Equation (2.86) together with the values of the rigorous Kerr model calibration factor,χ_k, complete the development of the calibrated Kerr-equivalent Pasternak model that yields the same results as the calibrated rigorous Kerr model (Worku, 2014). Instead of using calibration factors of generalized Kerr model in Equation (2.86) determined earlier (Worku and Degu, 2010), this thesis attempts to independently calibrate the Kerr- equivalent Pasternak-type model for beams under basic loading cases.

2.2 Analysis of Beams on Elastic Foundation

2.2.1 Formulation of the Differential Equation of the Beams

Beams are structural elements with a large length-to- width ratio and is subjected to loads that cause bending deflection in addition to stretching (Figure 2.10a).The transverse load q is assumed to be uniform at any section parallel to the x-axis, i.e., $q = q(x)$. In such a case, the vertical deflection w_0 of the beam is a functions of x only.

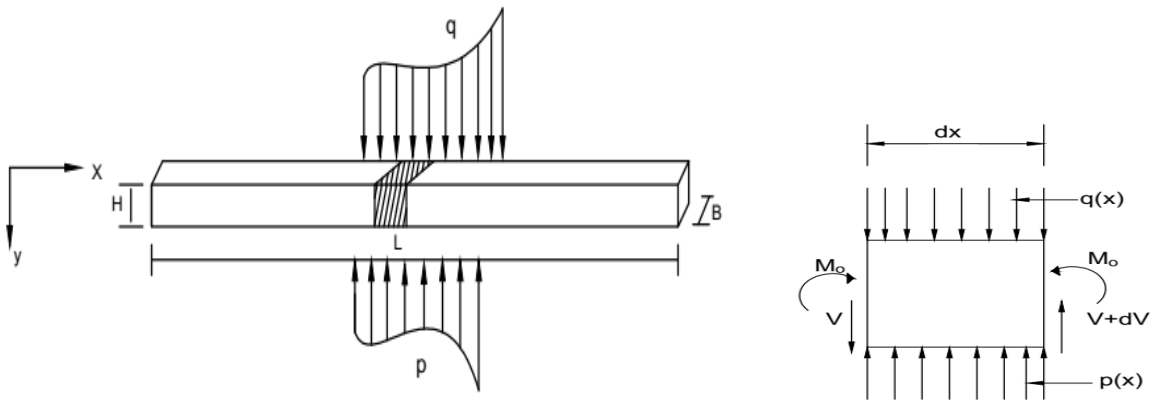

Figure 2.10: a) Beam Element b) section of Beam Element

Consider the equilibrium of the beam element shown in (Figure 2.10b) of length dx subjected

to the force systems shown.

$$\begin{aligned} &\sum F_y = 0 \\ &-V + (V + dV) + pdx - qdx = 0 \end{aligned} \tag{2.87}$$

$$-\frac{dV}{dx} = p(x) - q(x) \tag{2.88}$$

Where p is the contact pressure and q is the applied vertical surface pressure.
Using the relation, $V = \frac{dM}{dx}$,one can write

$$\frac{dV}{dx} = \frac{d^2M}{dx^2} = p - q \tag{2.89}$$

Using now the classical beam theory, $-M = EI\left(\frac{d^2w}{dx^2}\right)$, and differentiating twice one obtains the following relations for a beam of uniform rigidity EI

$$\frac{d^2M}{dx^2} = -EI\frac{d^4w(x)}{dx^4} \tag{2.90}$$

Combining Equation (2.90) with Equation (2.89) gives

$$EI\frac{d^4w}{dx^4} = q(x) - p(x) \tag{2.91}$$

In the following sections, the differential equations (DE) of beams on elastic subgrade are formulated for some typical subgrade models discussed in the previous chapter including single-parameter and two-parameter models.

2.2.2 Beams on Single-Parameter Subgrade Model

Hetenyi (1946), Selvadurai (1979), and Edward (2013), solved the problem of the beam on elastic foundation subjected to different loading conditions resting on Winkler's foundation. As discussed in the previous chapter, Winkler idealized the subgrade by a bed of equally spaced independent springs (Figure 2.11).

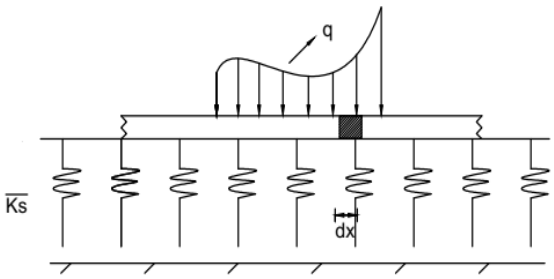

Figure 2.11: Winkler's mechanical model

Introducing Winkler's model, $p(x) = k_s w(x)$, into Equation (2.91), one obtains

$$EI\frac{d^4w(x)}{dx^4} + k_s w(x) = q(x) \tag{2.92}$$

B is the width of the beam and EI is its flexural rigidity.The homogeneous counterpart is given by

$$EI\frac{d^4w(x)}{dx^4} + k_s w(x) = 0 \tag{2.93}$$

Hetenyi (1946) solved Equation (2.93) and arrived at the following general solution for the beam.

$$w(x) = e^{\lambda x}(C_1 \cos \lambda x + C_2 \sin \lambda x) + e^{-\lambda x}(C_3 \cos \lambda x + C_4 \sin \lambda x) \tag{2.94}$$

Where
$\lambda = \sqrt[4]{\frac{K_s}{4EI}}$ is the soil-beam relative rigidity factor and C_i are integration constants.

2.2.2.1 Solution for Infinite Beams

By considering a beam of infinite length,Hetenyi (1946), solved the problem of beams subjected to different loading conditions resting on an elastic foundation. Since the deflection has to vanish at large distances,for axis symmetric problem considering the right portion of the beam (x≥0), C_1 and C_2 in Equation(2.94) should be zero. Such that, for an infinite beam

$$w(x) = e^{-\lambda x}(C_3 \cos \lambda x + C_4 \sin \lambda x) \tag{2.95}$$

2.2.2.1.1 An Infinite Beam Subjected to a Vertical Concentrated Force

Hetenyi (1946), and Selvadurai (1979), solved this problem by introducing the pertinent

boundary conditions (Figure 2.12). The origin of the coordinate system is located just under applied force,

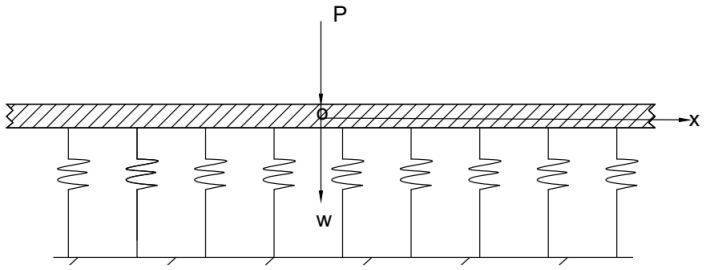

Figure 2.12: An infinite beam Subjected to a Concentrated Force

$$(a) w'(0) = 0$$
$$(b) EIw'''(0) = \frac{P}{2} \tag{2.96}$$

Then the following expressions are obtained for the various responses:

$$w(x) = \frac{P\lambda}{2K_s} A(\lambda x) \tag{2.97}$$

$$\theta(x) = -\frac{P\lambda^2}{K_s} B(\lambda x) \tag{2.98}$$

$$M(x) = \frac{P}{4\lambda} C(\lambda x) \tag{2.99}$$

$$V(x) = -\frac{P}{2} D(\lambda x) \tag{2.100}$$

Where, $w(x)$ is the deflection,$V(x)$ is the shear force,$M(x)$ is the moment, $\theta(x)$ is the slope, P is the applied force and $A(\lambda x)$ to $D(\lambda x)$ are dimensionless functions of the dimensionless

quantity λx given by;

$$\begin{aligned} A(\lambda x) &= e^{-\lambda x}(\cos \lambda x + \sin \lambda x) \\ B(\lambda x) &= e^{-\lambda x}(\sin \lambda x) \\ C(\lambda x) &= e^{-\lambda x}(\cos \lambda x - \sin \lambda x) \\ D(\lambda x) &= e^{-\lambda x}(\cos \lambda x) \end{aligned} \tag{2.101}$$

Equations (2.97) to (2.100) give the values of $w(x)$,$V(x)$,$M(x)$ and $\theta(x)$ for the right-hand side ($x \geq 0$) of the beam. On the left-hand side of the beam, ($x < 0$), $w(x)$ and $M(x)$ remain unchanged, whereas $\theta(x)$ and $V(x)$ change their signs.

2.2.2.1.2 An Infinite Beam Subjected to a Concentrated Moment

Hetenyi (1946),and Selvadurai (1979), solved the problem of an infinite beam subjected to a concentrated moment in a similar manner using a combination of two concentrated forces acting at a small distance t apart to yield a concentrated couple (Figure 2.13).

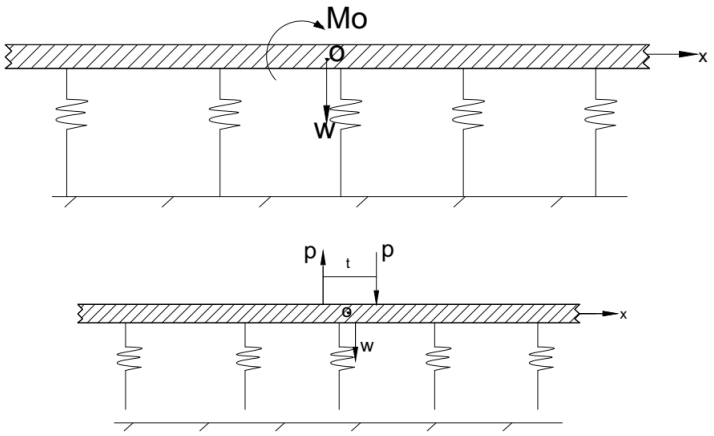

Figure 2.13: An Infinite Beam Subjected to a Concentrated Moment

They obtained the following expression:

$$w(x) = \frac{M_0 \lambda^2}{K_s} B(\lambda x) \tag{2.102}$$

$$\theta(x) = \frac{M_0 \lambda^3}{K_s} C(\lambda x) \tag{2.103}$$

$$M(x) = \frac{M_0}{2} D(\lambda x) \tag{2.104}$$

$$V(x) = -\frac{\lambda M_0}{2} A(\lambda x) \tag{2.105}$$

where, M_0 is the applied concentrated moment, $w(x)$ is the deflection, $V(x)$ is the shear force,$M(x)$ is the moment, $\theta(x)$ is the slope and $A(\lambda x)$ to $D(\lambda x)$ are the same functions of λx given by Equation(2.101). Equations (2.102) to (2.105) give the values of $w(x)$,$V(x)$,$M(x)$ and $\theta(x)$ for the right-hand side ($x \geq 0$) of the beam. For the left-hand side of the beam, ($x < 0$) $\theta(x)$ and $V(x)$, remain unchanged, whereas $w(x)$ and $M(x)$ change their signs.

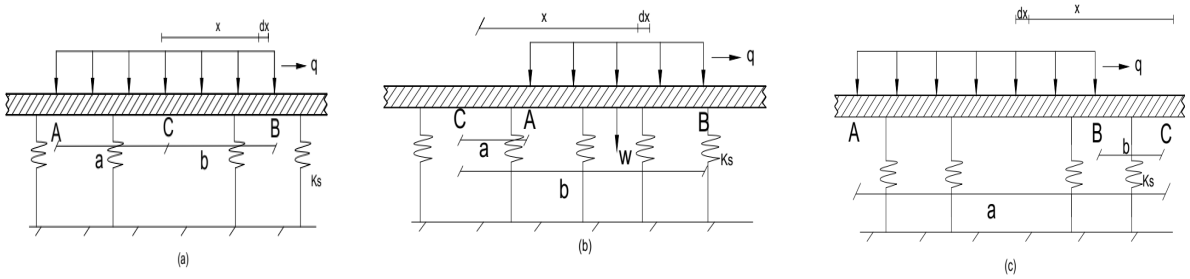

Figure 2.14: Infinite Beam on Winkler's model subjected to uniformly distributed load (a) point C is under the loaded region; (b) point C is to the left side of the loaded region; (c) point C is to the right of the loaded region

2.2.2.1.3 An Infinite Beam Subjected to a uniformly distributed load

Three cases,as shown (Figure 2.14), are considered depending on the location of the point at which deflections and internal actions are sought. The solution for each case are obtained by (Hetenyi 1946; Selvadurai 1979), and are given below:

(a) Case I: point C is below the loaded region

$$w(x) = \frac{q}{2K_s} [2 - D(\lambda a) - D(\lambda b)] \tag{2.106}$$

$$\theta(x) = \frac{q\lambda}{2K_s} [A(\lambda a) - A(\lambda b)] \tag{2.107}$$

$$M(x) = \frac{q}{4\lambda^2} [B(\lambda a) + B(\lambda b)] \tag{2.108}$$

$$V(x) = \frac{q}{4\lambda} [C(\lambda a) - C(\lambda b)] \tag{2.109}$$

(b) Case II:point C is to the left of the loaded region

$$w(x) = \frac{q}{2K_s}\left[D(\lambda a) - D(\lambda b)\right] \tag{2.110}$$

$$\theta(x) = \frac{q\lambda}{2K_s}\left[A(\lambda a) - A(\lambda b)\right] \tag{2.111}$$

$$M(x) = -\frac{q}{4\lambda^2}\left[B(\lambda a) - B(\lambda b)\right] \tag{2.112}$$

$$V(x) = \frac{q}{4\lambda}\left[C(\lambda a) - C(\lambda b)\right] \tag{2.113}$$

(c) Case III: point C is to the right of the loaded region

$$w(x) = -\frac{q}{2K_s}\left[D(\lambda a) - D(\lambda b)\right] \tag{2.114}$$

$$\theta(x) = \frac{q\lambda}{2K_s}\left[A(\lambda a) - A(\lambda b)\right] \tag{2.115}$$

$$M(x) = \frac{q}{4\lambda^2}\left[B(\lambda a) - B(\lambda b)\right] \tag{2.116}$$

$$V(x) = \frac{q}{4\lambda}\left[C(\lambda a) - C(\lambda b)\right] \tag{2.117}$$

2.2.2.2 Solution for Finite Beams

A finite beam may be considered as a portion of an infinite beam under the same loading. Hetenyi(1946) proposed the method of superposition for beams of finite length which are subjected to different external loading. Consider a beam of finite length subjected to a given loading P and q, as shown (Figure 2.15a).

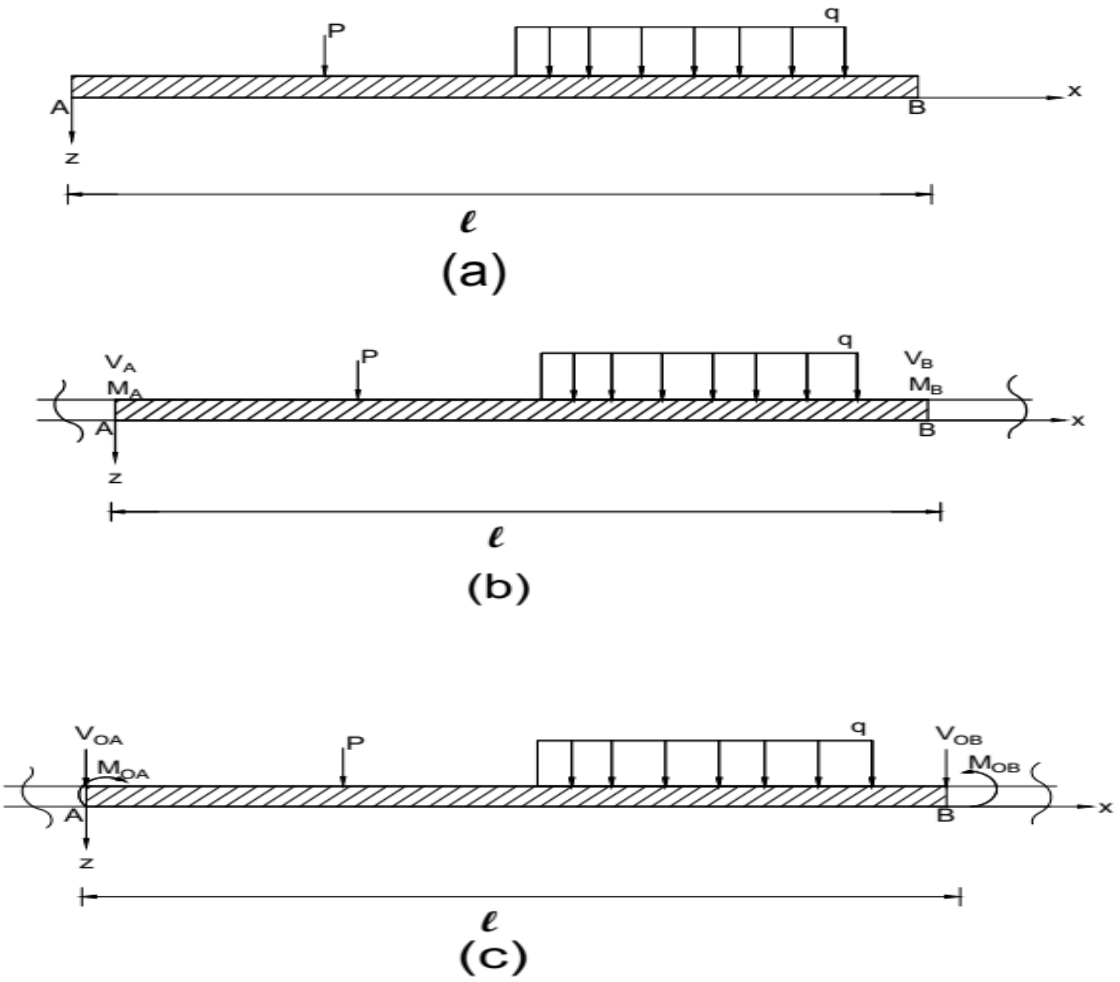

Figure 2.15: Finite beam on Winkler subgrade model

In Figure (2.15b) the bending moments (M_A, M_B), and shearing forces (V_A, V_A), are those in the infinite beam at the locations A and B, the ends of the finite beam, due to the given loads. But in Figure (2.15a) $M = 0$ and $V = 0$ in the finite beam. This condition is satisfied by applying the end conditioning shear forces $(V_{0A}$,$V_{0B})$, and moments $(M_{0A}$, $M_{0B})$ at those points (Figure 2.15c).

Shear forces V_{0A} and V_{0B}, give rise to the moments $V_{OA}\left(\frac{C}{4\lambda}\right)$ and $V_{OB}\left(\frac{C(\lambda l)}{4\lambda}\right)$, respectively,at A.

Similarly, the moments M_{0A} and M_{0B} give moments $M_{OA}\left(\frac{D}{2}\right)$ and $M_{OB}\left(\frac{D(\lambda l)}{2}\right)$, respectively,at A.

Therefore, to satisfy the zero-moment condition at A in the finite beam, the sum of these four should balance with M_A; i.e.

$$V_{OA}\left(\frac{C(\lambda)}{4\lambda}\right) + V_{OB}\left(\frac{C}{4\lambda}\right) + M_{OA}\left(\frac{D}{2}\right) + M_{OB}\left(\frac{D(\lambda l)}{2}\right) = -M_A \tag{2.118}$$

Conditions similar to Equation (2.118) derived for the remaining three boundary conditions.

As a result, we obtain simulations equations for the unknowns V_{0A} ,V_{0B}, M_{0A} and M_{0B}.

$$\begin{aligned}
&V_{OA}\frac{C}{4\lambda}+V_{OB}\frac{C(\lambda l)}{4\lambda}+M_{OA}\frac{D}{2}+M_{OB}\frac{D(\lambda l)}{2}+M_A=0\\
&V_{OA}\frac{C(\lambda l)}{4\lambda}+V_{OB}\frac{C}{4\lambda}+M_{OA}\frac{D(\lambda l)}{2}+M_{OB}\frac{D}{2}+M_B=0\\
&-V_{OA}\frac{D}{2}+V_{OB}\frac{D(\lambda l)}{2}-M_{OA}\frac{\lambda(A)}{2}+M_{OB}\frac{\lambda A(\lambda l)}{2}+V_A=0\\
&-V_{OA}\frac{D(\lambda l)}{2}+V_{OB}\frac{D}{2}-M_{OA}\frac{\lambda(A\lambda l)}{2}+M_{OB}\frac{\lambda A}{2}+V_B=0
\end{aligned} \tag{2.119}$$

Equation(2.119) can be represented in the matrix form:

$$\begin{bmatrix}
\frac{C}{4\lambda} & \frac{C(\lambda l)}{4\lambda} & \frac{D}{2} & \frac{D(\lambda l)}{2}\\
\frac{C(\lambda l)}{4\lambda} & \frac{C}{4\lambda} & \frac{D(\lambda l)}{2} & \frac{D}{2}\\
\frac{D}{2} & \frac{D(\lambda l)}{2} & \frac{\lambda A}{2} & \frac{\lambda A(\lambda l)}{2}\\
\frac{D(\lambda l)}{2} & \frac{D}{2} & \frac{\lambda(A\lambda l)}{2} & \frac{\lambda A}{2}
\end{bmatrix}
\begin{bmatrix} V_{OA}\\ V_{OB}\\ M_{OA}\\ M_{OB}\end{bmatrix}+
\begin{bmatrix} M_A\\ M_B\\ V_A\\ V_B\end{bmatrix}=0 \tag{2.120}$$

For conciseness Equation (2.120) can be written as

$$[C_w][R]=[F] \tag{2.121}$$

Where; $[C_w]$ is the coefficient matrix
$[R]$ unknown end conditioning force matrix
$[F]$ external force matrix
From the coefficient matrix $A(\lambda 0)$, $C(\lambda 0)$ and $D(\lambda 0)$ are unity. Using inverting matrix relationship in Equation (2.121) we have

$$[R]=[C_w]^{-1}[F] \tag{2.122}$$

Where $[C_w]^{-1}$ is the inverse of the coefficient matrix.
Hetenyi (1946), for a finite beam of freely supported ends, derived the following expressions for the end conditioning forces;

$$\begin{aligned}
V_{OA}&=P_0'+P"_0\\
V_{OB}&=P_0'-P"_0\\
M_{OA}&=M_0'+M"_0\\
M_{OB}&=M_0'-M"_0
\end{aligned} \tag{2.123}$$

Where;

$$\begin{aligned} P_0' &= 4E_1[S'A(1+D(\lambda l)) + \lambda M_A'(1-A(\lambda l))] \\ P_0'' &= 4E_2[S''A(1-D(\lambda l)) + \lambda M_A''(1+A(\lambda l))] \\ M_0' &= -\frac{2E_1}{\lambda}[S_A'(1+C(\lambda l)) + 2\,'_A(1-D(\lambda l))] \\ M_0'' &= -\frac{2E_2}{\lambda}[S_A''(1-C(\lambda l)) + 2\lambda M_A''(1-D(\lambda l))] \end{aligned} \tag{2.124}$$

$$\begin{aligned} S_A' &= \frac{1}{2}(V_A - V_B) \\ S_A'' &= \frac{1}{2}(V_A + V_B) \end{aligned} \tag{2.125}$$

$$\begin{aligned} M_A' &= \frac{1}{2}(M_A + M_B) \\ M_A'' &= \frac{1}{2}(M_A - M_B) \end{aligned} \tag{2.126}$$

$$\begin{aligned} E_1 &= [2(1+D(\lambda l))(1-D(\lambda l)) - (1-A(\lambda l))(1+C(\lambda l)]^{-1} \\ E_2 &= [2(1+D(\lambda l))(1-D(\lambda l)) - (1+A(\lambda l))(1-C(\lambda l)]^{-1} \end{aligned} \tag{2.127}$$

2.2.3 Beams on Two-Parameter Subgrade Models

As mentioned earlier, several researchers, recognizing the inherent problems with the Winkler model, attempted to make the model more realistic by introducing some form of interaction among the spring elements that represent the soil continuum. Pasternak introduced shear interaction among adjacent spring elements to improve the Winkler model and proposed the second parameter,G_p, which represents the stiffness of the vertical shear interaction (Figure 2.16).

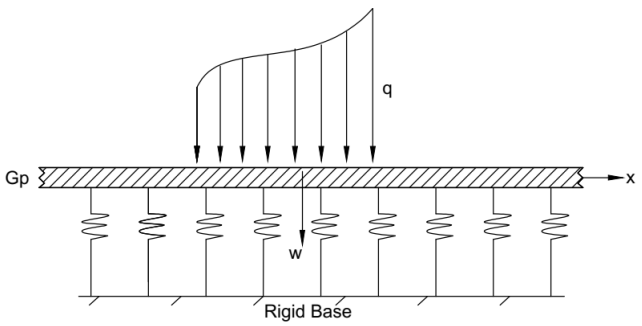

Figure 2.16: Pasternak's mechanical model

The mathematical model given for two parameter model in Equation (2.11) and is re-written as

$$p(x) = k_s w(x) - G_p \frac{d^2 w}{dx^2} \tag{2.128}$$

Combining Equation (2.128) with the beam equation of Equation (2.91) and rearranging, one obtains

$$EI\frac{d^4 w}{dx^4} + k_s w(x) - G_p \frac{d^2 w}{dx^2} = q(x) \tag{2.129}$$

The homogeneous counterpart is

$$EI\frac{d^4 w}{dx^4} + k_s w(x) - G_p \frac{d^2 w}{dx^2} = 0 \tag{2.130}$$

Where; $G_p = B\overline{G}_p$ and $k_s = B\overline{k}_s$

Equation (2.130) is an ODE with constant coefficients that has the known solution of the form $w = Ce^{mx}$. Substituting this into the equation and after some rearrangements,the following algebraic form is obtained;

$$m^4 - \frac{G_p}{EI}m^2 + \frac{k_s}{EI} = 0 \tag{2.131}$$

Equation(2.131) is a characteristic polynomial which may generally have four separate roots given by

$$m_{1,2,3,4} = \pm\sqrt[4]{\frac{G_p}{2EI} \pm i\sqrt{\frac{k_s}{EI} - \left(\frac{G_p}{2EI}\right)^2}} \tag{2.132}$$

The solution takes the form;

$$w(x) = C_1 e^{m_1 x} + C_2 e^{m_2 x} + C_3 e^{m_3 x} + C_4 e^{m_4 x} \tag{2.133}$$

Three cases are possible depending upon the internal square root value

Case (a) $D = \frac{G_p}{2\sqrt{K_s EI}} = 1$ mean when the shear interaction is equal to double the square root of the product of the beam rigidity and the soil stiffness. Then, the internal square root will be zero.

Case(b) $D = \frac{G_p}{2\sqrt{K_s EI}} > 1$ mean when the shear interaction is greater than to double the square root of the product of the beam rigidity and the soil stiffness. Then, the internal square root will be negative.

Case(c) $D = \frac{G_p}{2\sqrt{K_s EI}} < 1$ this case is the most common case in practice, as the shear interac-

tion can rarely be larger than double the square root of the product of the beam rigidity and the soil stiffness. In this case, the internal square root Equation (2.132) will be positive, and the four roots form two pairs of conjugate complex numbers expressed as;

$$m_{1,2,3,4} = \pm\sqrt{\alpha \pm i\beta} \tag{2.134}$$

where;

$$\beta = \sqrt{\lambda^2 - \frac{G_p}{4EI}} \tag{2.135}$$

$$\alpha = \sqrt{\lambda^2 + \frac{G_p}{4EI}} \tag{2.136}$$

Then by substituting the roots into Equation (2.133) and expanding the exponential functions, one obtains

$$w(x) = (C_1 e^{\alpha x} + C_2 e^{-\alpha x}) \cos \beta x + (C_3 e^{\alpha x} + C_4 e^{-\alpha x}) \sin \beta x \tag{2.137}$$

Only the solution case(c) is provided in here, whereas the expression for other two cases is provided in Annex A.

2.2.3.1 Solution for an Infinite Beams

For axis symmetric problem considering the right portion of the beam (x≥0) at large distance C_1 and C_3 in Equation (2.137) dwindle to zero. Such that, for an infinite beam as in case of Winkler's model

$$w(x) = e^{-\alpha x}(C_2 \cos \beta x + C_4 \cos \beta x) \tag{2.138}$$

2.2.3.1.1 An Infinite Beam Subjected to a Vertical Concentrated Force

The problem of an infinite length of the beam subjected to a vertical concentrated load resting on Pasternak foundation is solved by using the following boundary condition (Selvadurai,1979).

$$\begin{aligned} &(a) w'(0) = 0 \\ &(b) EIw'''(0) = \frac{p}{2} \end{aligned} \tag{2.139}$$

The first derivative of Equation (2.138) becomes

$$w'(x) = \alpha e^{-\alpha x}(-C_2 \cos \beta x - C_4 \sin \beta x) + \beta e^{-\alpha x}(-C_2 \sin \beta x + C_4 \cos \beta x) \tag{2.140}$$

Applying the boundary condition (a) to Equation (2.140), one obtains

$$-C_2\alpha + C_4\beta = 0 \tag{2.141}$$

$$C_4 = \frac{\alpha}{\beta}C_2 = \frac{\alpha}{\beta}C \tag{2.142}$$

Then Equation (2.140) becomes

$$w(x) = Ce^{-\alpha x}(\cos \beta x + \frac{\alpha}{\beta} \sin \beta x) \tag{2.143}$$

Applying the boundary condition (b) to Equation (2.143), one obtains

$$C = \frac{P\lambda^2}{2k_s\alpha} \tag{2.144}$$

Then Equation (2.143) becomes

$$w(x) = \frac{P\lambda^2}{2k_s\alpha\beta}e^{-\alpha x}(\beta \cos \beta x + \alpha \sin \beta x) = \frac{P\lambda^2}{2k_s}\tilde{A}(\alpha, \beta) \tag{2.145}$$

Successive differentiations of Equation (2.145) yield the expressions for slope, moment and shear force:

$$\theta(x) = -\frac{P}{4EI\alpha\beta}e^{-\alpha x}(\sin \beta x) = -\frac{P}{4EI}\tilde{B}(\alpha, \beta) \tag{2.146}$$

$$M(x) = \frac{P}{4\alpha\beta}e^{-\alpha x}(\beta \cos \beta x - \alpha \sin \beta x) = \frac{P}{4}\tilde{C}(\alpha, \beta) \tag{2.147}$$

$$V(x) = -\frac{P}{4\alpha\beta}e^{-\alpha x}(\cos \beta x + (\alpha^2 - \beta^2)2 \sin \beta x) = -\frac{P}{4}\tilde{D}(\alpha, \beta) \tag{2.148}$$

Where;

$$\begin{aligned}
\tilde{A}(\alpha,\beta) &= \frac{1}{\alpha\beta}e^{-\alpha x}(\beta\cos\beta x + \alpha\sin\beta x)\\
\tilde{B}(\alpha,\beta) &= \frac{1}{\alpha\beta}e^{-\alpha x}\alpha\sin\beta x\\
\tilde{C}(\alpha,\beta) &= \frac{1}{\alpha\beta}e^{-\alpha x}(\beta\cos\beta x - \alpha\sin\beta x)\\
\tilde{D}(\alpha,\beta) &= \frac{1}{\alpha\beta}e^{-\alpha x}(2\alpha\beta\cos\beta x + (\alpha^2-\beta^2)\sin\beta x)
\end{aligned} \tag{2.149}$$

Equations (2.145) to (2.148) give the values of $w(x)$,$V(x)$,$M(x)$ and $\theta(x)$ for the right-hand side ($x \geq 0$) of the beam. On the left-hand side of the beam, ($x < 0$) $w(x)$ and $M(x)$, remain unchanged, whereas $\theta(x)$ and $V(x)$ change their signs.

2.2.3.1.2 An Infinite Beam Subjected to a Concentrated Moment

Selvadurai (1979) solved the case of an infinite beam subjected to a concentrated clockwise moment at the point O of the beam resting on Pasternak foundation. For the common case of $D < 1$, he obtained the following expressions;

$$w(x) = \frac{M_0}{4EI\alpha\beta}e^{-\alpha x}\sin\beta x = \frac{M_0}{4EI}\tilde{b}(\alpha,\beta) \tag{2.150}$$

$$\theta(x) = \frac{M_0}{4EI\alpha\beta}e^{-\alpha x}(\beta\cos\beta x - \alpha\sin\beta x) = \frac{M_0}{4EI}\tilde{c}(\alpha,\beta) \tag{2.151}$$

$$M(x) = \frac{M_0}{4\alpha\beta}e^{-\alpha x}\left(2\alpha\beta\cos\beta x - (\alpha^2-\beta^2)\sin\beta x\right) = \frac{M_0}{4}\tilde{D}^*(\alpha,\beta) \tag{2.152}$$

$$V(x) = -\frac{M_0\lambda^2}{2\alpha\beta}e^{-\alpha x}(\beta\cos\beta x + \alpha\sin\beta x) = -\frac{M_0}{4EI}\tilde{A}(\alpha,\beta) \tag{2.153}$$

Where,$\tilde{D}^*(\alpha,\beta) = \frac{1}{\alpha\beta}e^{-\alpha x}\,(2\alpha\beta\cos\beta x - (\alpha^2-\beta^2)\sin\beta x)$and $\tilde{A}(\alpha,\beta)$ to $\tilde{C}(\alpha,\beta)$ are the same to given by Equation(2.149).

Equations (2.150) to (2.153) give the values of $w(x)$,$V(x)$,$M(x)$ and $\theta(x)$ for the right-hand side ($x \geq 0$) of the beam. On the left hand-side of the beam, ($x < 0$) $\theta(x)$ and $V(x)$, remain unchanged, whereas $w(x)$ and $M(x)$ change their signs.

2.2.3.1.3 An Infinite Beam Subjected to uniformly distributed load

Selvadurai (1979) also solved the problem of an infinite beam subjected to a uniformly dis-

tributed load q on Pasternak foundation in a similar manner to that of the distributed load in Winkler foundation and obtained the following expressions;

(a) Case I: when point C is below the loaded region

$$w(x) = \frac{q}{2k_s}\left[4 - \tilde{D}(\alpha,\beta,a) - \tilde{D}(\alpha,\beta,b)\right] \tag{2.154}$$

$$\theta(x) = \frac{q\lambda^2}{2k_s}\left[\tilde{A}(\alpha,\beta,a) - \tilde{A}(\alpha,\beta,b)\right] \tag{2.155}$$

$$M(x) = \frac{q}{4}\left[\tilde{B}(\alpha,\beta,a) + \tilde{B}(\alpha,\beta,b)\right] \tag{2.156}$$

$$V(x) = \frac{q}{4}\left[\tilde{C}(\alpha,\beta,a) - \tilde{C}(\alpha,\beta,b)\right] \tag{2.157}$$

(b) Case II: when point C is to the left of the loaded region

$$w(x) = \frac{q}{2k_s}\left[\tilde{D}(\alpha,\beta,a) - \tilde{D}(\alpha,\beta,b)\right] \tag{2.158}$$

$$\theta(x) = \frac{q\lambda}{2k_s}\left[\tilde{A}(\alpha,\beta,a) - \tilde{A}(\alpha,\beta,b)\right] \tag{2.159}$$

$$M(x) = -\frac{q}{4}\left[\tilde{B}(\alpha,\beta,a) - \tilde{B}(\alpha,\beta,b)\right] \tag{2.160}$$

$$V(x) = \frac{q}{4}\left[\tilde{C}(\alpha,\beta,a) - \tilde{C}(\alpha,\beta,b)\right] \tag{2.161}$$

(c) Case III: when point C is to the right of the loaded region

$$w(x) = -\frac{q}{2k_s}\left[\tilde{D}(\alpha,\beta,a) - \tilde{D}(\alpha,\beta,b)\right] \tag{2.162}$$

$$\theta(x) = \frac{q\lambda}{2k_s}\left[\tilde{A}(\alpha,\beta,a) - \tilde{A}(\alpha,\beta,b)\right] \tag{2.163}$$

$$M(x) = \frac{q}{4}\left[\tilde{B}(\alpha,\beta,a) - \tilde{B}(\alpha,\beta,b)\right] \tag{2.164}$$

$$V(x) = \frac{q}{4}\left[\tilde{C}(\alpha,\beta,a) - \tilde{C}(\alpha,\beta,b)\right] \tag{2.165}$$

2.2.3.2 Finite Beams on a Pasternak Subgrade

Owing to the continuous character of the two-parameter soil model it is necessary to define a generalized shearing force which takes into account the effects of shearing stresses in the soil medium and beam Selvadurai (1979).

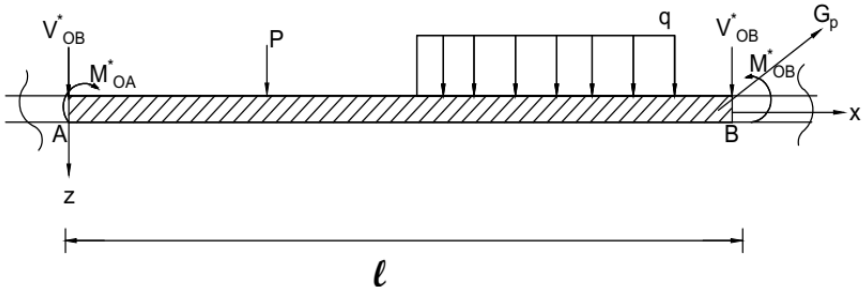

Figure 2.17: Finite beam on Pasternak subgrade model

The prevailing boundary conditions considered at $x = 0$ or $x = l$ are

$$\begin{aligned} &(a)\tilde{V}(x) - BG_p\frac{dw_e}{dx} = 0 \\ &(b)M(x) = 0 \end{aligned} \tag{2.166}$$

Where w_e is the surface displacement in the appropriate region exterior to the beam, B is width of the beam. $\tilde{V}(x)$ is the generalized shear force defined by

$$\tilde{V}(x) = V(x) + G_p\frac{dw}{dx} \tag{2.167}$$

Where; $\tilde{V}(x)$ generalized shearing force

$V(x) = -E_bI\frac{d^3w}{dx^3}$ the classical shear force of the beam

$G_p\frac{dw}{dx}$ shear stresses in the soil medium

For the regions $x < 0$ and $x > l$, the surface displacement of the two-parameter medium are of

the form

$$\begin{aligned} w_e(x) &= w_0 e^{\xi x} \quad for x < 0 \\ w_e(x) &= w_l e^{-\xi(x-l)} \quad for x > 0 \end{aligned} \tag{2.168}$$

Where $\xi^2 = \frac{k_s}{G_p}$ and w_0, w_l deflections of the beam at its edges. Hence using, Equation (2.168),the boundary condition corresponding to Equation (2.166) reduced to the form

$$\begin{aligned} \tilde{V}(0) &= -\xi B G_p w_0 \\ \tilde{V}(l) &= -\xi B G_p w_l \end{aligned} \tag{2.169}$$

Make the moments and shear forces vanish at point A and B on the infinite beam, by applying the end conditioning moments, (M^*_{OA}, M^*_{OB}) and shearing forces (V^*_{OA},V^*_{OB}) at those points (Figure 2.17).
The deflection of the beam at point A and B due to end conditioning moments and shear forces becomes

$$\begin{aligned} w_0 &= \frac{V^*_{OA}\lambda^2}{2k_s}A(\alpha,\beta,0) + \frac{V^*_{OB}\lambda^2}{2k_s}A(\alpha,\beta,l) + \frac{M^*_{OA}}{4EI}B(\alpha,\beta,0) + \frac{M^*_{OA}}{4EI}B(\alpha,\beta,l) + w^*_A \\ w_l &= \frac{V^*_{OA}\lambda^2}{2k_s}A(\alpha,\beta,l) + \frac{V^*_{OB}\lambda^2}{2k_s}A(\alpha,\beta,0) + \frac{M^*_{OA}}{4EI}B(\alpha,\beta,l) + \frac{M^*_{OA}}{4EI}B(\alpha,\beta,0) + w^*_B \end{aligned} \tag{2.170}$$

Where w^*_A and w^*_B are the deflection in the infinite beam, at the location A and B due to external loads
The shear forces V^*_{0A} and V^*_{0B} give rise to the moments $V^*_{OA}\left(\frac{\tilde{C}(\alpha,\beta,0)}{4}\right)$ and $V^*_{OB}\left(\frac{\tilde{C}(\alpha,\beta,l)}{4}\right)$, respectively,at A.

Similarly, the moments M^*_{0A} and M^*_{0B} give moments $M^*_{OA}\left(\frac{\tilde{D^*}(\alpha,\beta,0)}{4}\right)$and $M^*_{OB}\left(\frac{\tilde{D^*}(\alpha,\beta,l)}{4}\right)$, respectively,at A.

Therefore, To satisfy the zero-moment condition at A in the finite beam, the sum of these four should balance with M^*_A ; i.e.

$$V^*_{OA}\left(\frac{\tilde{C}(\alpha,\beta,0)}{4}\right) + V^*_{OB}\left(\frac{\tilde{C}(\alpha,\beta,l)}{4}\right) + M^*_{OA}\left(\frac{\tilde{D}(\alpha,\beta,0)}{4}\right) + M*_{OB}\left(\frac{\tilde{D}(\alpha,\beta,l)}{4}\right) = -M^*_A \tag{2.171}$$

Conditions similar to Equation (2.171) derived for the remaining three boundary conditions.

As a result, we obtain simulations equations for the unknowns N^*_{0A} ,N^*_{0B}, M^*_{0A} and M^*_{0B}.

$$\begin{aligned}
&-V^*_{OA}\frac{\tilde{D}(\alpha,\beta,0)}{4}+V^*_{OB}\frac{\tilde{C}(\alpha,\beta,l)}{4}-M^*_{OA}\frac{\lambda^2\tilde{A}(\alpha,\beta,0)}{2}+M^*_{OB}\frac{\lambda^2\tilde{A}(\alpha,\beta,l)}{2}=-\tilde{V}_A+\xi BG_pw^*_A\\
&-V^*_{OA}\frac{\tilde{D}(\alpha,\beta,l)}{4}+V^*_{OB}\frac{\tilde{D}(\alpha,\beta,0)}{4}-M^*_{OA}\frac{\lambda^2\tilde{A}(\alpha,\beta,l)}{2}+M^*_{OB}\frac{\lambda^2\tilde{A}(\alpha,\beta,0)}{2}=-\tilde{V}_B-\xi BG_pw^*_B\\
&V^*_{OA}\frac{\tilde{C}(\alpha,\beta,0)}{4}+V^*_{OB}\frac{\tilde{C}(\alpha,\beta,l)}{4}+M^*_{OA}\frac{\tilde{D}^*(\alpha,\beta,0)}{4}+M^*_{OB}\frac{\tilde{D}^*(\alpha,\beta,l)}{4}=-M^*_A\\
&V^*_{OA}\frac{\tilde{C}(\alpha,\beta,l)}{4}+V^*_{OB}\frac{\tilde{C}(\alpha,\beta,0)}{4}+M^*_{OA}\frac{\tilde{D}^*(\alpha,\beta,l)}{4}+M^*_{OB}\frac{\tilde{D}^*(\alpha,\beta,0)}{4}=-M^*_B
\end{aligned} \tag{2.172}$$

Equation (2.119) can be represented in a matrix form

$$\begin{bmatrix}
\frac{\tilde{C}(\alpha,\beta,0)}{2} & \frac{\tilde{C}(\alpha,\beta,l)}{2} & \frac{\bar{D}(\alpha,\beta,0)}{4} & \frac{\tilde{D}^*(\alpha,\beta,l)}{4}\\
\frac{C(\alpha,\beta,l)}{2} & \frac{C(\alpha,\beta,0)}{2} & \frac{\tilde{D}^*(\alpha,\beta,l)}{4} & \frac{\bar{D}(\alpha,\beta,0)}{4}\\
-\frac{\tilde{D}(\alpha,\beta,0)}{4} & \frac{\tilde{D}(\alpha,\beta,l)}{4} & -\frac{\lambda^2\tilde{A}(\lambda(\alpha,\beta,0)}{2} & \frac{\lambda^2\tilde{A}(\lambda(\alpha,\beta,l)}{2}\\
-\frac{\tilde{D}(\alpha,\beta,0)}{4} & \frac{\tilde{D}(\alpha,\beta,l)}{4} & -\frac{\lambda^2\tilde{A}(\lambda(\alpha,\beta,0)}{2} & \frac{\lambda^2\tilde{A}(\lambda(\alpha,\beta,l)}{2}
\end{bmatrix}
\begin{bmatrix} V^*_{OA}\\ V^*_{OB}\\ M^*_{OA}\\ M^*_{OB}\end{bmatrix}=
\begin{bmatrix} -M^*_A\\ -M^*_B\\ -\tilde{V}_A+\xi B^*G_pw^*_A\\ -\tilde{V}_B-\xi B^*G_pw^*_B\end{bmatrix} \tag{2.173}$$

For conciseness Equation (2.173) can be written as

$$[C^*_w][R^*]=[F^*] \tag{2.174}$$

Where; $[C^*_w]$ is the coefficient matrix
$[R^*]$ unknown end conditioning force matrix
$[F^*]$ external force matrix
Using inverting matrix relationship in Equation (2.174) we have

$$[R^*]=[C^*_w]^{-1}[F^*] \tag{2.175}$$

Where $[C_w]^{-1}$ is the inverse of the coefficient matrix.

2.2.3.3 Beams on a Three-Parameter Subgrade Model

As described earlier, the Kerr model consists of two linear elastic spring layers of constants k_u and k_l interconnected by a unit thickness shear layer of constant G_k and unit thickness. The governing deferential equation describing the deflection behavior of beams on elastic Kerr foundation is found by combining the Kerr's mathematical model (Figure 2.18) with the PDE of the beam.

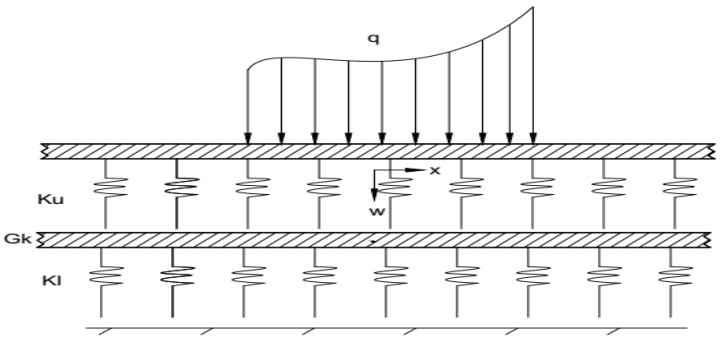

Figure 2.18: Kerr's Mechanical Model

Kerr's mathematical model is given by

$$(1+\frac{k_l}{k_u})p(x)-\frac{G_k}{k_u}\frac{d^2p(x)}{dx^2}=k_lw(x)-G_k\frac{d^2w(x)}{dx^2} \tag{2.176}$$

Combining Equation (2.176) with the beam equation of Equation (2.91) and rearranging ,one obtains

$$\frac{G_k}{k_u}EI\frac{d^6w}{dx^6}-EI\left[1+\frac{k_l}{k_u}\right]\frac{d^4w}{dx^4}+G_k\frac{d^2w}{dx^2}-k_lw=\frac{G_k}{k_u}\frac{d^2q}{dx^2}-\left[1+\frac{k_l}{k_u}\right]q \tag{2.177}$$

The homogeneous counterpart of the governing differential equation is

$$\frac{G_k}{k_u}EI\frac{d^6w}{dx^6}-EI\left[1+\frac{k_l}{k_u}\right]\frac{d^4w}{dx^4}+G_k\frac{d^2w}{dx^2}-k_lw=0 \tag{2.178}$$

The three parameter models are not further dealt with in this work ,because for routine analysis purposes the two-parameter Pasternak model is more convenient. Instead,two-parameter model proposed by Worku (2014), is employed, as it yields results of the same level of accuracy as Kerr's model while computation simplicity is achieved.

2.3 Analysis of Beams Using Finite Element Software

2.3.1 Finite Element Software-Plaxis

Plaxis is a finite element program for geotechnical applications and in foundation engineering in which models are used to simulate the soil behavior. The program code and soil models have been developed with great care. Although a lot of testing and validation has been performed, it cannot be guaranteed that the plaxis code is free of errors. Moreover, the simulation of geotechnical problems by means of the finite element method implicitly involves some inevitable numerical and modelling errors in general. The accuracy at which reality is approximated depends highly on the expertise of the user regarding the modelling of the problem, the understanding of the soil models and their limitations, the selection of model parameters, and

the ability to judge the reliability of the computational results. There are 2D and 3D versions of Plaxis, where the 2D package is intended for the two-dimensional analysis of deformation and stability in geotechnical engineering. Plaxis 3D Foundation is a three-dimensional Plaxis program, developed for the analysis of foundation constructions including raft foundations and offshore structures. Beams on elastic foundation can be modeled by using both 2D and 3D versions of Plaxis.

Finite element calculations for geotechnical applications give special requirements to the finite element model being used. When structures are involved, structural behavior as well as soil-structure interaction needs to be taken into account. Soil model, interface elements, and the coarseness of finite element mesh play an important role.

2.3.1.1 Soil Models and Properties

The choice of an appropriate soil constitutive model may have significant influence on the accuracy of soil-structure interaction analyses. For this work from the available Plaxis 2D soil models linear elastic model is used. The model used to perform linear elastic analysis. The model is based on Hokes's Law of isotropic elasticity. It involves two basic elastic parameters, i.e., Young's modulus (E_s) and Poisson's ratio (υ) (Gowthaman, 2017; Plaxis 2D, 2002).

2.3.1.2 Interface elements

Many geotechnical applications involve the interaction between soil and structures in or on the soil. Soil-structure interaction problems can be modelled using interface elements with limited shear strength and tension capacity. Several factors such as structural material, soil properties, and surface roughness have been investigated to better understand their effects on the interface characteristics. Interface was categorized into three zones: "smooth," "intermediate," and "rough". The shear strength in the interface can conveniently be related to the shear strength of the surrounding soil by using an interface strength reduction factor (R_{inter}). Interaction between a structure and the soil is intermediate between smooth and fully rough. The roughness of the interaction is modelled by choosing a suitable value for the strength reduction factor in the interface (R_{inter}). Rigid option is used when the interface should not have a reduced strength with respect to the surrounding soil (which corresponds to $R_{inter} = 1.0$) (Gowthaman, 2017; Plaxis 3D, 2006).

Strength properties in the interaction zone between soil and structures are lower than the adjacent soil. This reduction can be specified using the R_{inter} parameter. Hence, using $R_{inter} < 1.0$ gives a reduced interface friction and adhesion compared to the friction angle and the cohesion in the adjacent soil. R_{inter} greater than 1 would not normally be used (Gowthaman, 2017).

2.3.1.3 Meshing

In particular for stability and bearing capacity problems, the accuracy of the solution depends on the type and size of the elements. Upon global or local mesh refinement, the accuracy of results tends to improve. In addition to the refinement of the mesh the quality of the mesh has to be considered. It is preferable when the quality becomes 1.

Chapter 3

Numerical Analysis

In this chapter, a numerical study is conducted using the different solutions obtained for finite and infinite beams under several loading conditions. Calibration factor for Winkler and Kerr-equivalent Pasternak-type subgrade models developed by Worku are determined. Among the different solution cases that ascended in the previous chapter under beams on a two-parameter subgrade, only case III, D <1, considered. Because for the practical purposes, the other two cases are very unlikely to take place. This observation can be made by plotting the parameter D against another carefully selected parameter combining all factors that influence D for selected values of the thickness of the stratum, H. D is a function of modulus of elasticity of the beam(E), modulus of elasticity of the soil(E_s), and Poisson's ratio of the soil(υ). Poulos (2002), suggested the use of the following dimensionless stiffness factor or relative rigidity of soil-beam system.

$$k_r = \frac{16EI(1-\upsilon^2)}{\pi E_s(2l)^4} \tag{3.1}$$

Where l is half the length of the beam, and k_r is the relative rigidity of the soil-beam system. The soil and beam properties taken to identify the case are given in Table 3.1. Taking these values the effect of relative rigidity on D for several values of stratum thickness are shown in (Figure 3.1).

Table 3.1: Soil and beam Properties (Bowles, 1997; Briaud, 2013)

Soil parameters			Beam Property		
	E_s(Mpa)	υ		B(m)	H(m)
Loose sand	25	0.36	Short beam	0.3	0.3
Medium dense sand	50	0.3			
Dense sand	120	0.25	Medium beam	0.3	0.5
Soft clay	15	0.4			
Medium stiff clay	30	0.35	Long beam	0.5	1
Stiff clay	100	0.25	E_c(Gpa)	30	
			υ_c	0.2	

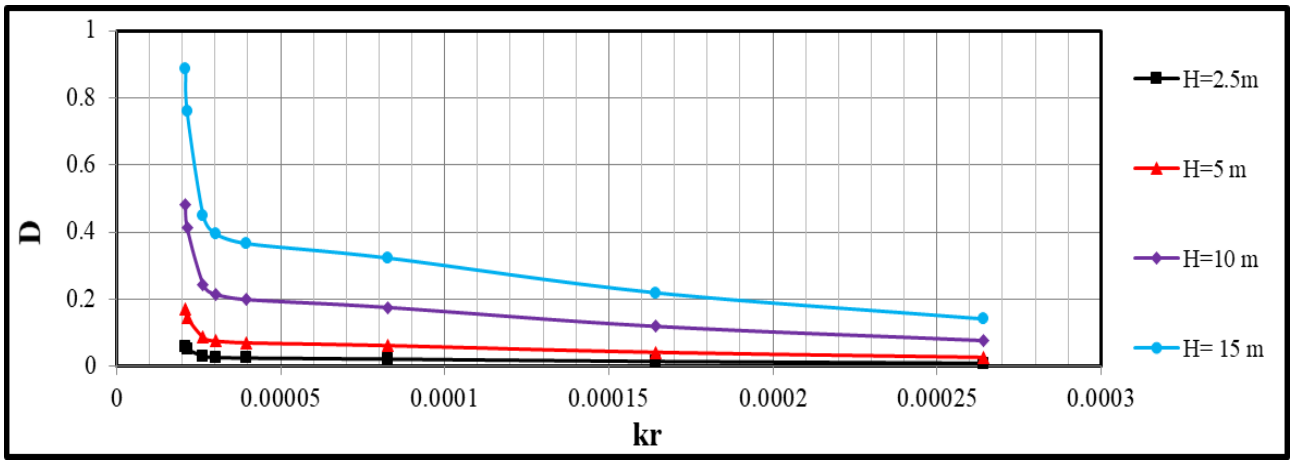

Figure 3.1: Effects of k_r and H on D

The above plots of D against k_r for a wide range of stratum thickness revealed that the value of D lies in case III (D <1). Therefore, it can be concluded that for all practical purposes, it is sufficient to consider the case of D<1 only.

3.1 Calibration of the Winkler-type and Pasternak-type Continuum models

Calibration is possible with the use of existing theoretical results, FE-based software, or lab model testing. For this paper calibration efforts have been made using the FE-based Plaxis 2D software.

All continuum models including the generalized continuum models developed by Worku are sensitive to the thickness, (H), of the stratum. When the thickness of the soil layer increases, it may give unrealistic or excessive deformation. Therefore, it is important to calibrate this model by using Finite Element based Plaxis model; whereby a calibration factor associated with H is introduced by using Plaxis software as a tool.The first step in this process to select between the 2D and 3D versions of the software. To this effect analysis of selected cases of both finite and infinite beams using the two versions are shown in Figures (3.2) to (3.9). For this purpose and subsequent analysis the beam parameters and soil type employed are listed Table 3.2.

Table 3.2: Soil and beam Properties

Soil parameters			Beam Property		
	E_s(Mpa)	υ		B(m)	H(m)
Loose soil	25	0.36	Beam	0.3	0.3
Hard soil	110	0.25			

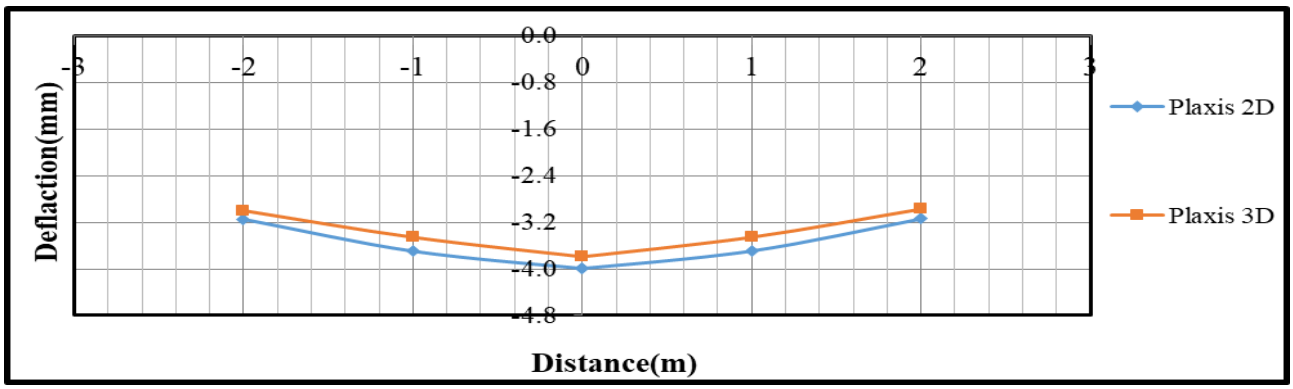

Figure 3.2: Finite beam resting on loose soil subjected to concentrated force

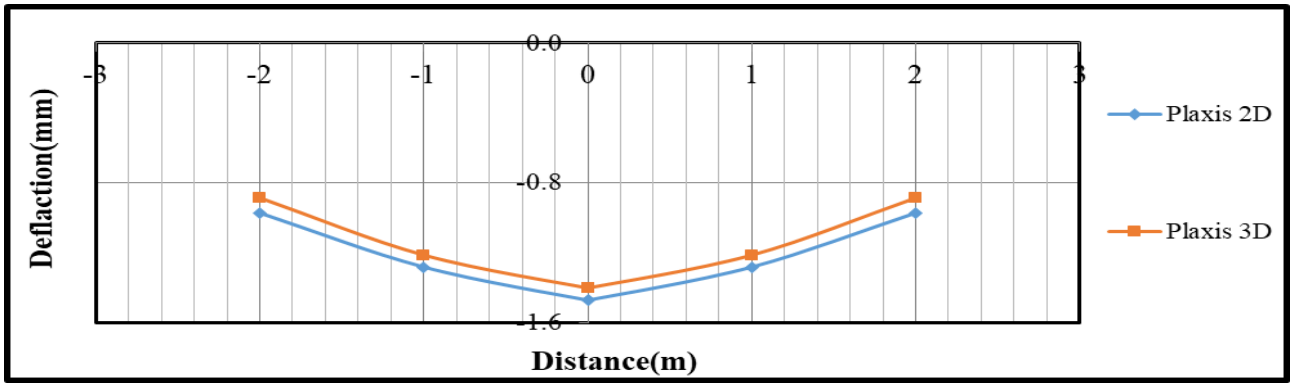

Figure 3.3: Finite beam resting on hard soil subjected to concentrated force

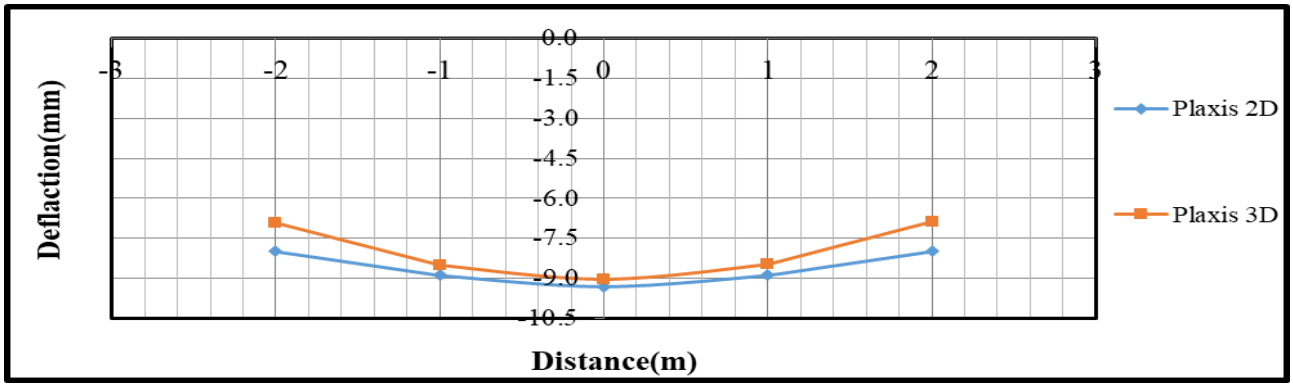

Figure 3.4: Finite beam resting on loose soil subjected to uniformly distributed load

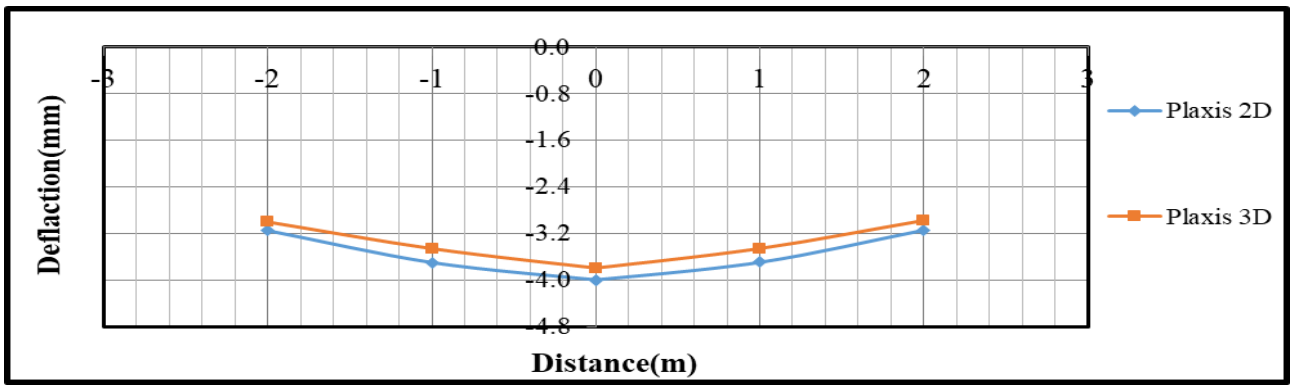

Figure 3.5: Finite beam resting on hard soil subjected to uniformly distributed load

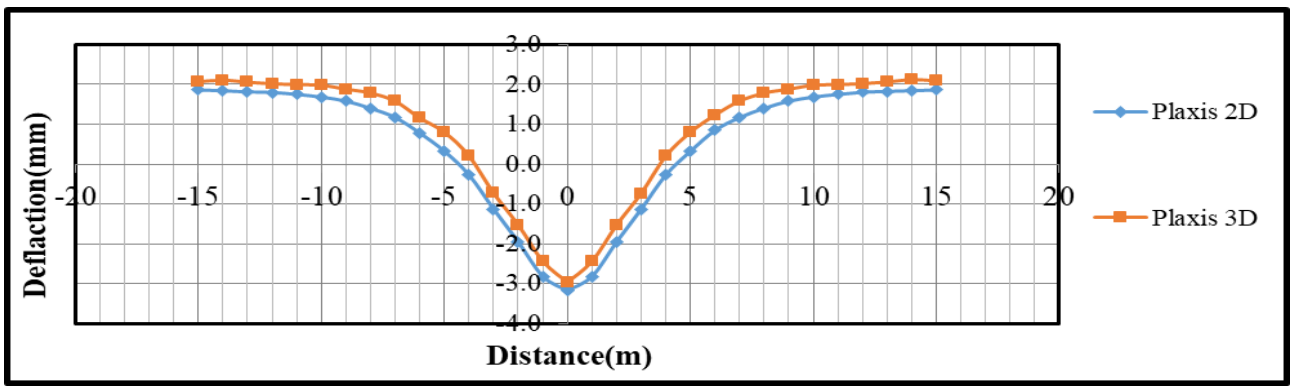

Figure 3.6: Infinite beam resting on loose soil subjected to concentrated force

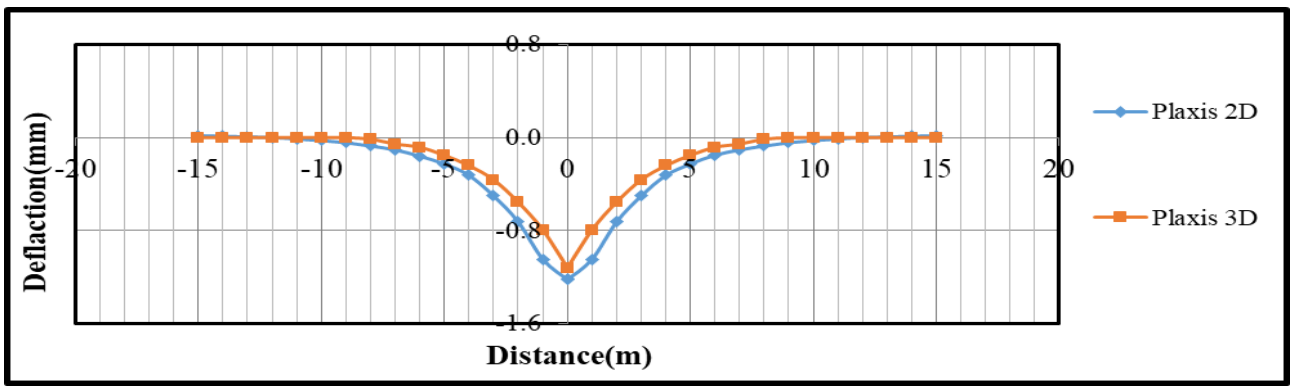

Figure 3.7: Infinite beam resting on hard soil subjected to concentrated force

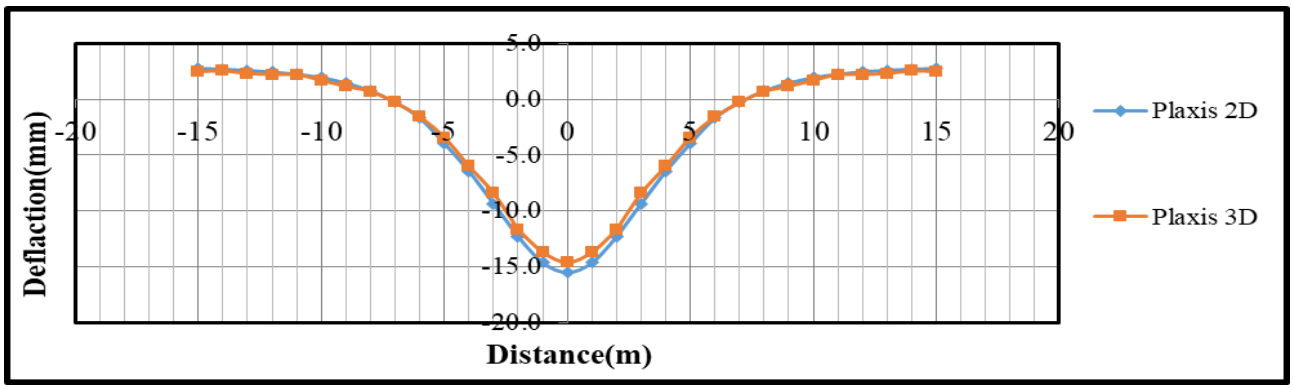

Figure 3.8: Infinite beam resting on loose soil subjected to uniformly distributed load

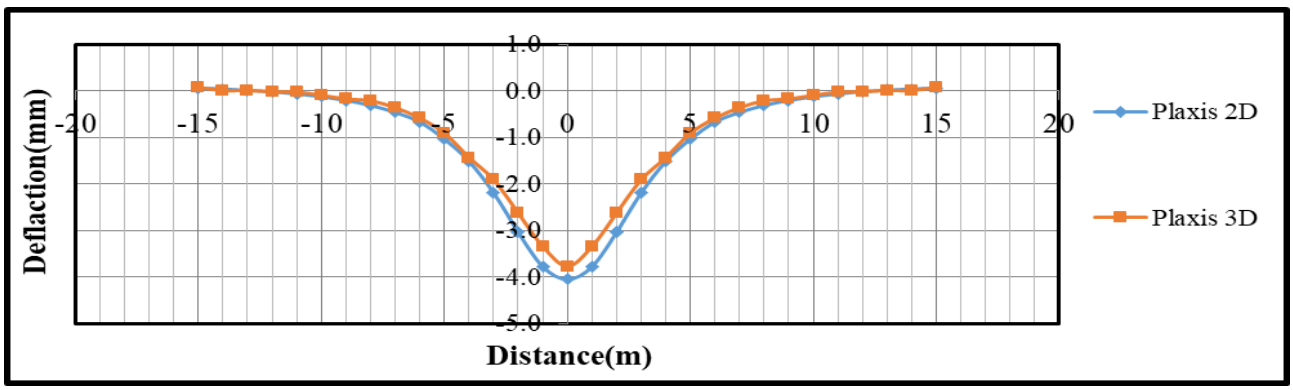

Figure 3.9: Infinite beam resting on hard soil subjected to uniformly distributed load

As we can see in Figures (3.2) to (3.9) the deflection results using Plaxis 2D and 3D models are almost the same for both finite and infinite beams. For this reason, and for the simplicity of computation, Plaxis 2D is used in this paper.

Then the next step is fix the interface element and the mesh type. This is due to the fact that all the output of the Plaxis is affected by the mesh size and could be influenced by interface element used. When the mesh size is decreased, more accurate results will be obtained. But it will take a longer time to get the results. Hence, it is necessary find the optimum mesh size and see the effect of interface element. The effect of interface reduction factor on deflection for beam and soil parameters given in Table 3.2 are shown in Figure (3.17) to (3.17).

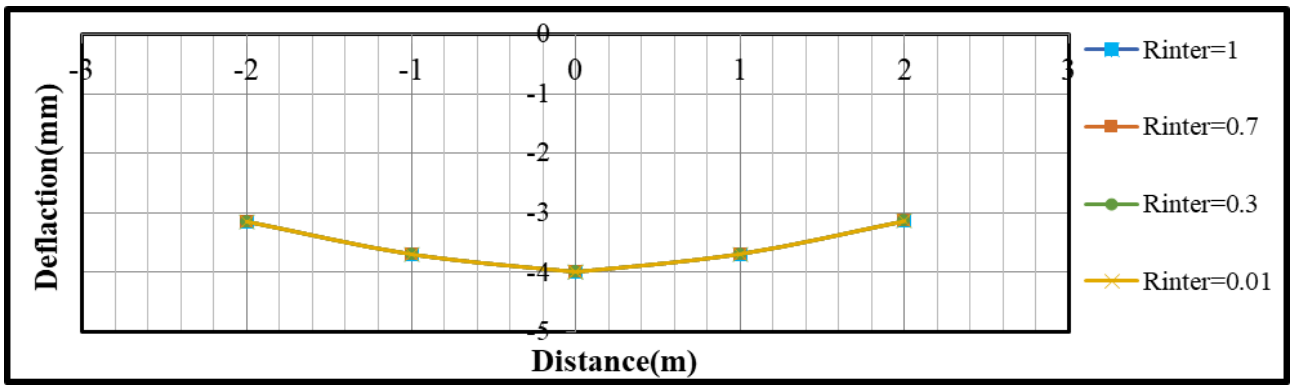

Figure 3.10: Finite beam resting on loose soil subjected to concentrated force

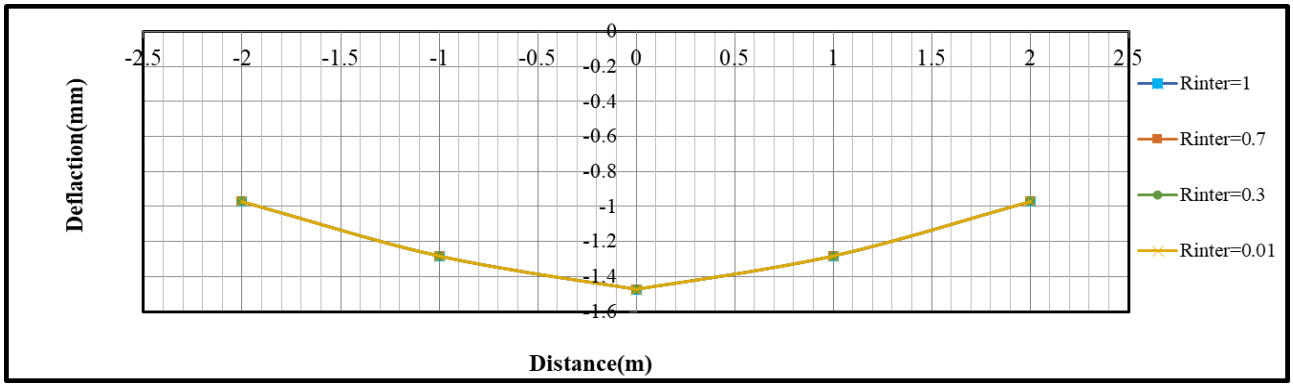

Figure 3.11: Finite beam resting on hard soil subjected to concentrated force

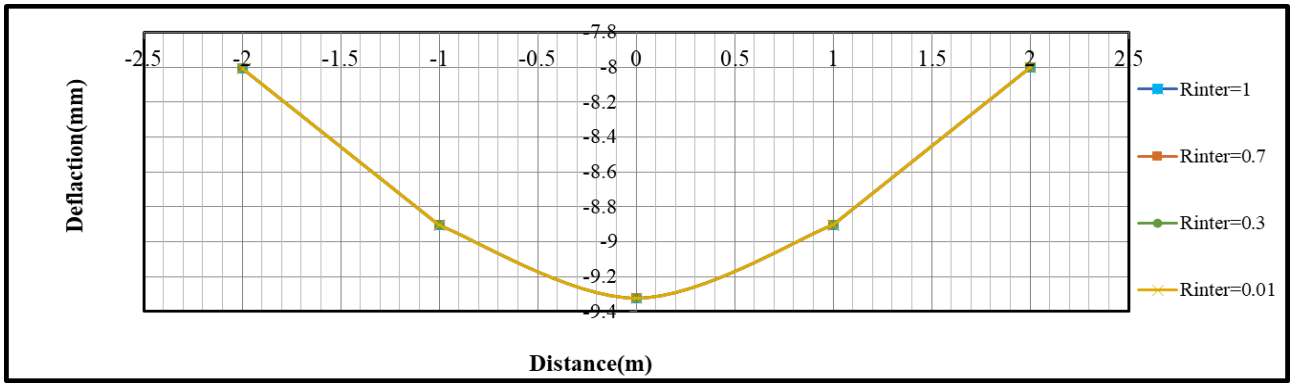

Figure 3.12: Finite beam resting on loose soil subjected to uniformly distributed load

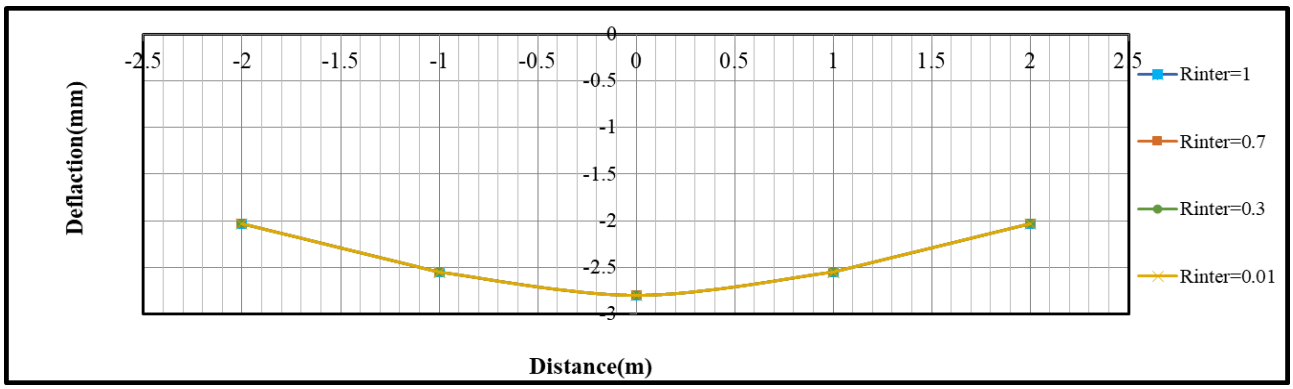

Figure 3.13: Finite beam resting on hard soil subjected to uniformly distributed load

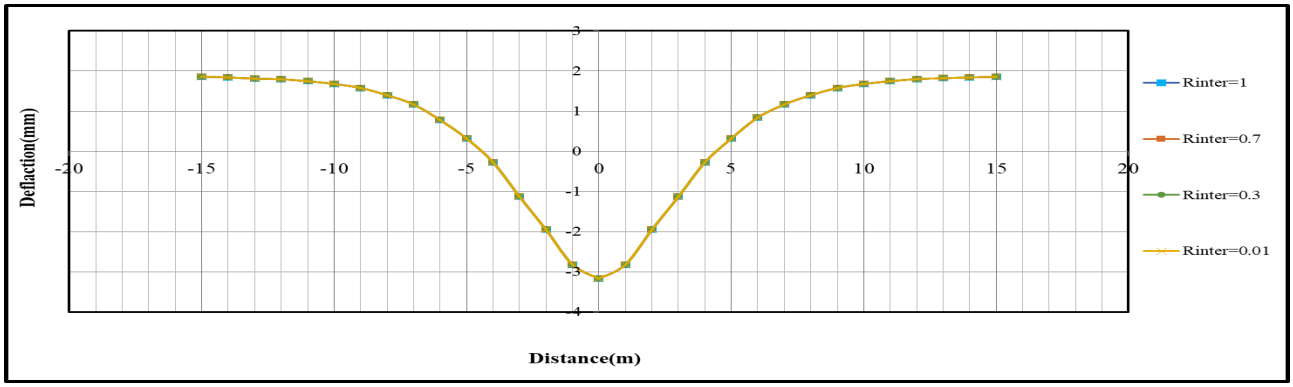

Figure 3.14: Infinite beam resting on loose soil subjected to concentrated force

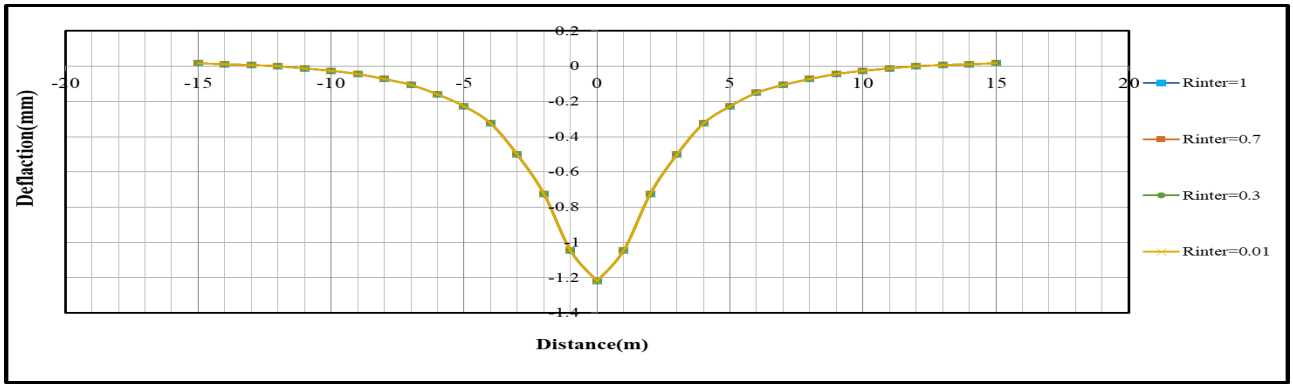

Figure 3.15: Infinite beam resting on hard soil subjected to concentrated force

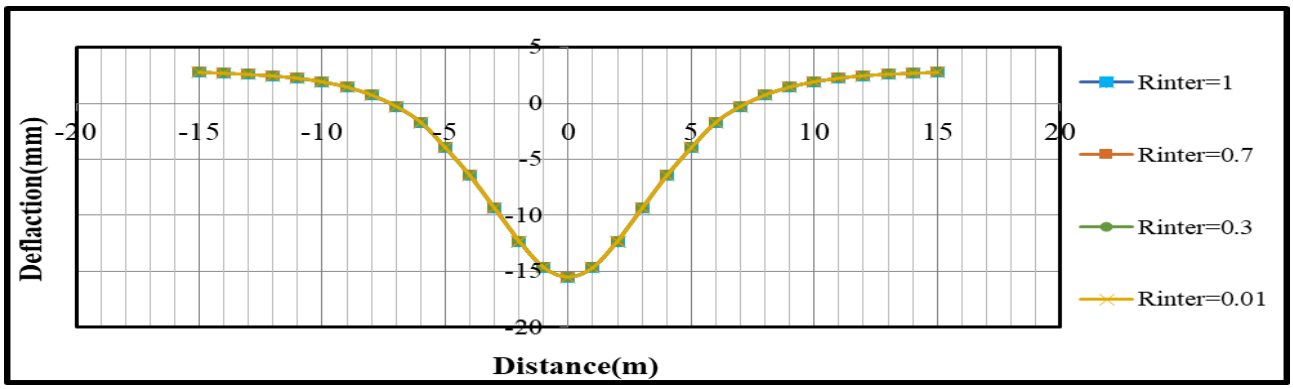

Figure 3.16: Infinite beam resting on loose soil subjected to uniformly distributed load

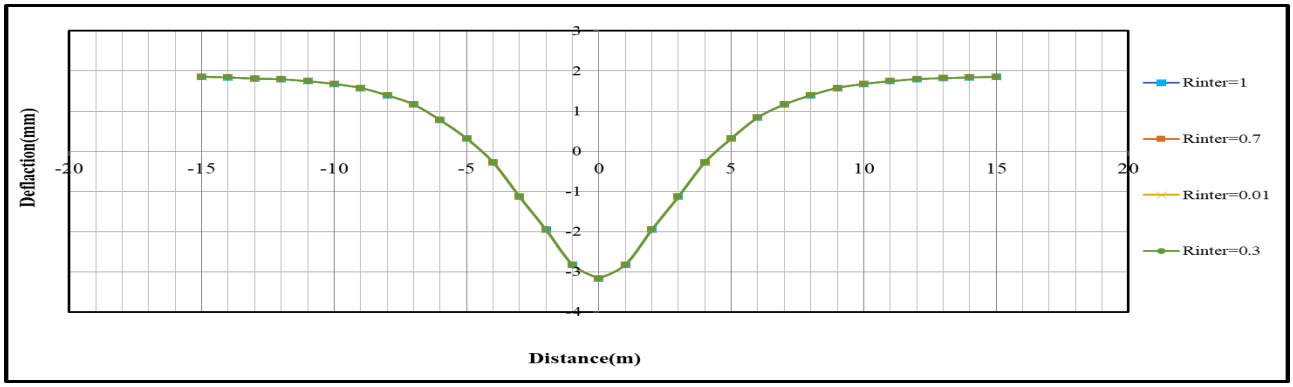

Figure 3.17: Infinite beam resting on hard soil subjected to uniformly distributed load

As could be seen in Figures (3.2) to (3.9) regardless of the interface reduction factor ranging from smooth to rough for the problem on hand the deflection is independent to the interface reduction factor.

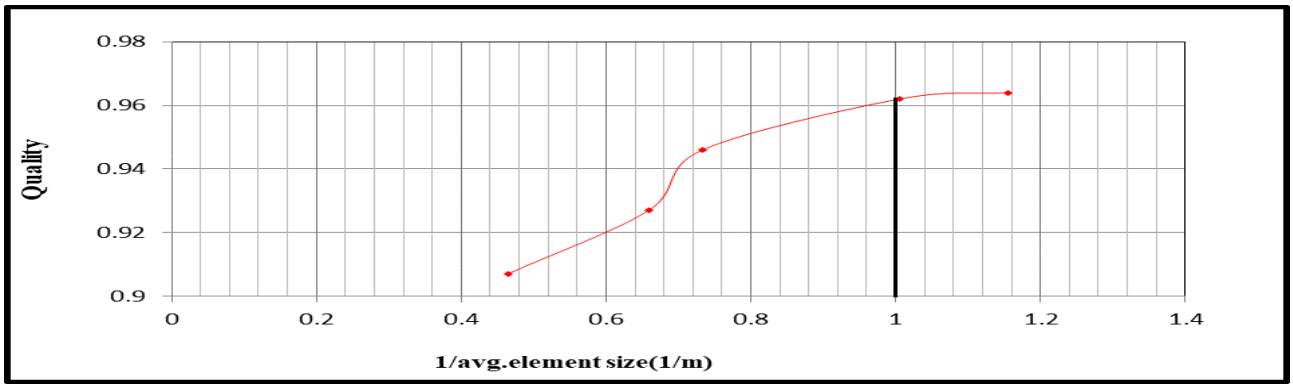

Figure 3.18: Quality of the mesh

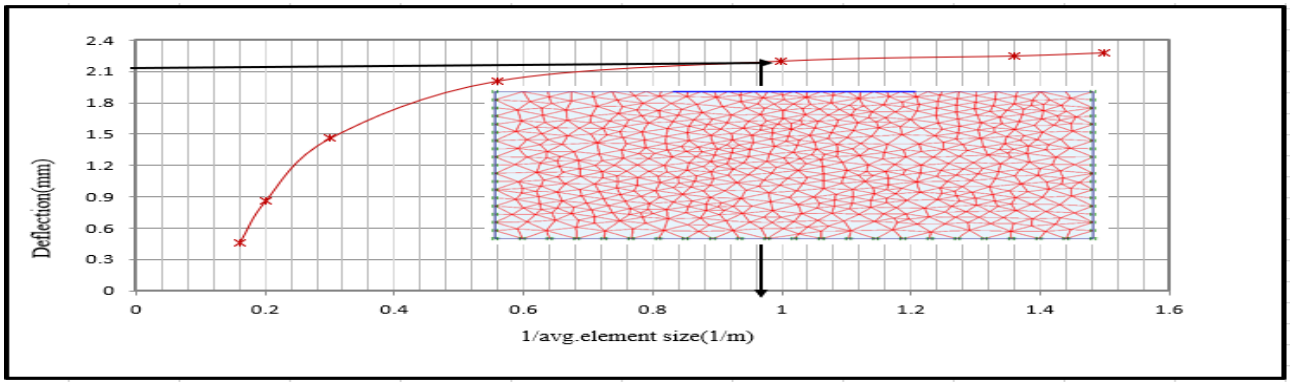

Figure 3.19: Effects of mesh size on deflection

As it is shown in the (Figure 3.19), the average mesh size is determined by drawing a horizontal tangent line where the plot becomes almost constant.
The next step is the calibration of the Winkler-Type and Pasternak–type continuum models of Worku. This is attained after a large number of analysis involving different types of soils is conducted, with various relative thickness of the stratum. Subsequently, the maximum deflection (w_{max}), is plotted against χ for finite and infinite length beams subjected to different loading cases (Figure 3.20).

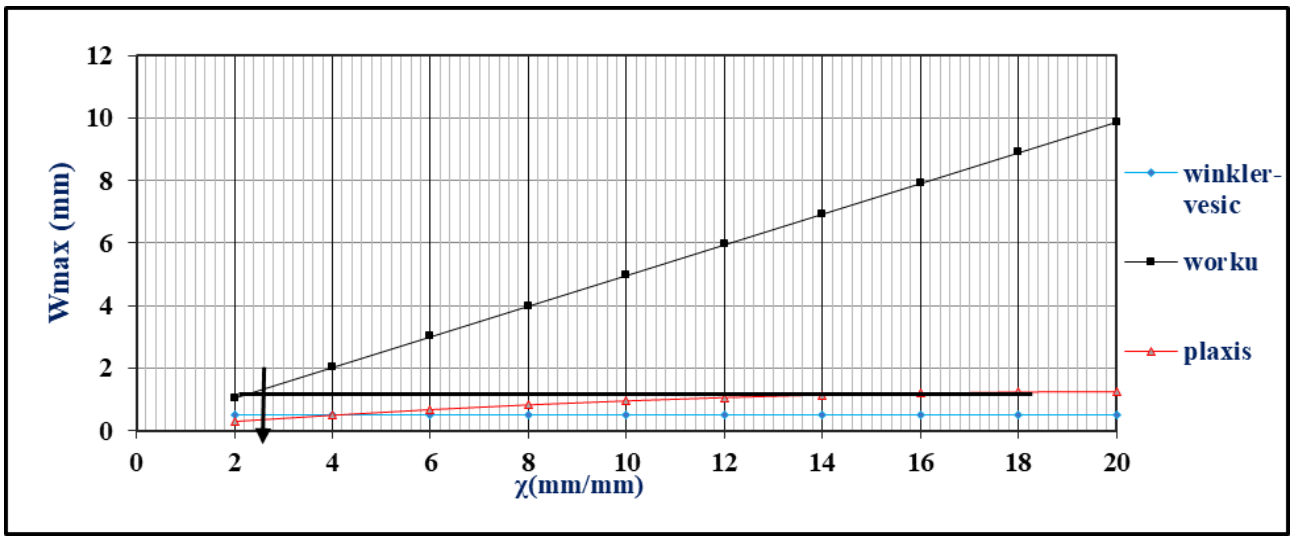

Figure 3.20: Determination of χ

Finally, a calibration factor for each combination of representative type of soil and loading condition is obtained by establishing best fitting trend between the identified range of values of χ against λ. These plots are presented in Figures (3.21) to (3.28). In addition to the soil beam properties given in Table 3.1 the following parameters are used as input for calibration:

- Length of the beam
  - Finite beam 4m

  - Infinite beam 30m

- Vertical Concentrated force
  - P=100 kN
- Concentrated moment
  - M=100 kNm
- Uniformly distributed load
  - q=100 kN/m
  - Loaded region
    - 10m for infinite beam
    - 2m for finite beam
- Combined load
  - P=100 kN,M=100kNm and q=100kN/m

(a) Calibration of Winkler's subgrade model subjected to different beam and soil type combinations

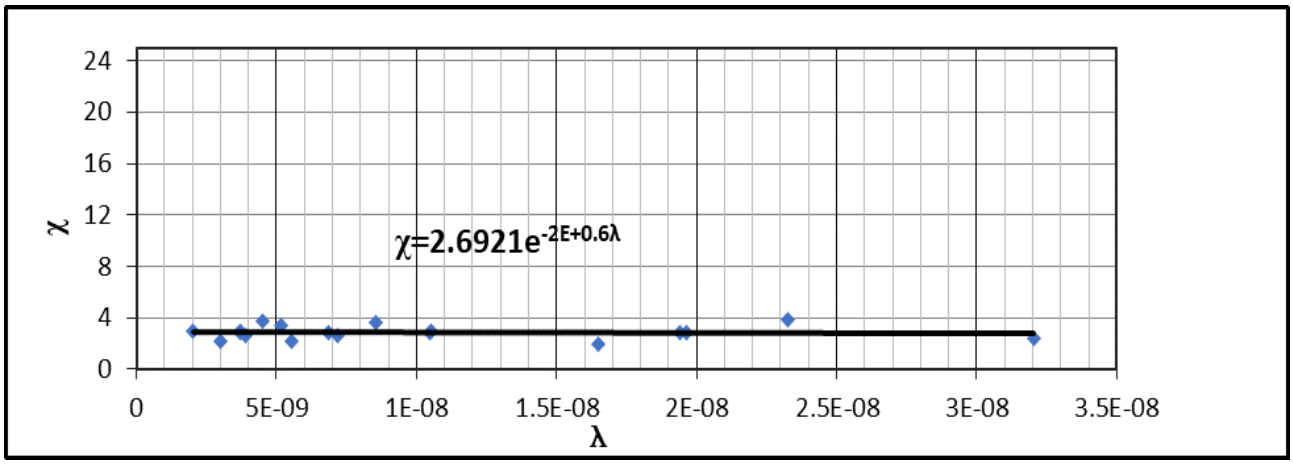

Figure 3.21: χ for beams subjected to a concentrated force

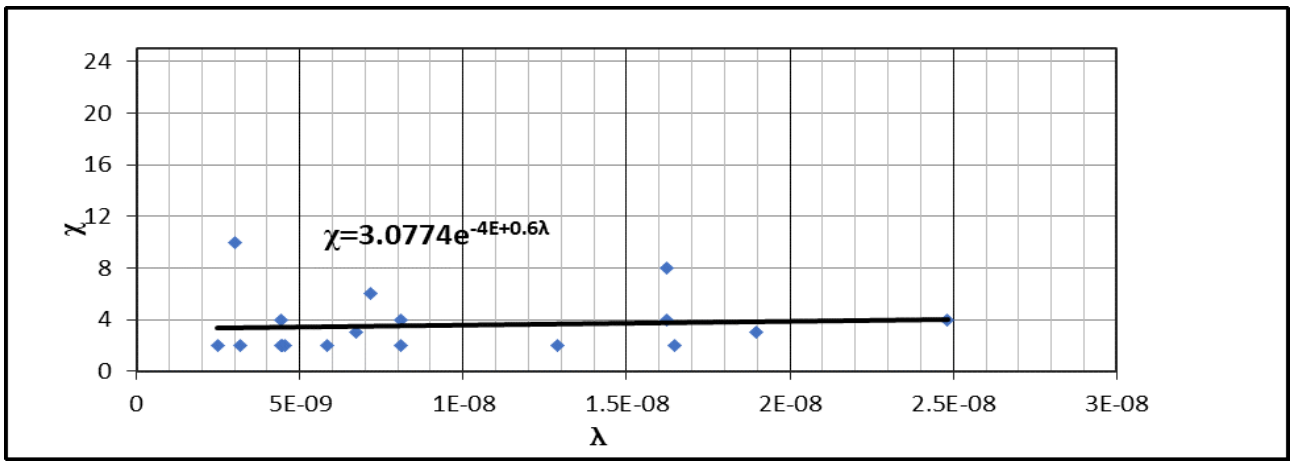

Figure 3.22: χ for beams subjected to a concentrated moment

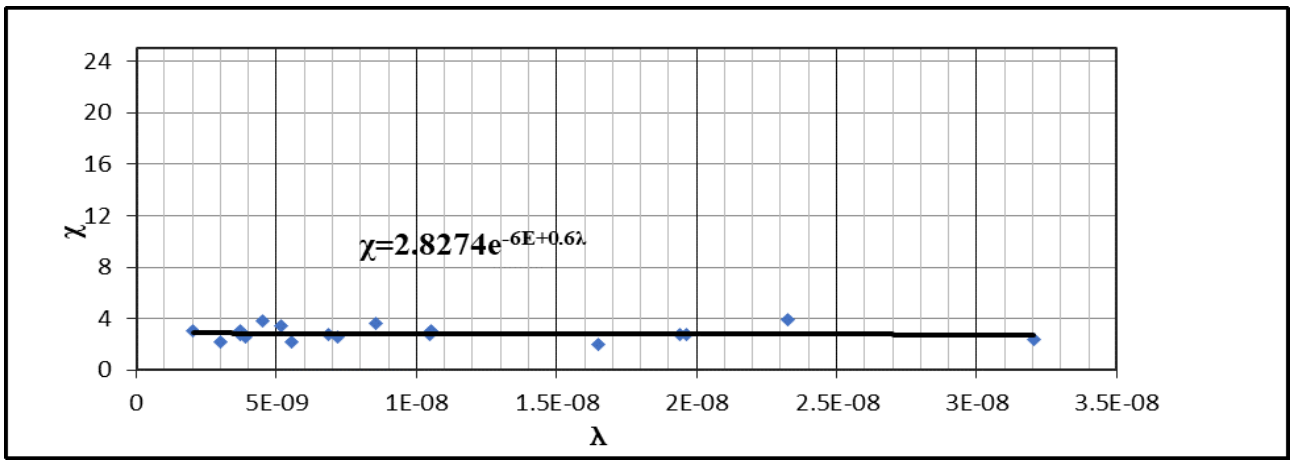

Figure 3.23: χ for beams subjected to a distributed load

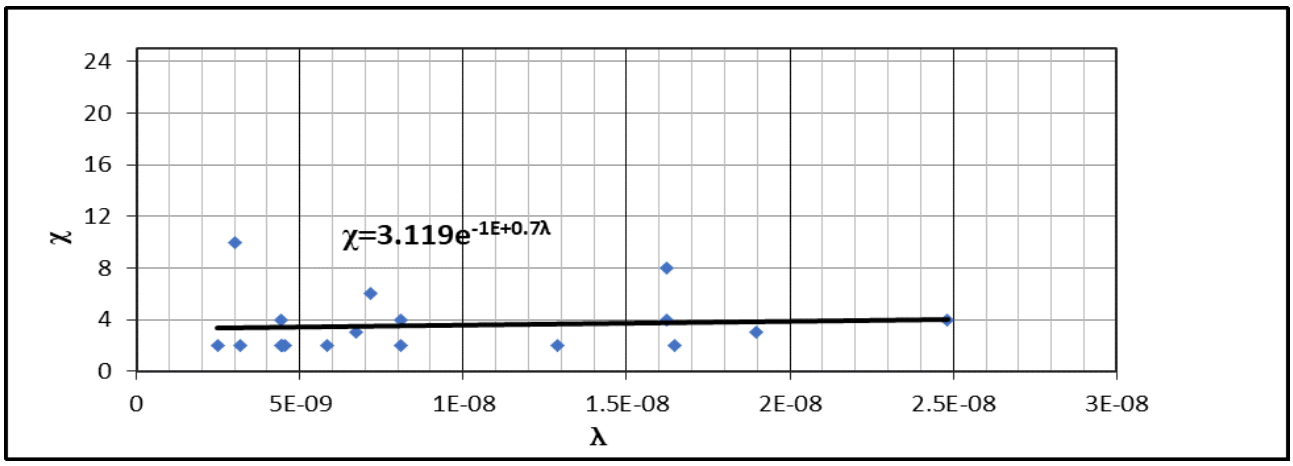

Figure 3.24: χ for beams subjected to combined loading

(b) Calibration of Pasternak's subgrade model subjected to different beam and soil type combinations

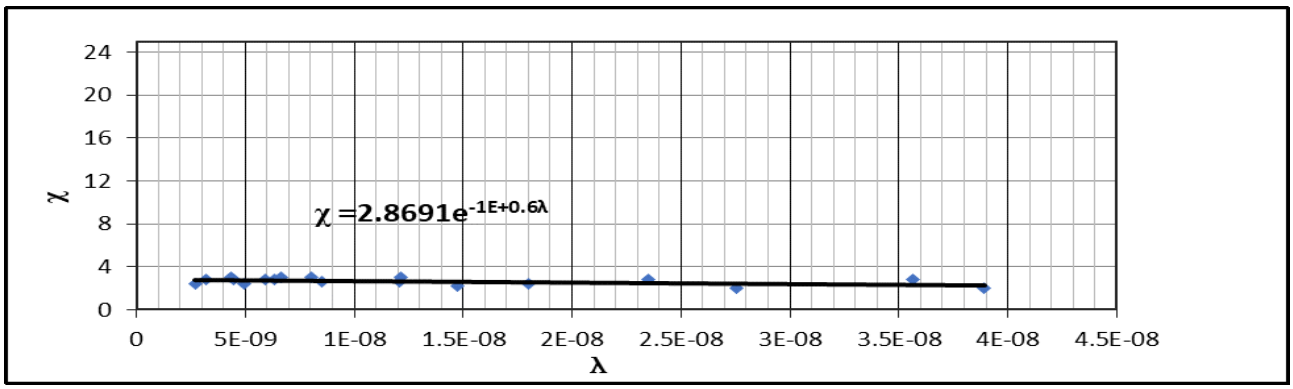

Figure 3.25: χ for beams subjected to a concentrated force

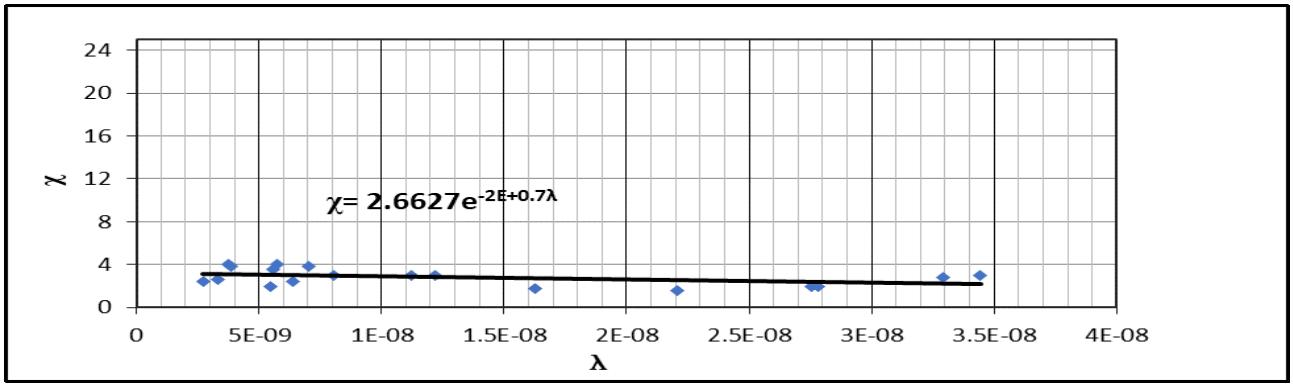

Figure 3.26: χ for beams subjected to a concentrated moment

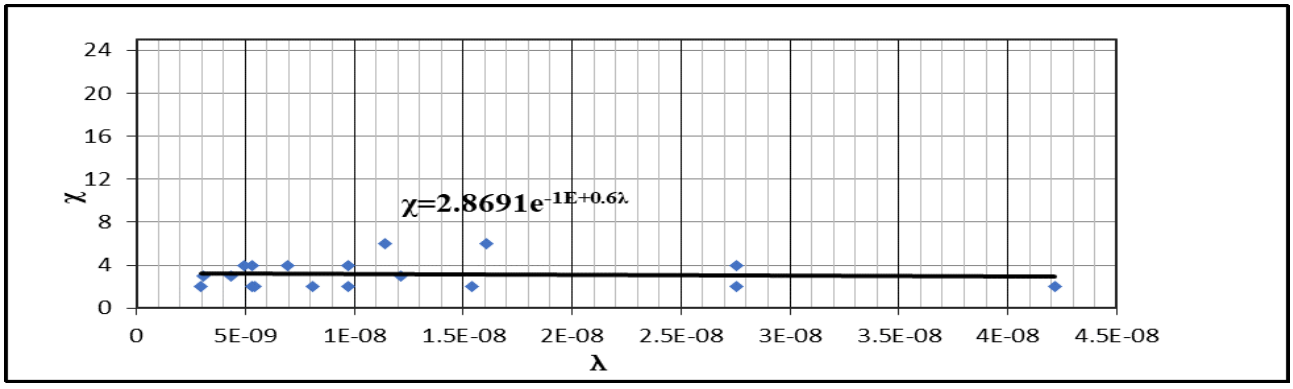

Figure 3.27: χ for beams subjected to a distributed load

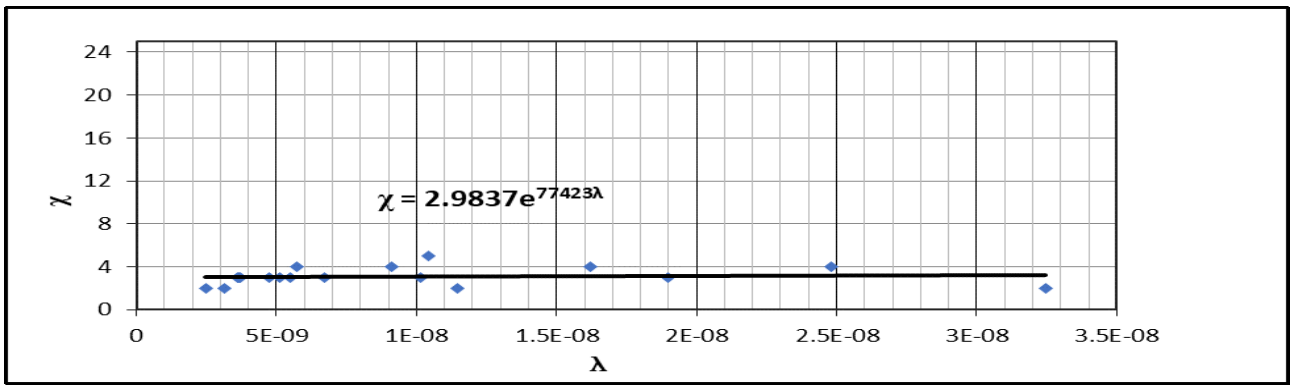

Figure 3.28: χ for beams subjected to combined loading

As shown in the above plots of χ versus the soil-beam relative rigidity factor λ, it can be seen clearly that almost all points lie on a narrow horizontal band and the plots of both models show consistent trend irrespective of the loading type. Also Pasternak's model exhibits lower values of χ compared to Winkler's model and less scattering of data. The recommended calibration factors for a beam to selected loading cases as established from the plots are presented in Table 3.3 and Table 3.4.

Table 3.3: χ for Winkler's subgrade model

Recommended value of calibration factor χ for Winkler's subgrade model	
Load type	χ_w
Concentrated force	2.69
Concentrated moment	3.08
Uniformly distributed load	2.83
Combined load	3.13

Table 3.4: χ for Pasternak's subgrade model

Recommended value of calibration factor χ for Pasternak's subgrade model	
Load type	χ_p
Concentrated force	2.87
Concentrated moment	2.66
Uniformly distributed load	2.87
Combined load	2.98

Since continuum models generally are sensitive to the thickness of the stratum for an actual stratum with $H > \chi B$,the calibration factors given in Tables 3.3-3.4 are to be employed; whereas when $H < \chi B$, the actual soil stratum thickness is used.

3.2 Calibrated Model Parameters

The Calibration parameter, which relates the soil layer thickness to the beam width, was introduced through the relation:

$$\chi = \frac{H}{B} \tag{3.2}$$

Where H is the thickness of the soil,B is the width of the beam and χ is the calibration factor for the subgrade model given in Tables 3.3-3.4.
Introducing Equation (3.2) in Equation (2.68) and Equation (2.86), one obtains the calibrated model parameters of Worku's model as given below:
Winkler's Type model

$$\overline{K}_w = \frac{E_s}{(1-0.4\upsilon)B\chi_w} \tag{3.3}$$

Pasternak's Type model

$$\begin{aligned} k_p &= \frac{(0.4\upsilon+0.67)E_s}{B\chi_p} \\ G_p &= (1.36\upsilon+2.28)GB\chi_p \end{aligned} \tag{3.4}$$

3.3 Numerical Comparison

In this part of the work numerical comparison of the response of beams on single-parameter and two-parameter subgrade models with FE-based Plaxis 2D are performed. The comparison is done for beams having finite and infinite length subjected to selected loading conditions and different soil-beam rigidity. The comparison includes Worku's calibrated models as well as selected other models that enjoy wide usage. Hetenyi (1946), classified beams as finite and infinite based on their beam length and soil-beam rigidity λ.

- $\lambda l \geq 6$ infinite beam
- $\lambda l < 6$ finite beam

This classification is used in the analysis presented in the following sections.

3.4 Infinite Beam

Numerical computations for an infinite (long length) beam subjected to a concentrated vertical force,a concentrated moment, a uniformly distributed load, and combined loads are carried out for different types of soil. Subsequently, the results obtained from single-parameter and two-parameter subgrade models and finite- element-based Plaxis 2D model are compared. The input parameters are given below.

Excel Program Input Parameters:

A) Beam Properties (Concrete)

- Elastic modulus of the beam (E_c) =30 GPa
- Width of the beam (B) = 0.3 m
- Depth of the beam (d) =0.3m
- Poisson's ratio(υ_c) = 0.2

B) Soil data taken from (Briaud ,2013).

- Stratum thickens H=10m for all types of soil
- Hard/Dense Soil
  i. Elastic modulus of the soil (Es) = 110MPa
  ii. Poisson's ratio (υ) = 0.25
- Soft/ Loose Soil
  i. Elastic modulus of the soil (Es) = 20MPa
  ii. Poisson's ratio (υ) = 0.35

C) Loading Conditions

i. Vertical Concentrated force
- P=100 kN

ii. Concentrated moment
- M=100 kNm

iii. Uniformly distributed load
- q=100 kN/m , Loaded region 8m

iv. Combined load
- P=100 kN,M=100kNm and q=100kN/m

Finite Element (Plaxis 2D) Inputs

(a) Rough foundation soil interaction ($R_{inter} = 1$)

(b) Soil model
- Linear elastic model

(c) Material model for the beam
- Elastic model

(d) Mesh type
- Fine

Subgrade Models:

A) Single parameter subgrade models

- Biot
- Vesic
- Horvath
- Worku Winkler type

B) Two parameter subgrade models

- Vlasov

$$\begin{cases} \gamma = 0 \\ \gamma = 10 \end{cases}$$

- Horvath
- Worku Pasternak type model

For Vlasov model the γ values between 0 to 10 is a wide range to represent the model.The results of deflection, moment and shear force are evaluated and presented graphically for an infinite beam and soil parameters given above. Plaxis 2D analysis sample output for different loadings are graphically presented in Annex B.

Infinite beam subjected to a vertical concentrated force on a single-parameter subgrade model

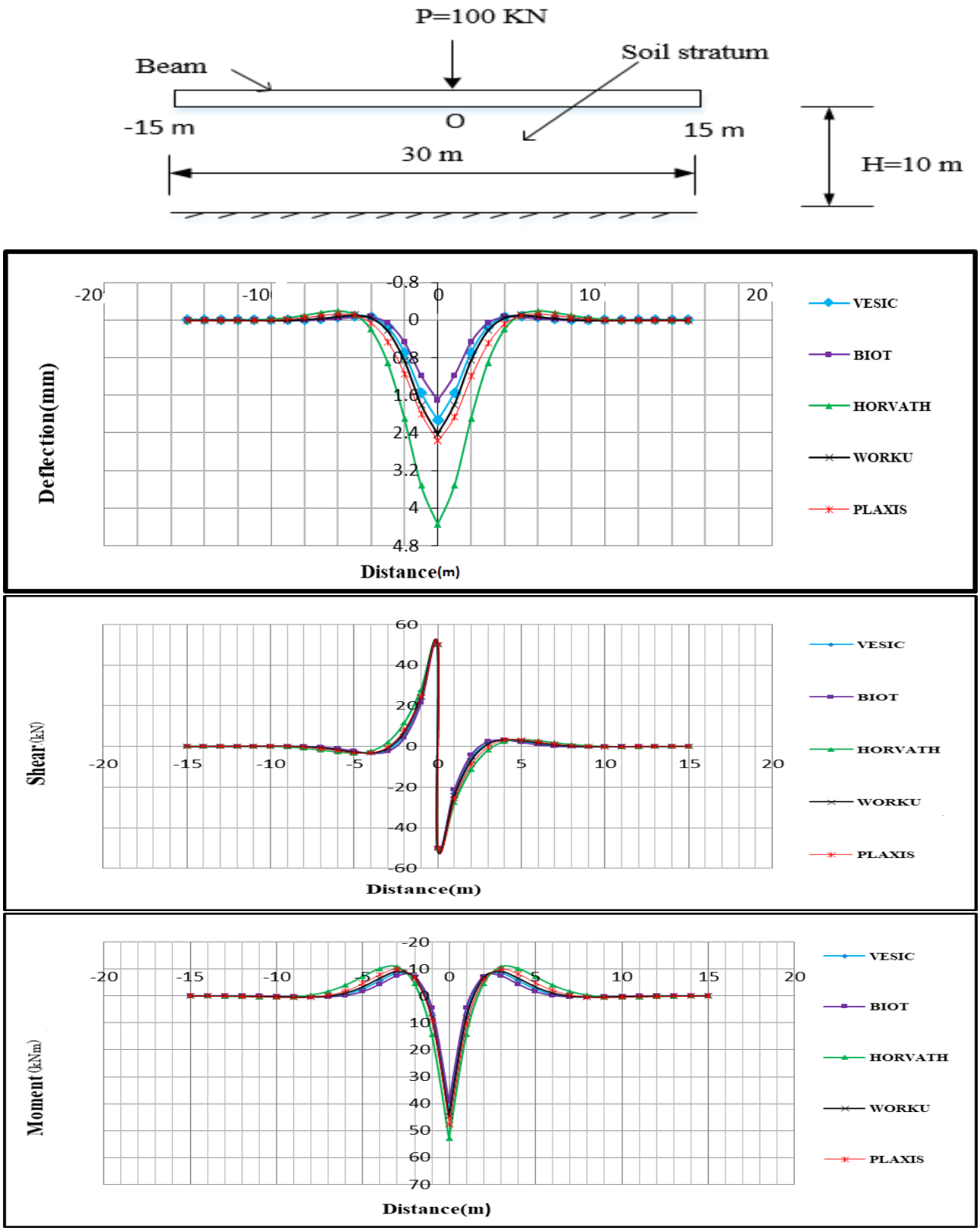

Figure 3.29: Infinite beam resting on soft/loose soil subjected to a vertical concentrated force on a single-parameter subgrade model

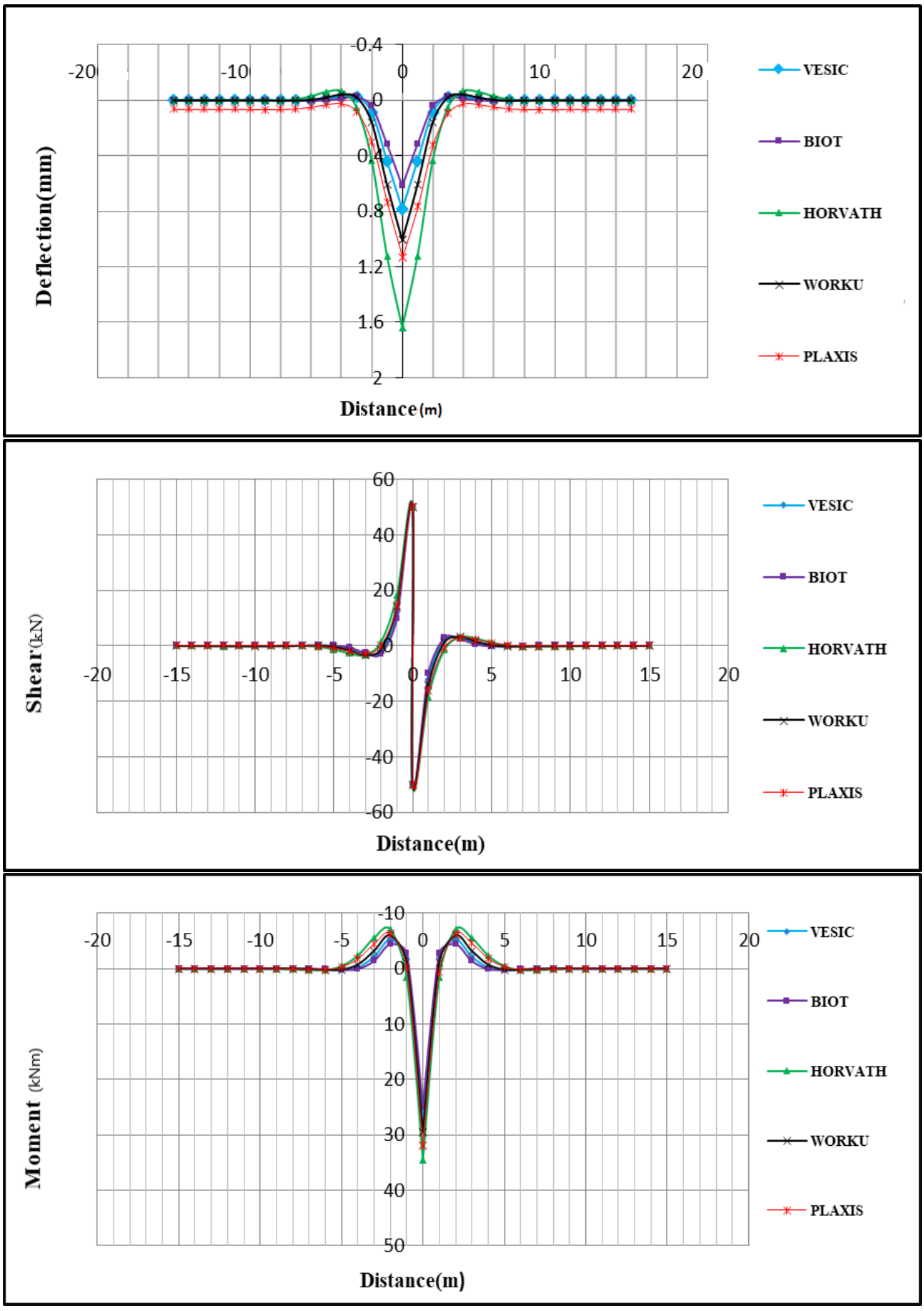

Figure 3.30: Infinite beam resting on hard/dense soil subjected to a vertical concentrated force on a single-parameter subgrade model

A review of the curves reveals a number of significant observations:

- Deflection shows deviation near the mid-span and becomes much better elsewhere.
- The deflection obtained by Worku model is in a very good agreement with the FE based Plaxis 2D model throughout the beam span.
- In the particular case of hard/dense soil, FE based Plaxis 2D has shown a variation outside the mid-span deviation that may,however, amount up to 5% only.
- Horvath subgrade model gives the highest deflection compared to the other models.
- Vesic and Biot subgrade models give a lower deflection value when compared to Plaxis 2D.
- Shear and moment are not affected in comparison to the deflection.

Infinite beam subjected to a vertical concentrated force on a two-parameter subgrade model

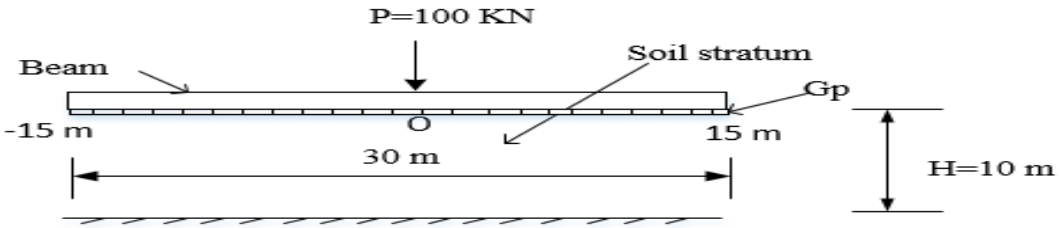

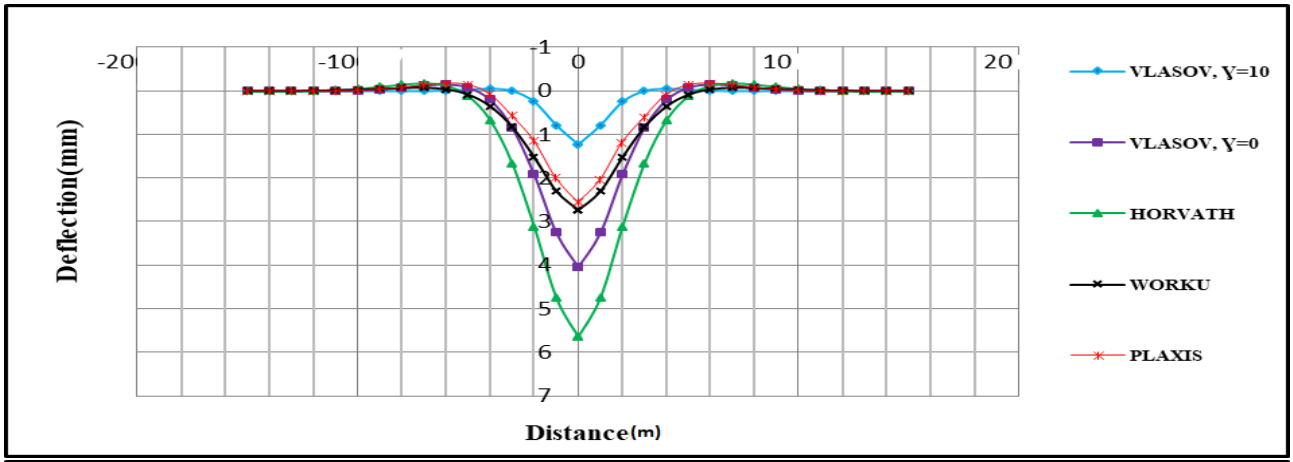

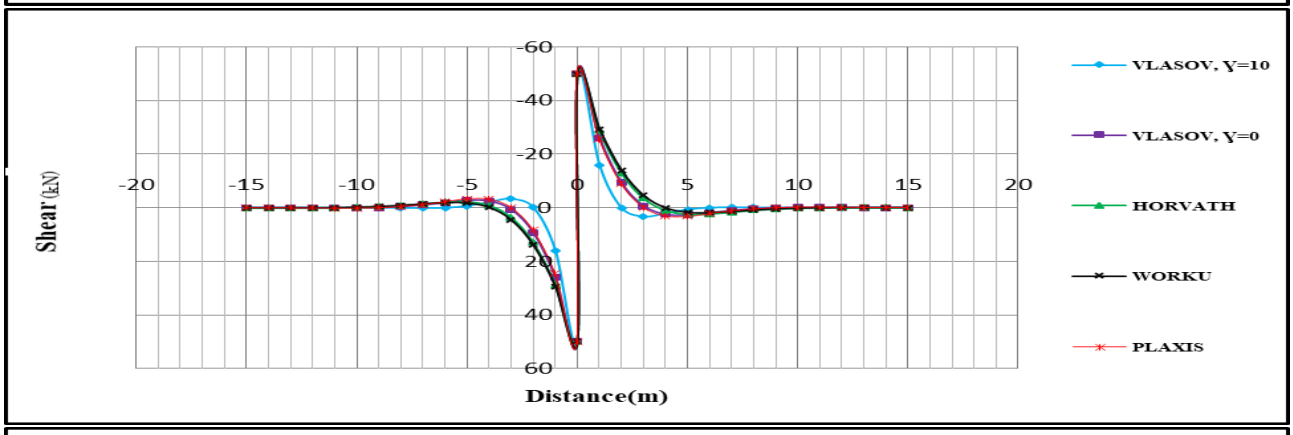

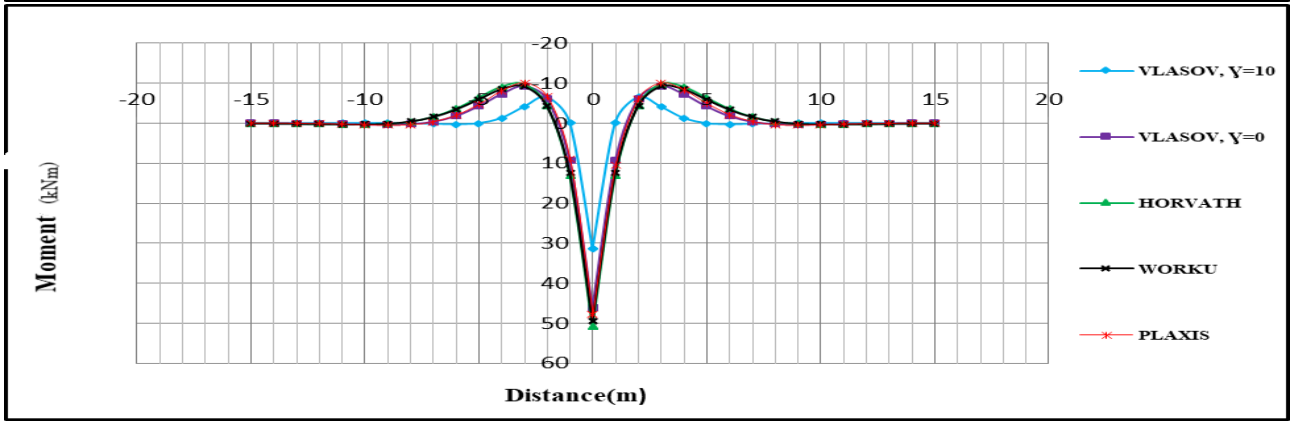

Figure 3.31: Infinite beam resting on soft/loose soil subjected to a vertical concentrated force on a two-parameter subgrade model

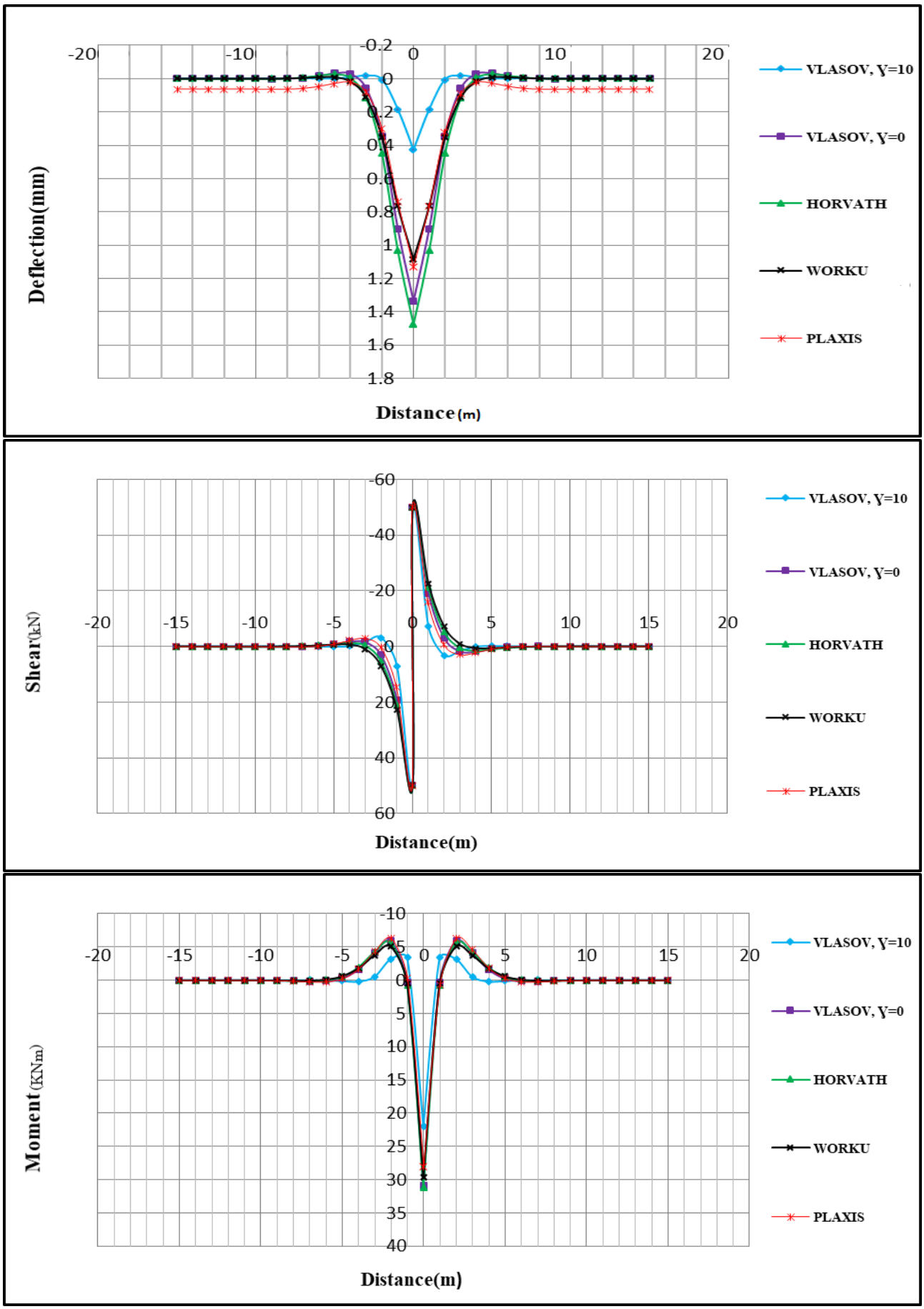

Figure 3.32: Infinite beam resting on hard/dense soil subjected to a vertical concentrated force on a two-parameter subgrade model

A review of the curves reveals a number of significant observations:

- Deflection shows deviation near the mid-span and is much better elsewhere.
- The deflection obtained by Worku model is in a very good agreement with the FE based Plaxis 2D model throughout the beam span.
- In the particular case of hard/dense soil, FE based Plaxis 2D has shown a variation outside the mid-span deviation that not exceed 3%.
- Vlasov subgrade model underestimates the deflection compared to Plaxis 2D when $\gamma = 10$.
- Vlasov subgrade model has shown deflection, shear and moment variation compared to the other models when $\gamma = 10$.
- Shear and moment are not affected in comparison to deflection for most models other-than Vlasov's model for $\gamma = 10$.
- Vlasov's model overlaps with the generalized Kerr-Equivalent Pasternak model of Worku when $\gamma = 2.5$ and $\gamma = 2$ for loose and hard soil, respectively.

Infinite beam subjected to a Concentrated moment on a single-parameter subgrade model

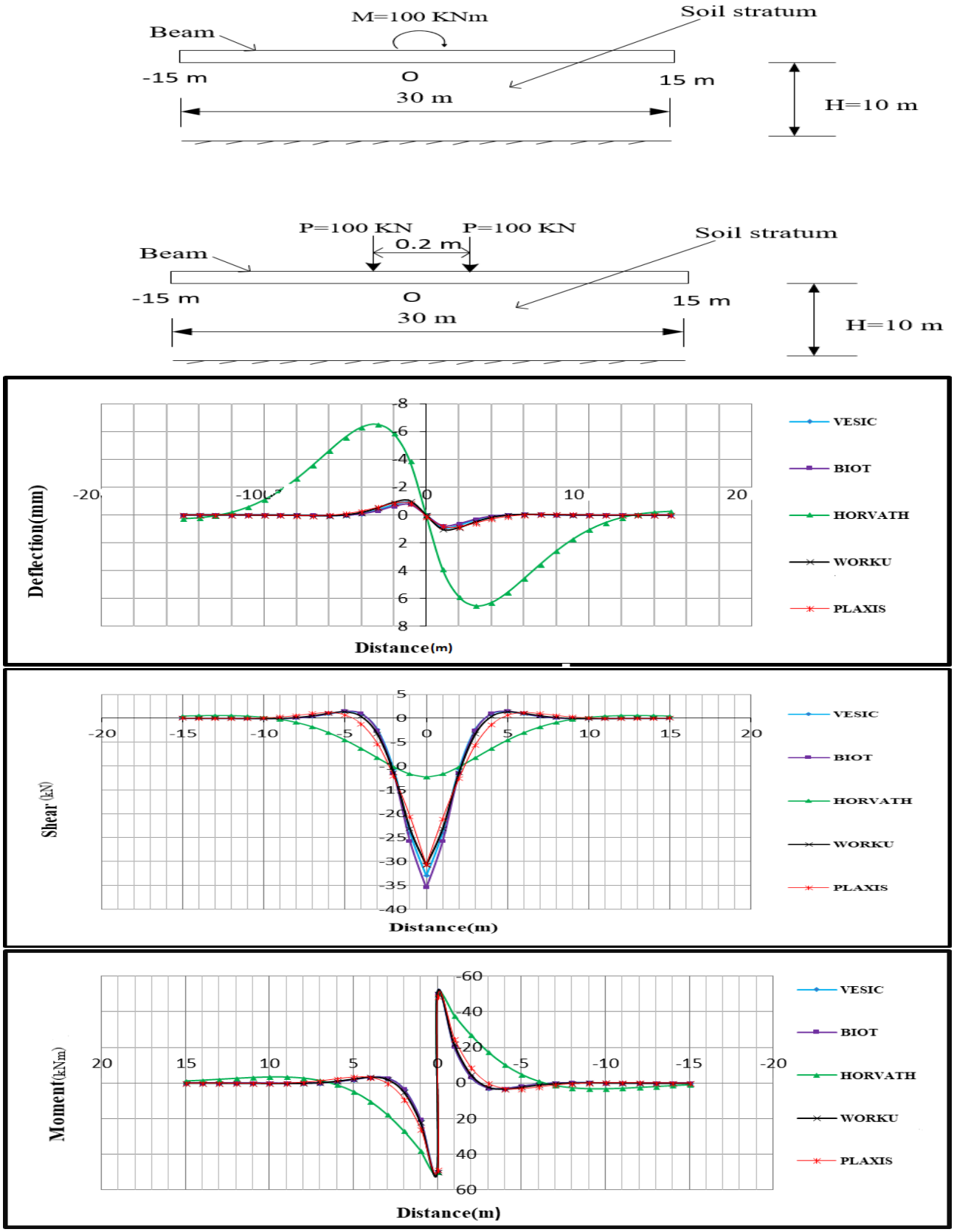

Figure 3.33: Infinite beam resting on soft/loose soil subjected to a concentrated moment on a single-parameter subgrade model

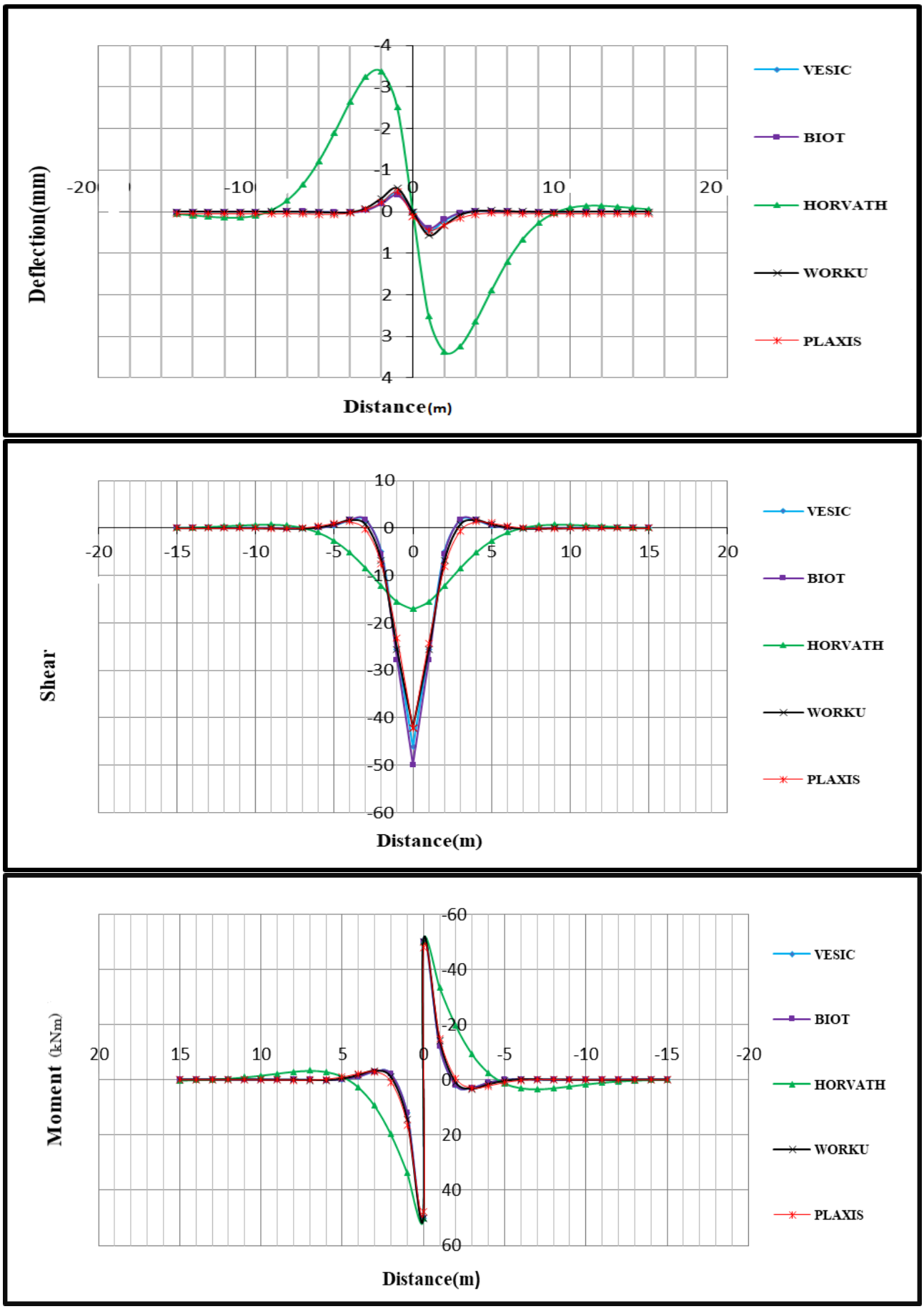

Figure 3.34: Infinite beam resting on hard/dense soil subjected to a concentrated moment on a single-parameter subgrade model

A review of the curves reveals a number of significant observations:

- The deflection obtained by the Worku model is in a very good agreement with the FE based Plaxis 2D model throughout the beam span.
- Horvath subgrade model has shown large deflection (more than six fold), shear and moment variation compared to the other models, its use thus questionable.
- Shear and moment are not affected in comparison to deflection for other models otherthan Horvath.

Infinite beam subjected to a Concentrated moment on a two-parameter subgrade model

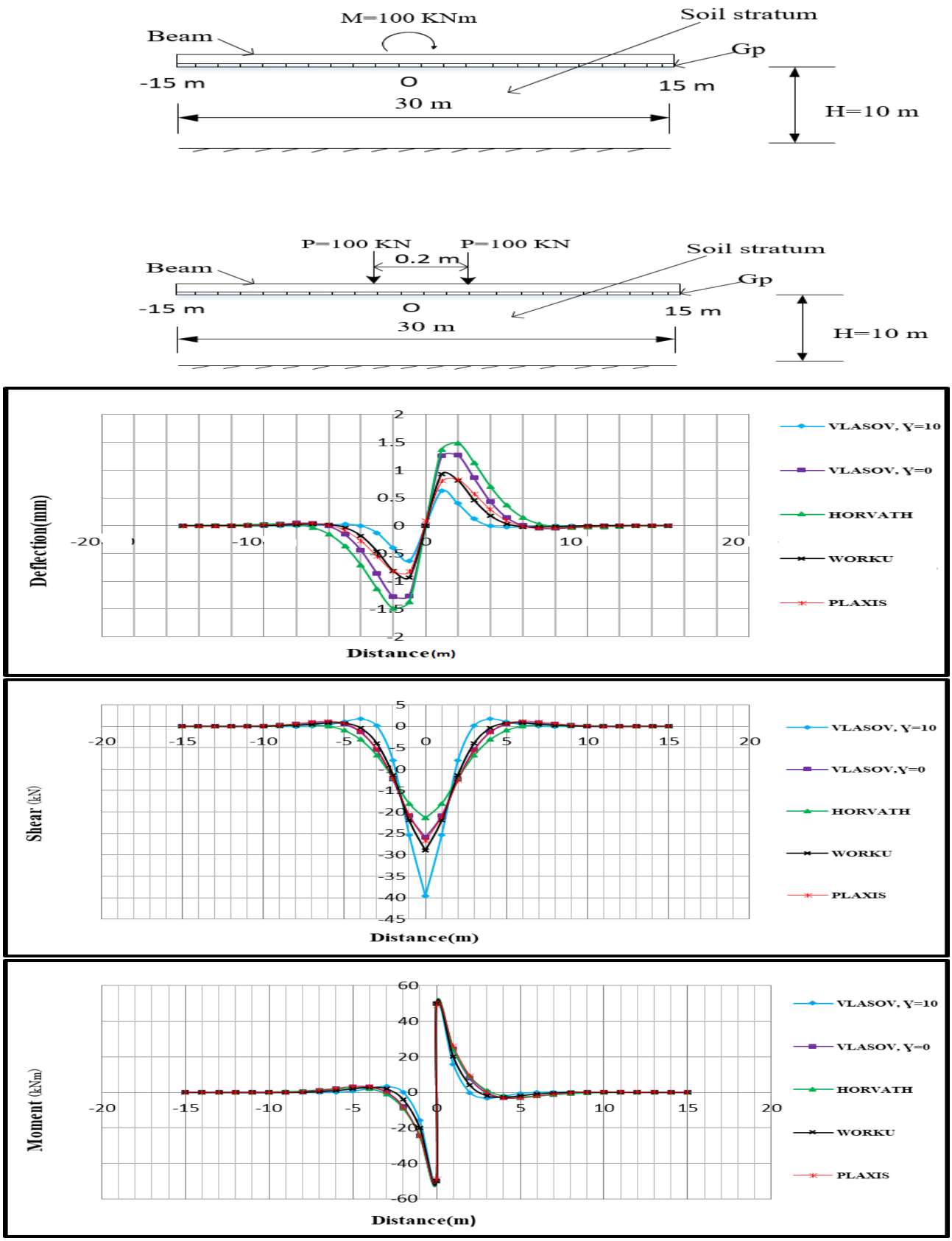

Figure 3.35: Infinite beam resting on soft/loose soil subjected to a concentrated moment on a two-parameter subgrade model

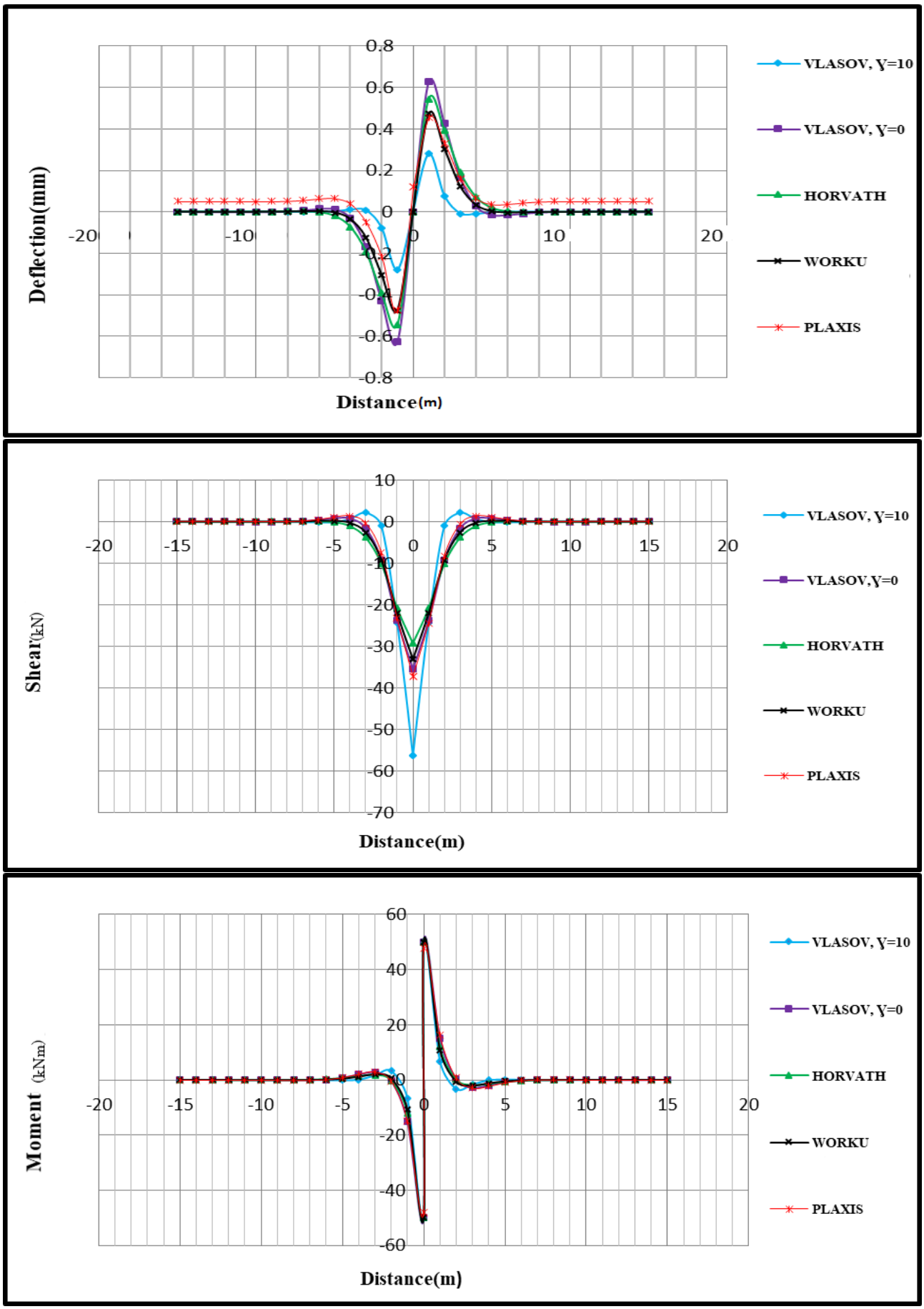

Figure 3.36: Infinite beam resting on hard/dense soil subjected to a concentrated moment on a two-parameter subgrade model

A review of the curves reveals a number of significant observations:

- The deflection obtained by Worku model is in a very good agreement with the FE based Plaxis 2D model throughout the beam span.
- In the particular case of hard/dense soil, FE based Plaxis 2D shows a variation outside the mid-span deviation not exceeding 3%.
- Vlasov subgrade model underestimates the deflection and overestimates the maximum shear when $\gamma = 10$, compared to the other models.
- Vlasov subgrade model has shown deflection, shear and moment variation compared to the other models when $\gamma = 10$.
- Moment is barely affected in comparison to deflection and shear.
- Vlasov's model overlaps with the generalized Kerr-Equivalent Pasternak model of Worku when $\gamma = 5$ and $\gamma = 4$ for loose and hard soil, respectively.

Infinite beam subjected to a Uniformly distributed load on a single-parameter subgrade model

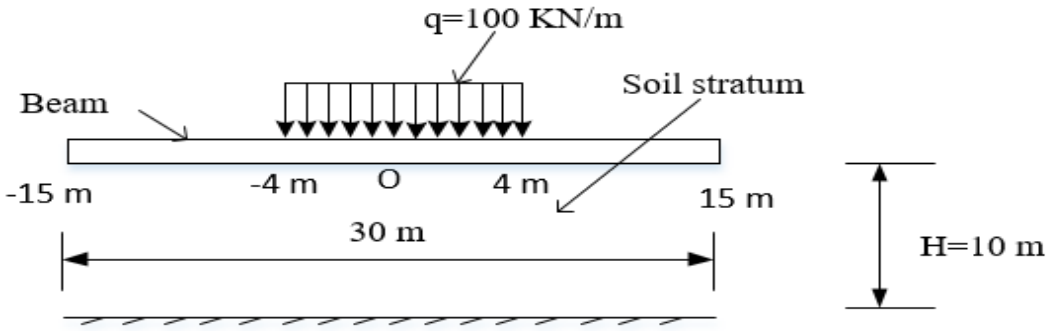

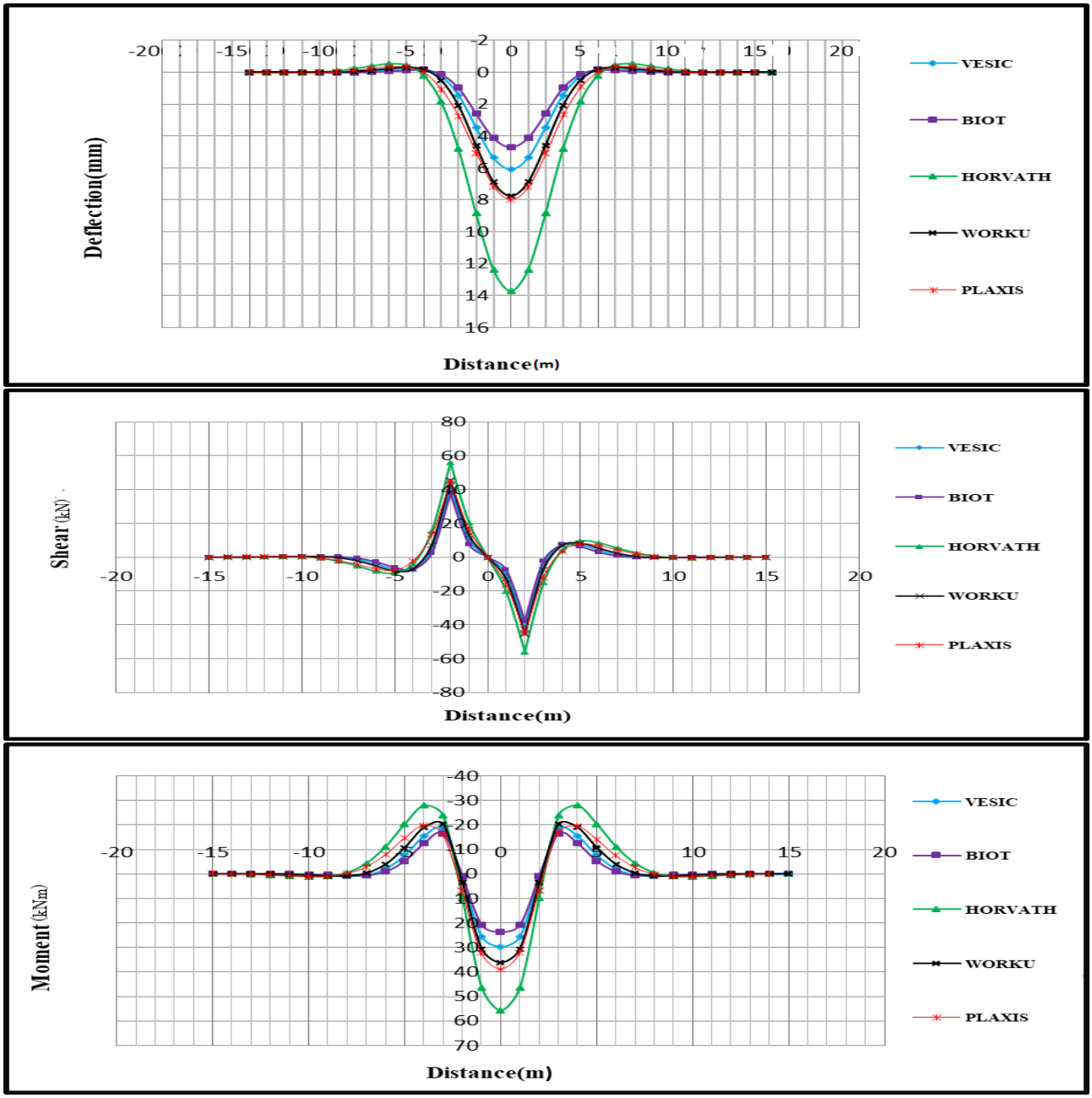

Figure 3.37: Infinite beam resting on loose/soft soil subjected to a uniformly distributed load on a single- parameter subgrade model

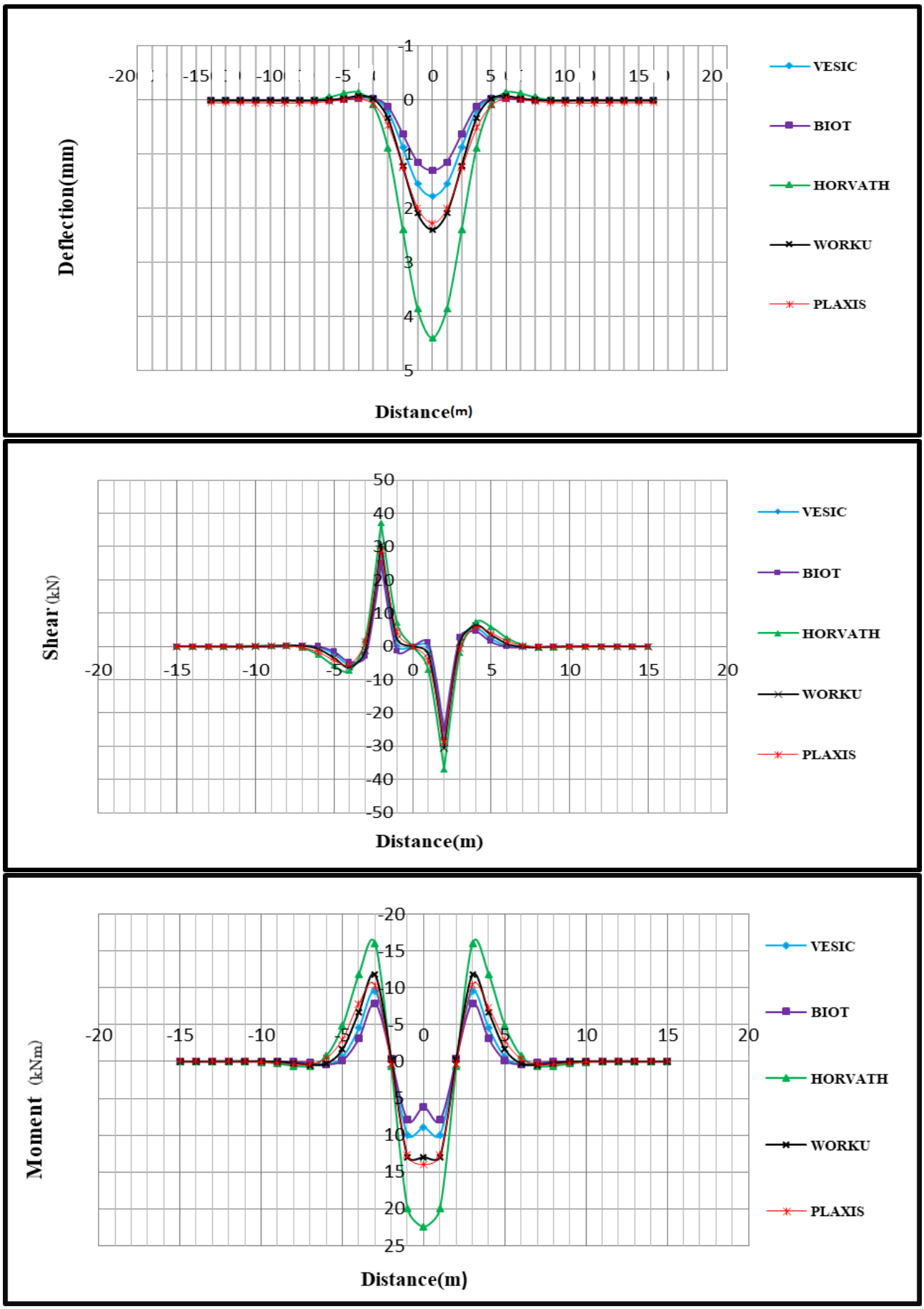

Figure 3.38: Infinite beam resting on hard/dense soil subjected to a uniformly distributed load on a single- parameter subgrade model

A review of the curves reveals a number of significant observations:

- The deflection obtained by Worku model is in a very good agreement with the FE based Plaxis 2D model throughout the beam span.
- Horvath subgrade model shows the highest deviation and moment compared to the other models.
- Shear is not affected in comparison to the deflection and moment.

Infinite beam subjected to a Uniformly distributed load on a two-parameter subgrade model

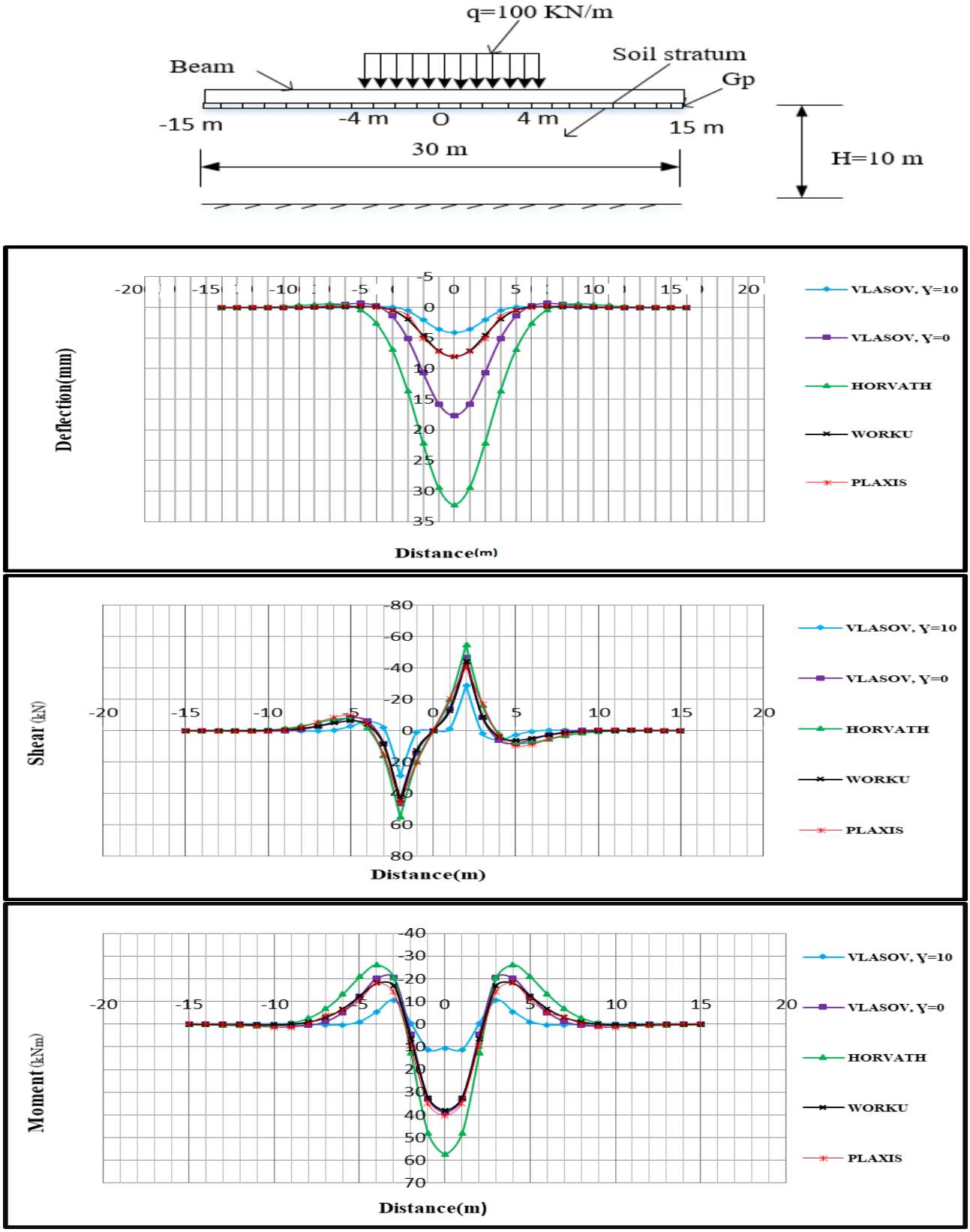

Figure 3.39: Infinite beam resting on loose/soft soil subjected to a uniformly distributed load on a two- parameter subgrade model

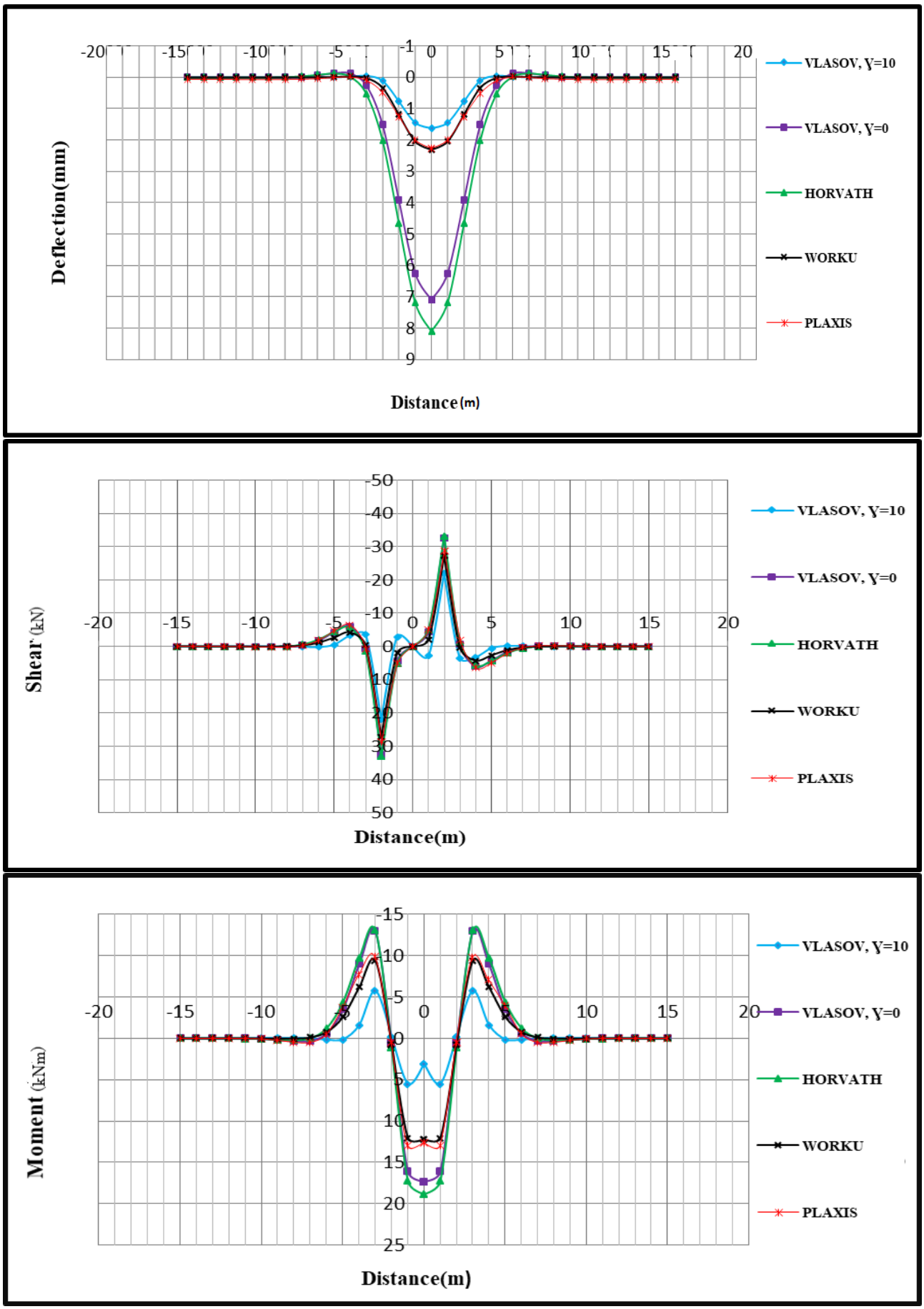

Figure 3.40: Infinite beam resting on hard/dense soil subjected to a uniformly distributed load on a two- parameter subgrade model

A review of the curves reveals a number of significant observations:

- Deflection shows deviation near the mid-span and much better beyond.
- The deflection obtained by Worku model is in a very good agreement with the FE based Plaxis 2D model throughout the beam span.
- Vlasov subgrade model highly underestimates the deflection when $\gamma = 10$, in contrast to Horvath's model underestimates it significantly.
- Vlasov subgrade model has shown deflection, shear and moment variation compared to the other models when $\gamma = 10$.
- Vlasov's model overlaps with the generalized Kerr-Equivalent Pasternak model of Worku when $\gamma = 6$ and $\gamma = 5$ for loose and hard soil, respectively.

Infinite beam subjected to a combined load on a single-parameter subgrade model

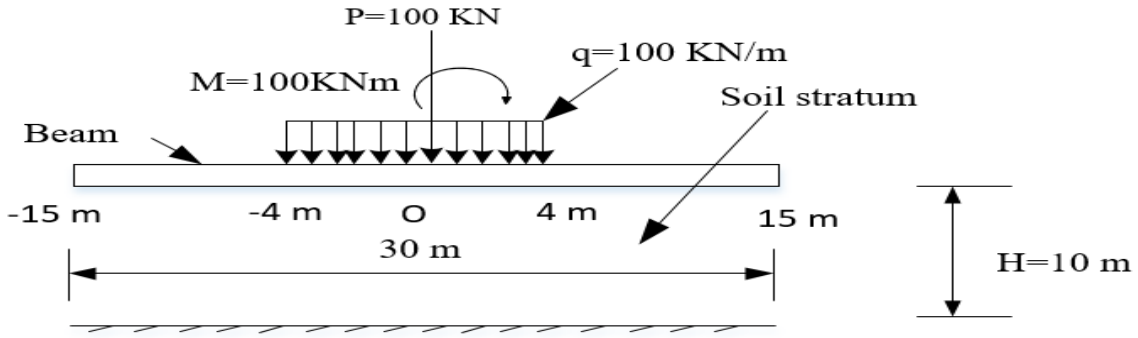

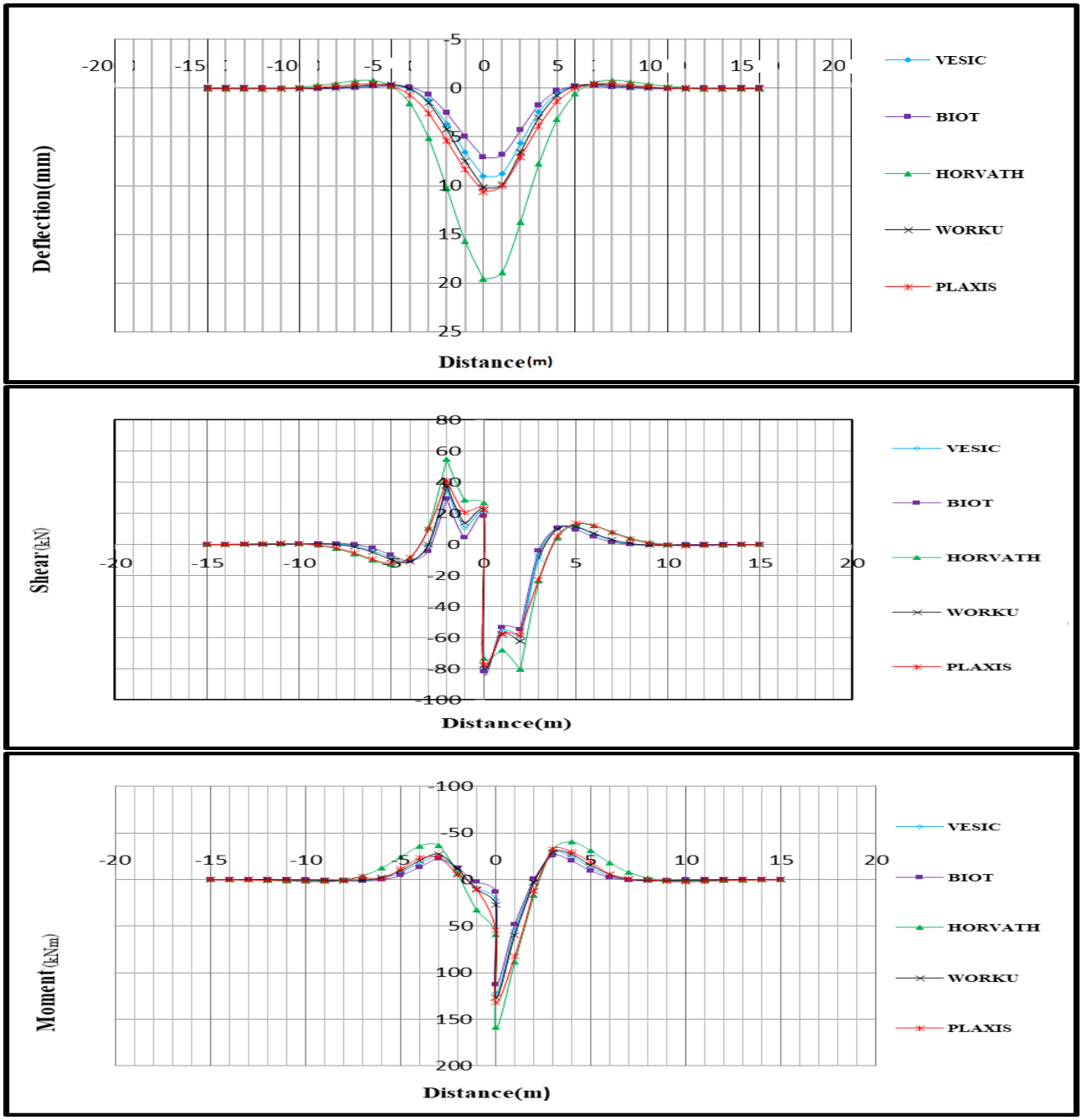

Figure 3.41: Deflection ,shear force and moment for the case of infinite beam resting on loose/soft soil subjected to a combined load in single parameter subgrade model

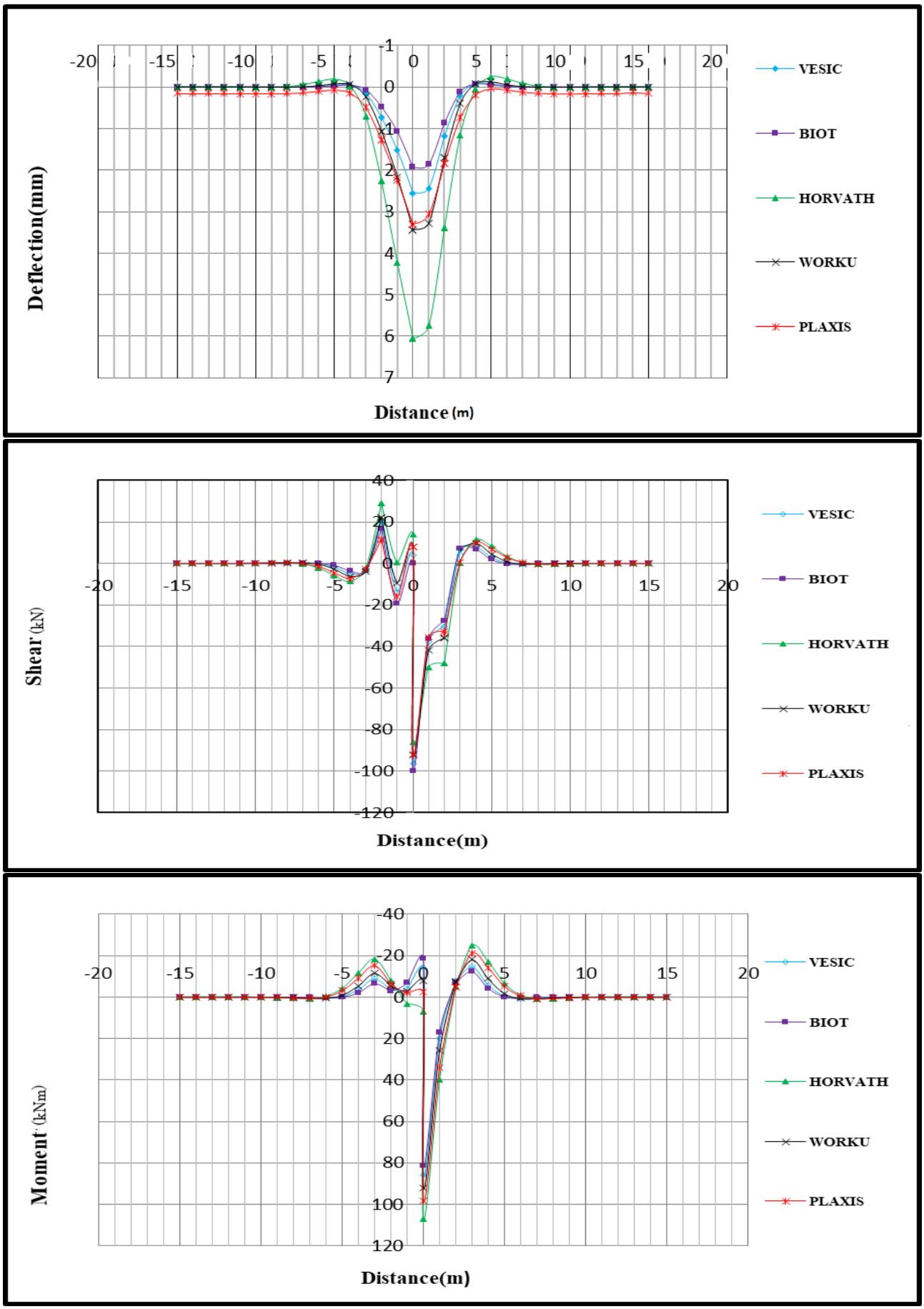

Figure 3.42: Infinite beam resting on hard/dense soil subjected to a combined load on a single-parameter subgrade model

A review of the curves reveals a number of significant observations:

- The deflection obtained by Worku model is in a very good agreement with the FE based Plaxis 2D model throughout the beam span.
- In the particular case of hard/dense soil FE based Plaxis 2D shows a variation outside the midspan deviation does not exceed 5%.
- Horvath's subgrade model gives the highest deflection compared to the other models.
- Shear and moment are not affected in comparison to the deflection.

Infinite beam subjected to a combined load on a two-parameter subgrade model

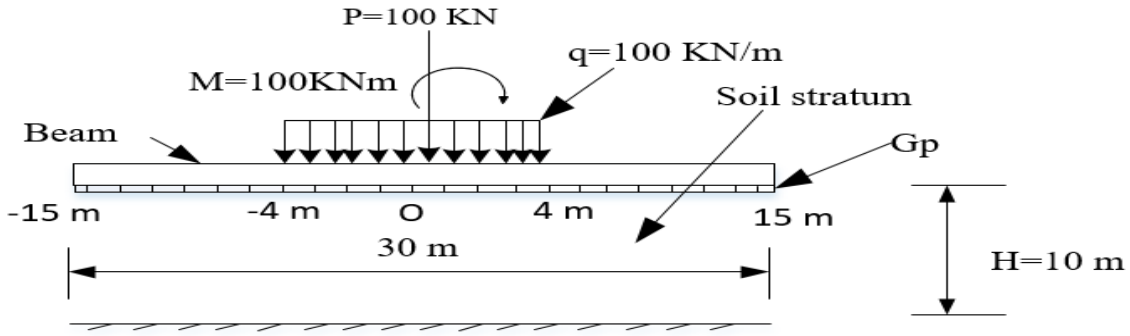

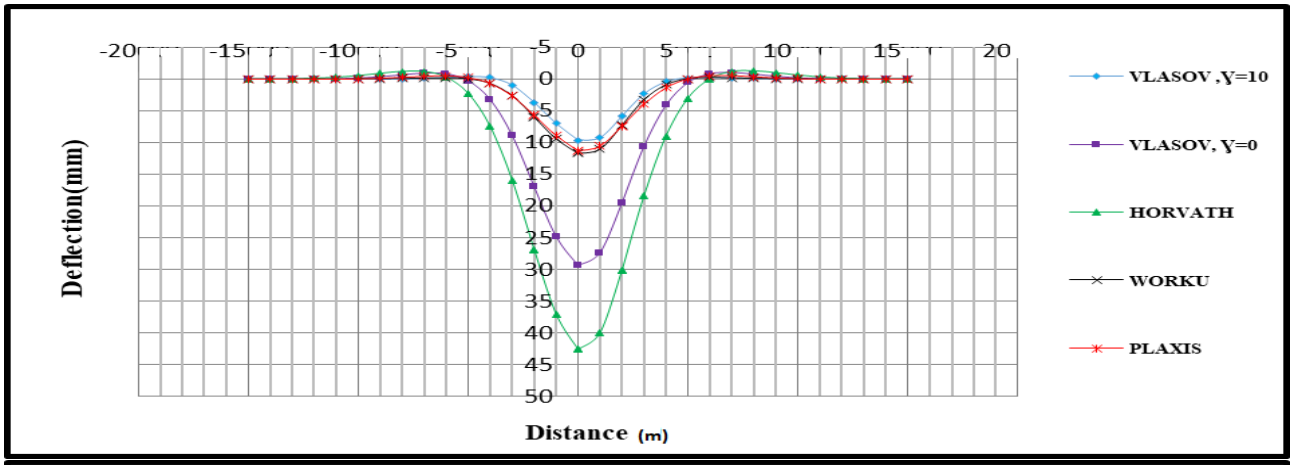

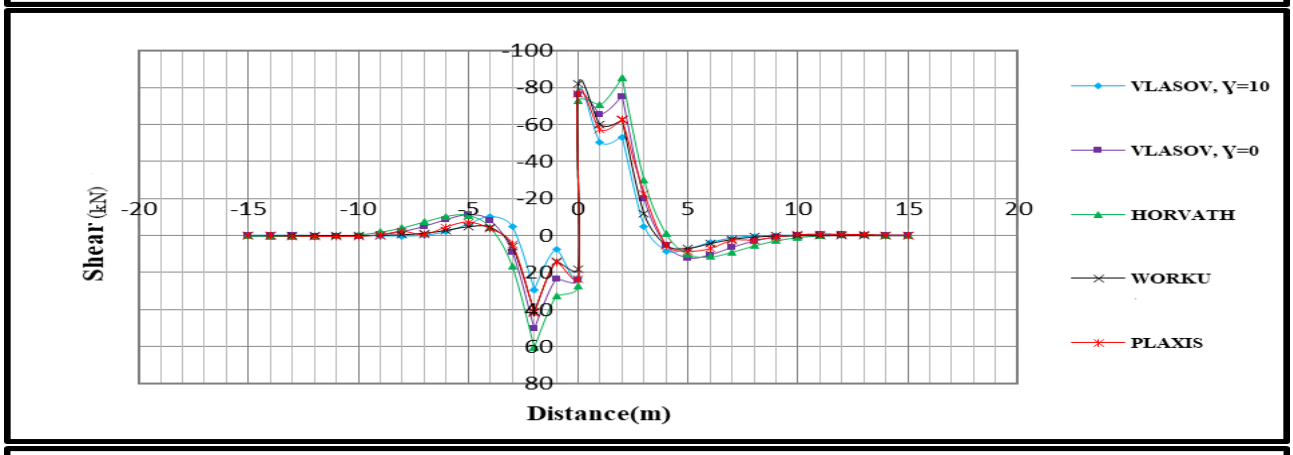

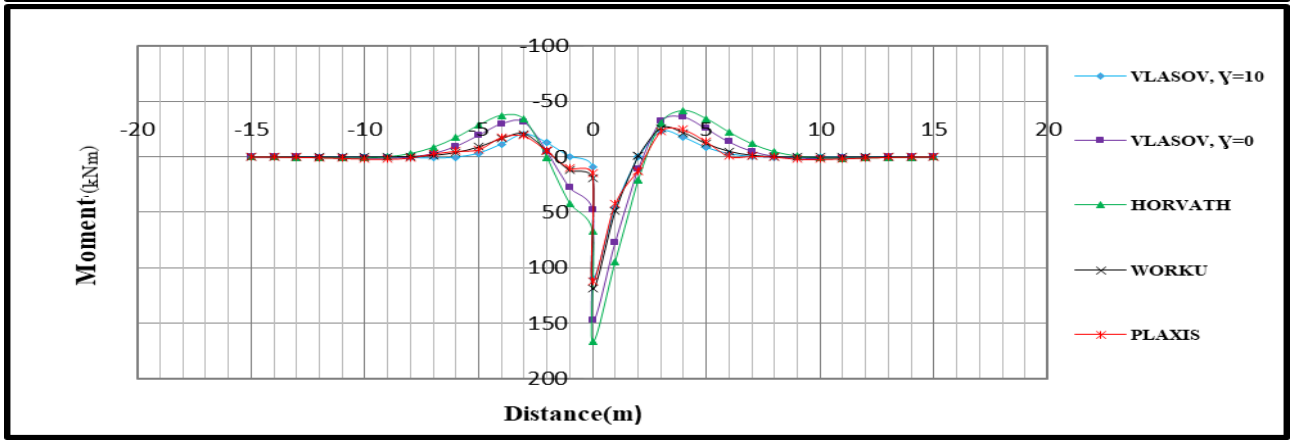

Figure 3.43: Infinite beam resting on loose/soft soil subjected to a combined load on a two-parameter subgrade model

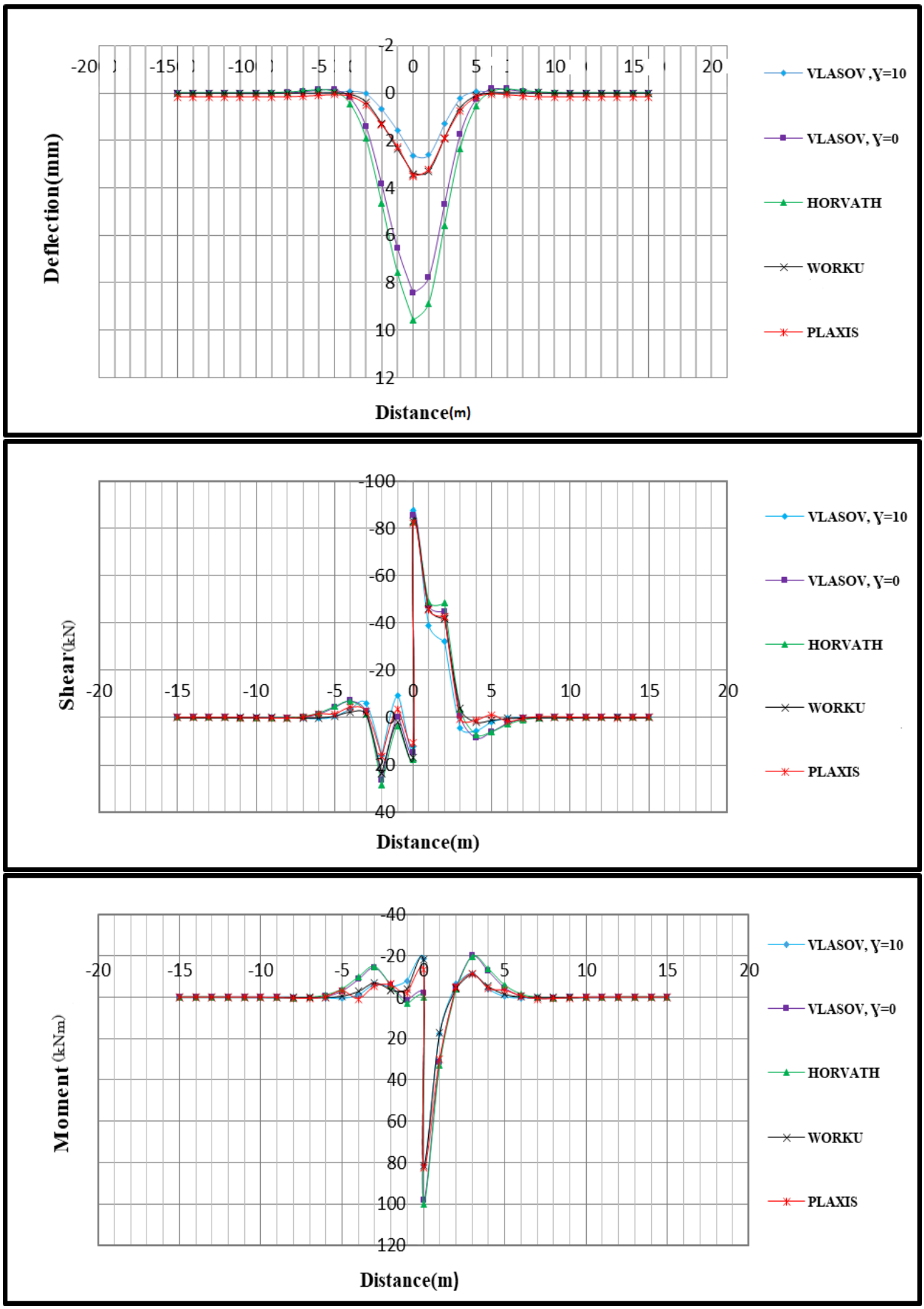

Figure 3.44: Infinite beam resting on hard/dense soil subjected to a combined load on a two -parameter subgrade mode

A review of the curves reveals a number of significant observations.

- Deflection shows deviation near the midspan and become less affected elsewhere.
- The deflection obtained Worku model is in a very good agreement with the FE based Plaxis 2D model throughout the beam span.
- In the particular case of hard/dense soil, FE based Plaxis 2D has shown a variation outside the mid-span deviation does not exceed 2.5%.
- Vlasov's subgrade model underestimates the deflection when $\gamma = 10$, compared to the other models.
- Vlasov's subgrade model has shown significant deviation deflection, shear and moment compared to the other models when $\gamma = 10$.
- Vlasov's model overlaps with the generalized Kerr-Equivalent Pasternak model of Worku when $\gamma = 4$ and $\gamma = 3$ for loose and hard soil, respectively.

The maximum deflection obtained by the two models of Worku is in a very good agreement with the FE based Plaxis 2D model. However, there is a modest deviation of deflection when moving away from the mid-span. This becomes more pronounced in the Winkler-Type model especially in hard/dense soils in both concentrated force and combined load cases. This is due to the fact that Winkler-Type model does not consider the shear interaction behavior of the soil from the outset despite the calibration. Additionally, because the calibration factor determined is solely dependent on the maximum deflection, it is not surprising to have deviations when moving away from this location.
Unlike the deflection, the bending moment and shear force show little deviation between the models and the Plaxis 2D outputs, in all cases of loading conditions. Furthermore, in the case of a concentrated vertical force, the shear force is invariably the same for all models at the mid-point. Furthermore, in the case of a concentrated moment, the bending moment is consistently the same for all models at the midpoint. This implies that midpoint span shear force and bending moment are independent of soil rigidity in the case of the concentrated force and bending moment, respectively. Biot's model consistently underestimates the response more than Vesic's model does.To be noted is that both vesic's and Biot's models were derived based on semi analytical studies on beams specifically with the objective to propose relationship for k_s while sticking to Winkler's model. On the other hand, Horvath's models (both single and two parameter) result in excessively overestimated response. These models are not recommended for practical use. In the case of Vlasov's model, its overall capacity to predict the soil-foundation response further depends on values of γ.

Table 3.5: γ values for infinite beam where Vlasov's model gives the closest result to Plaxis 2D and Worku's model

Load type	γ	
	Loose soil	Hard soil
Concentrated force	2.5	2
Concentrated moment	5	4
Combined loading	3	4
Uniformly distributed load Partially loaded	6	5

In general, the two-parameter Worku calibrated Kerr Equivalent Pasternak-type model gives more compatible results to the Plaxis 2D output than the Winkler-type model in all loading cases. The calibrated Winkler- type model of Worku has also performed quite well in many cases.

3.5 Finite Beams

Numerical computations for a finite beam subjected to a concentrated vertical force, a concentrated moment, and uniformly distributed load are carried out for different types of soils. Subsequently, the results obtained from single-parameter and two-parameter subgrade models and Finite Element based Plaxis 2D model are compared. The input parameters are given below.

Excel Program Input Parameters:

A) Beam Properties (Concrete)

- Elastic modulus of the beam (E_c) =30 GPa
- Width of the beam (B) = 0.3 m
- Depth of the beam (d) =0.3m
- Poisson's ratio(υ_c) = 0.2
- Length of the beam (l)

Case 1 $\lambda l < 6$ for different soil-beam combinations $l = 2m$

Case 2 $\lambda l = 6$ for different soil-beam combinations $l = 4m$

B) Soil data taken from (Briaud ,2013).

- Stratum thickens H=10m for all types of soil
- Hard/Dense Soil

i. Elastic modulus of the soil (Es) = 110MPa

ii. Poisson's ratio (υ) = 0.25

- Soft/ Loose Soil

i. Elastic modulus of the soil (Es) = 20MPa

ii. Poisson's ratio (υ) = 0.35

C) Loading Conditions

i. Vertical Concentrated force

- P=100 kN

ii. Concentrated moment

- M=100 kNm

iii. Uniformly distributed load

- q=100 kN/m , Loaded region 2m and 4m

Finite Element (Plaxis 2D) Inputs

(a) Rough foundation soil interaction ($R_{inter} = 1$)

(b) Soil model

- Linear elastic model

(c) Material model for the beam

- Elastic model

(d) Mesh type

- Fine

Subgrade Models:

A) Single parameter subgrade models

- Biot
- Vesic
- Horvath
- Worku Winkler type

B) Two parameter subgrade models

- Vlasov

$$\begin{cases} \gamma = 0 \\ \gamma = 10 \end{cases}$$

- Horvath
- Worku Pasternak type model

The results of the deflection, moment and shear force are evaluated and presented graphically for a finite beam and soil parameters given above. Plaxis analysis sample output for different loadings are graphically presented in Annex C.

Finite beam subjected to a vertical concentrated force on single-parameter subgrade model

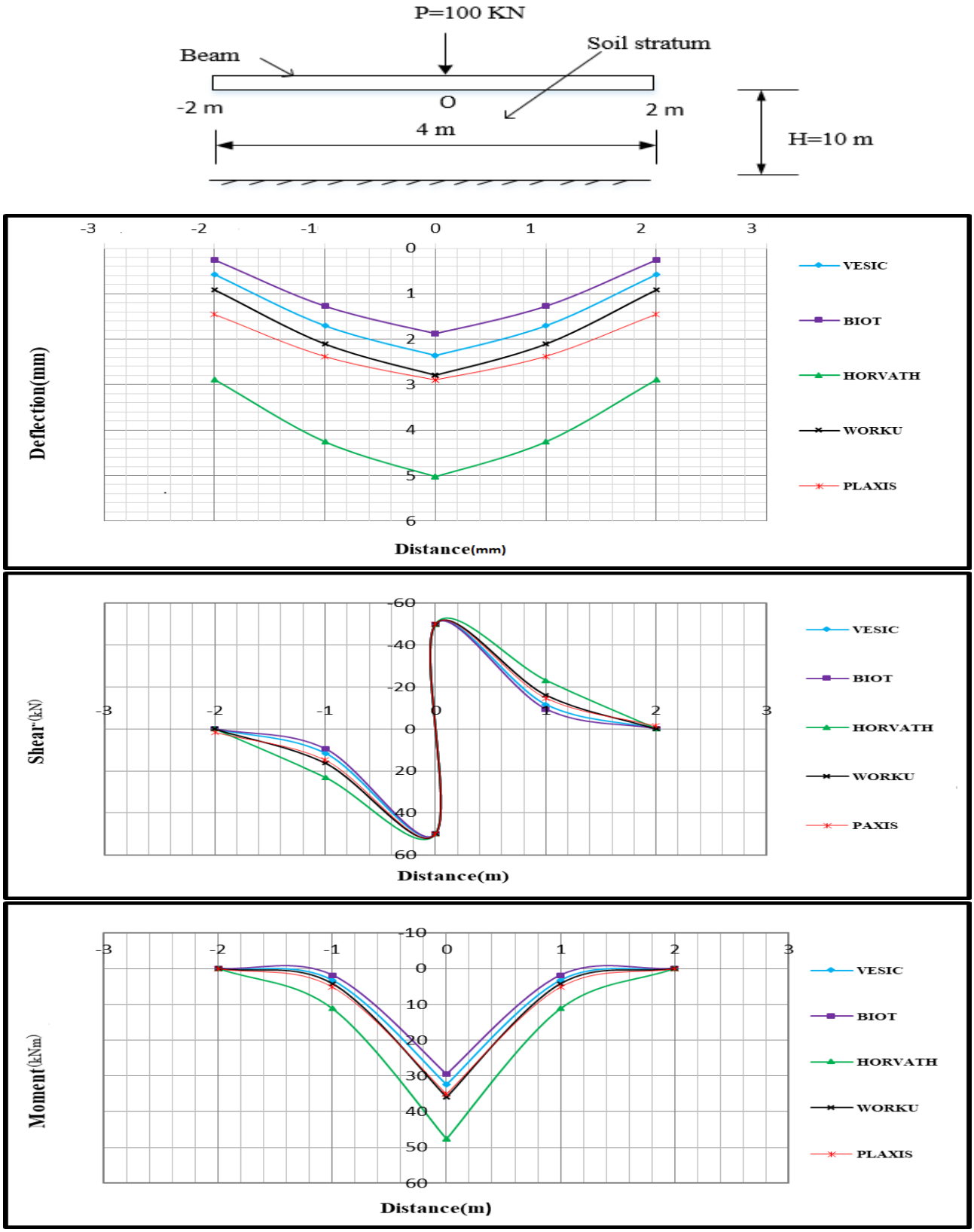

Figure 3.45: Finite beam resting on soft/loose soil subjected to a vertical concentrated force on a single-parameter subgrade model

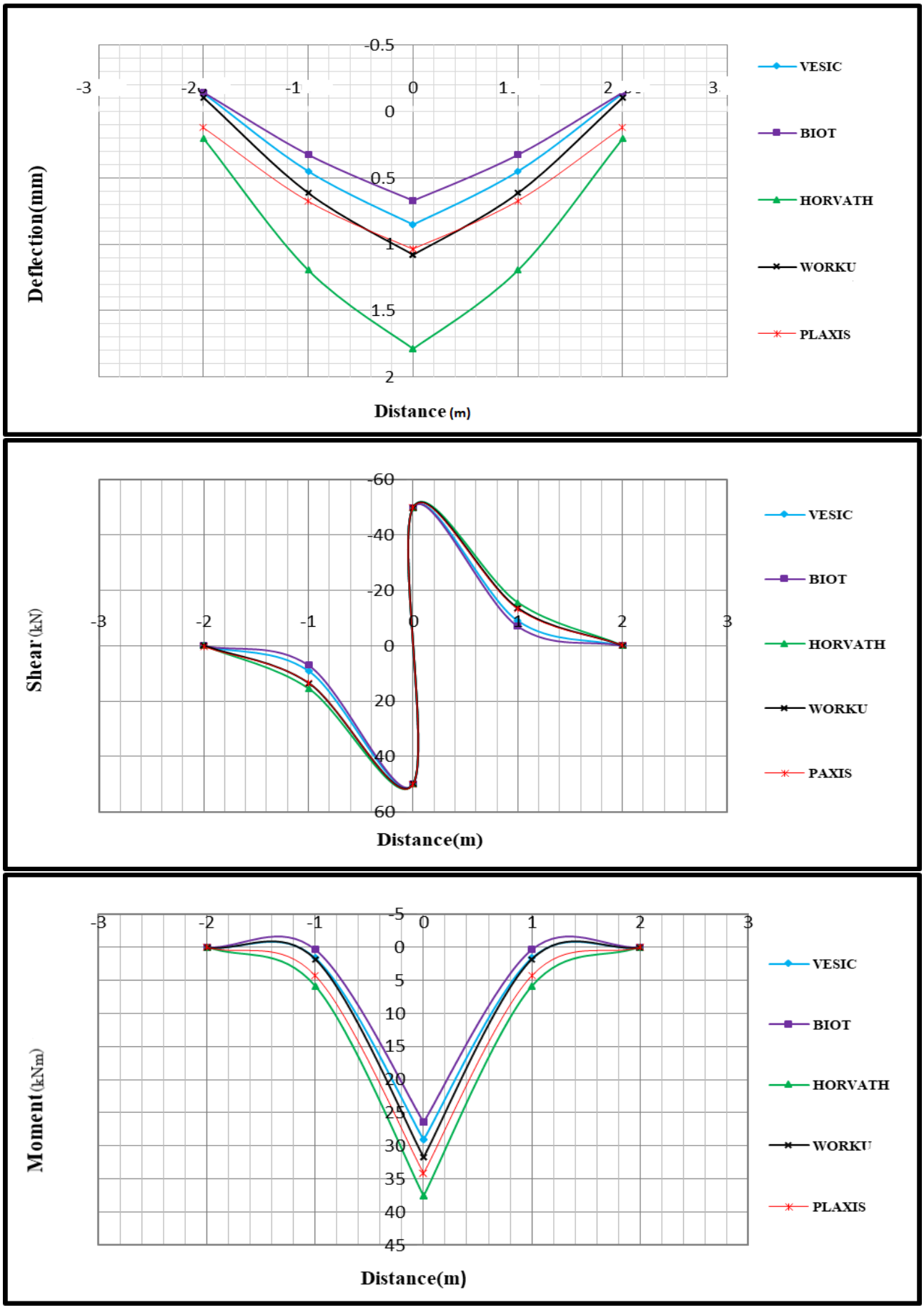

Figure 3.46: Finite beam resting on hard/dense soil subjected to a vertical concentrated force on a single-parameter subgrade model

A review of the curves reveals a number of significant observations:

- The maximum deflection obtained by Worku model is in a very good agreement with the FE based Plaxis 2D model. However, there is a deviation of deflection when moving away from the mid-span of the beam.
- Horvath subgrade model gives the highest deviations compared to the other models.
- Vesic and Biot subgrade models give a lower deflection value when compared to Plaxis 2D, this was not pronounced in the case of infinite beams.
- Shear and moment are least affected in comparison.

Finite beam subjected to a vertical concentrated force on a two-parameter subgrade model

case(a) $\lambda l = 6$

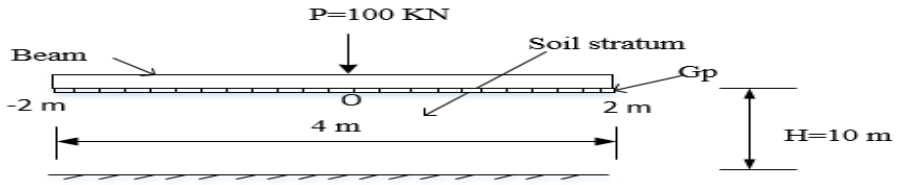

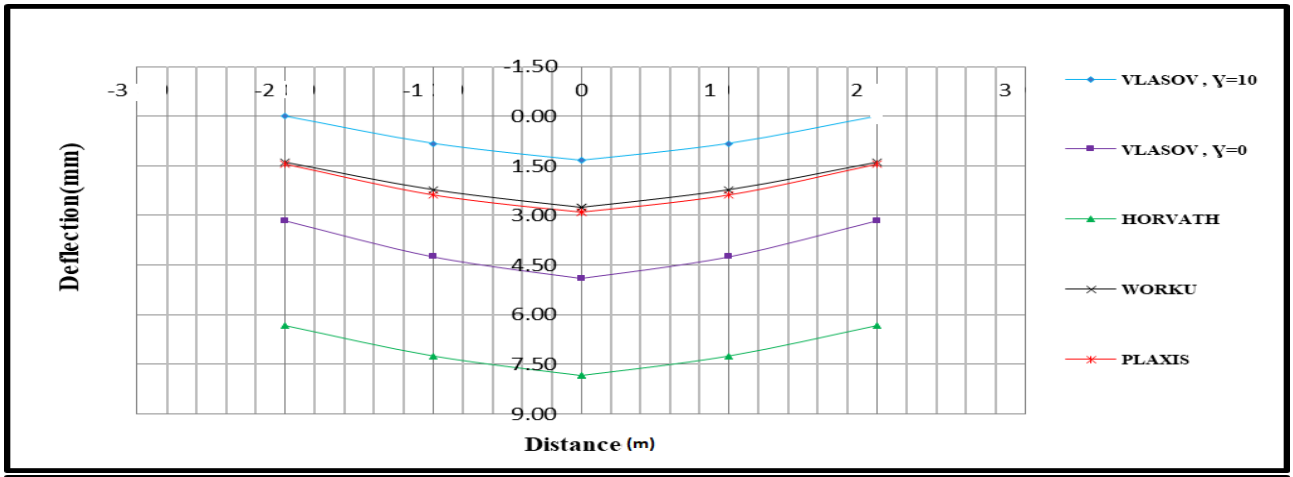

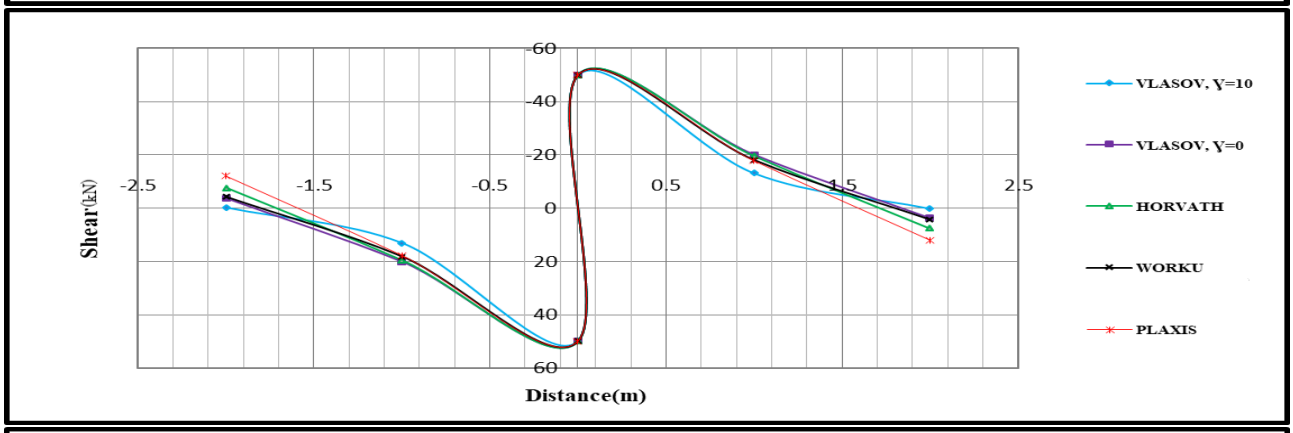

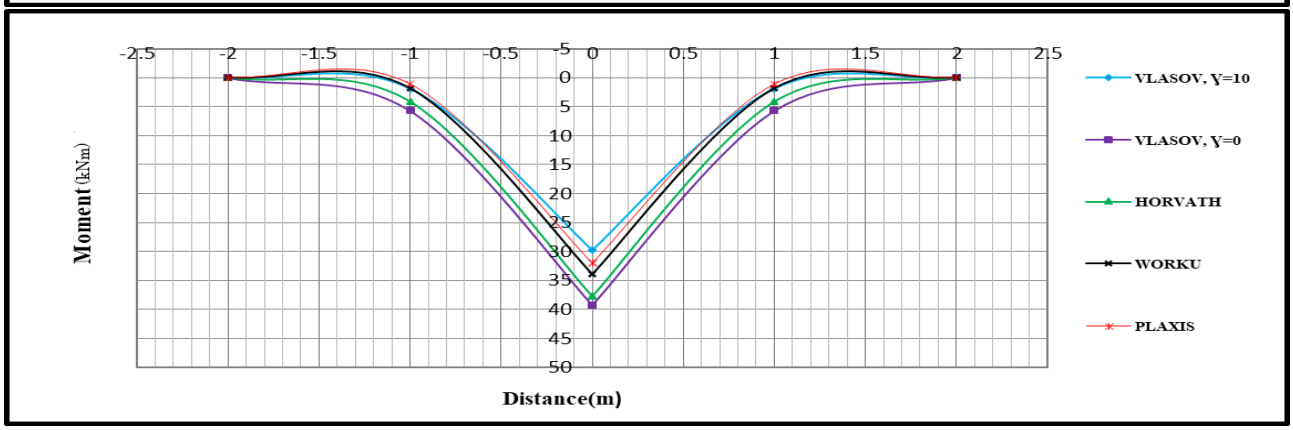

Figure 3.47: Finite beam resting on soft/loose soil subjected to a vertical concentrated force on a two-parameter subgrade model

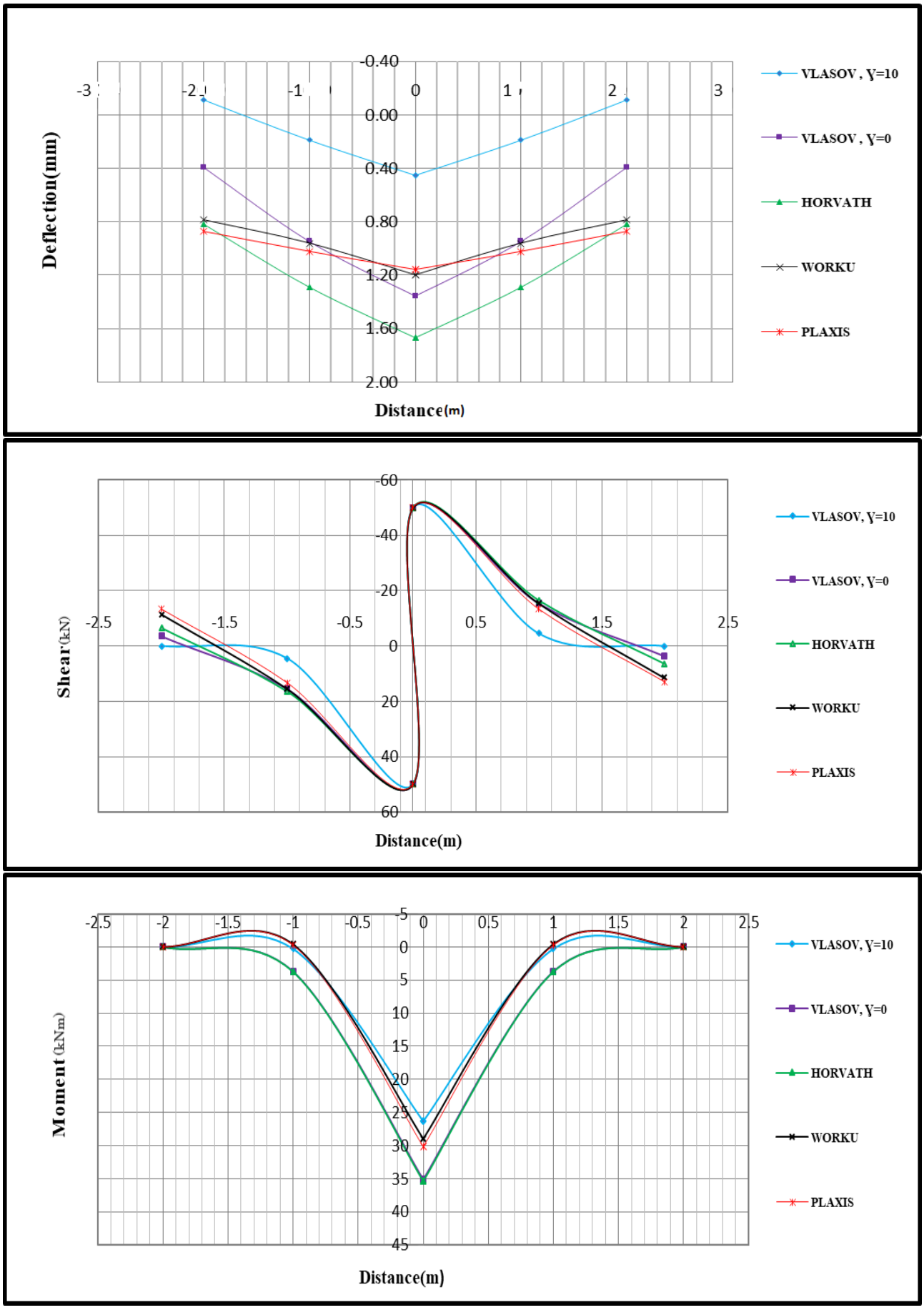

Figure 3.48: Finite beam resting on hard/dense soil subjected to a vertical concentrated force on a two-parameter subgrade model

A review of the curves reveals a number of significant observations:

- The deflection obtained by the calibrated model of Worku is in a very good agreement with the FE based Plaxis 2D model throughout the beam span.
- Vlasov's subgrade model underestimates the deflection when $\gamma = 10$, for $\gamma = 0$, the model gives deflection that deviate noticeably over the majority of the beam length.
- Vlasov subgrade model has shown deflection and shear variation compared to the other models when $\gamma = 10$.
- Horvath subgrade model gives the highest deflection and moment compared to other models.
- Vlasov's model overlaps with the generalized Kerr-Equivalent Pasternak model of Worku at $\gamma = 3.5$ and $\gamma = 2$ for loose and hard soil, respectively.

case(b) $\lambda l < 6$

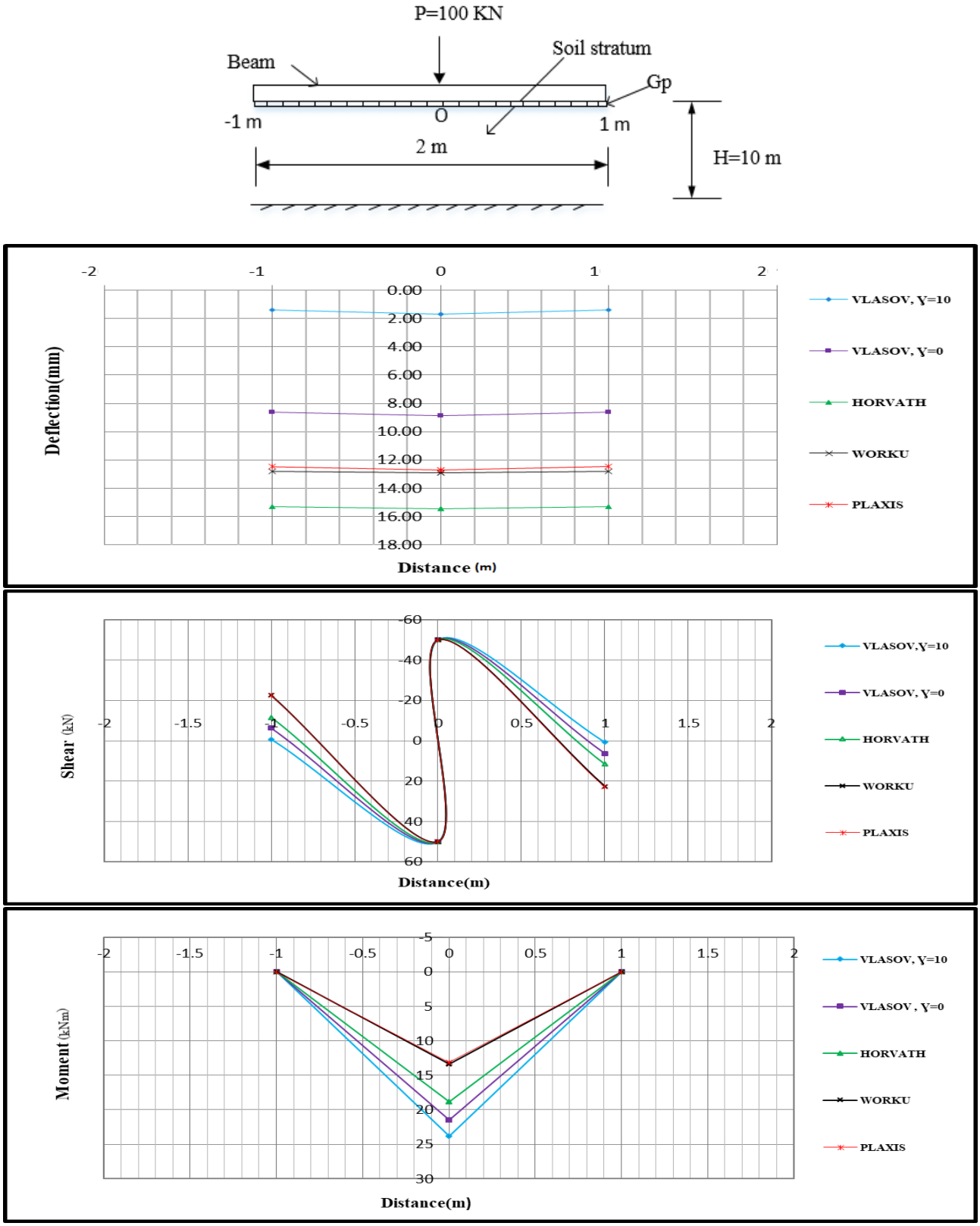

Figure 3.49: Finite beam resting on soft/loose soil subjected to a vertical concentrated force on a two-parameter subgrade model

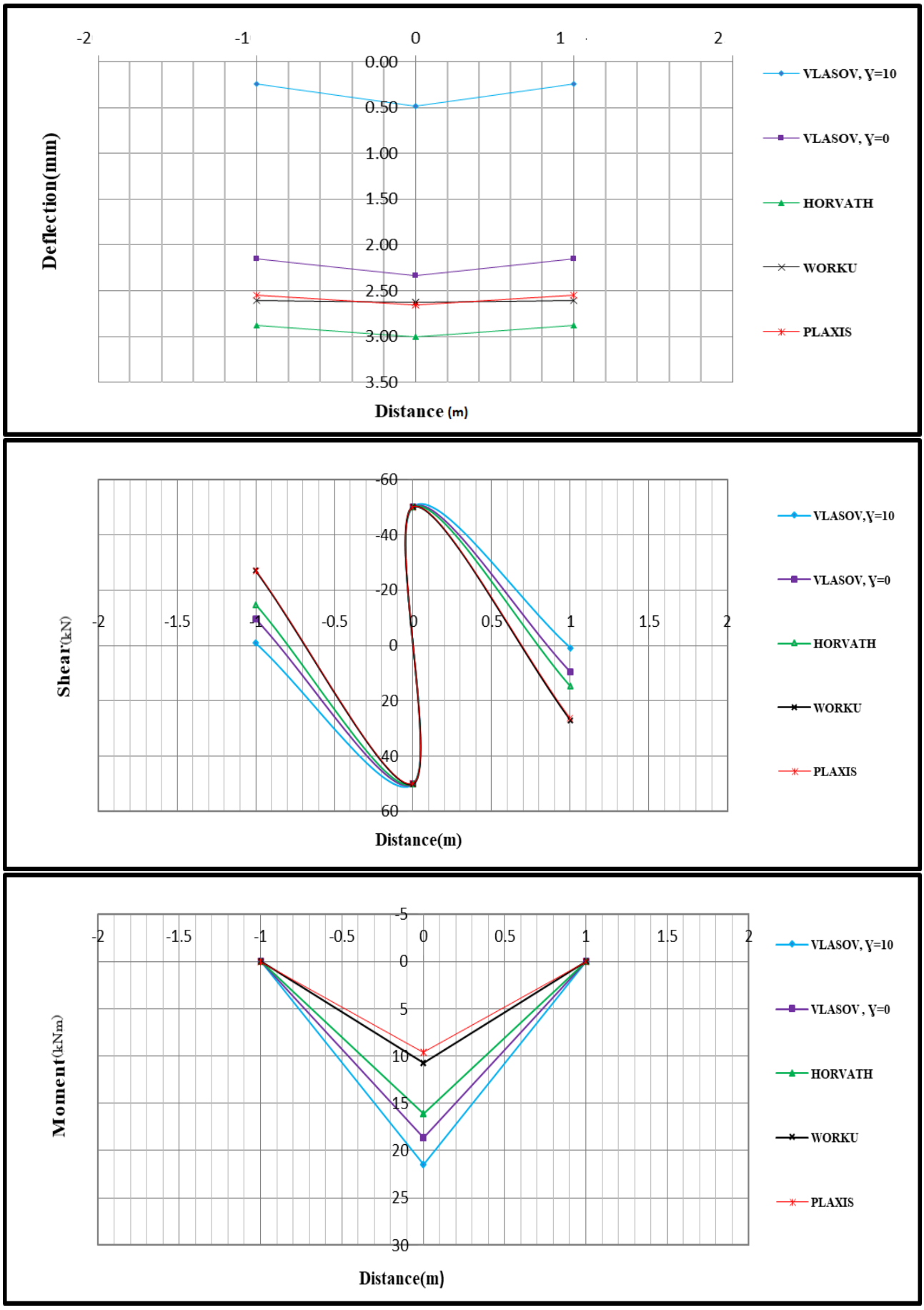

Figure 3.50: Finite beam resting on hard/dense soil subjected to a vertical concentrated force on a two-parameter subgrade model

A review of the curves reveals a number of significant observations:

- The deflection obtained by Worku model is again in a very good agreement with the FE based Plaxis 2D model throughout the beam span.
- Horvath subgrade model gives the highest deflection and moment compared to other models.
- Vlasov subgrade model underestimates the deflection in both values of γ compared to Plaxis 2D.

Comparison of case(a) with case(b) shows that when the length of the beam decreases maximum deflection and moment increases. Kerr-Equivalent Pasternak model of Worku is in a very good agreement with the FE based Plaxis 2D for both cases.In case(b) Vlasov's model underestimates the deflection for both γ values compared to the other models also, increasing value of γ make Vlasov's model further deteriorate the deflection.

Finite beam subjected to a Concentrated moment on a single-parameter subgrade model

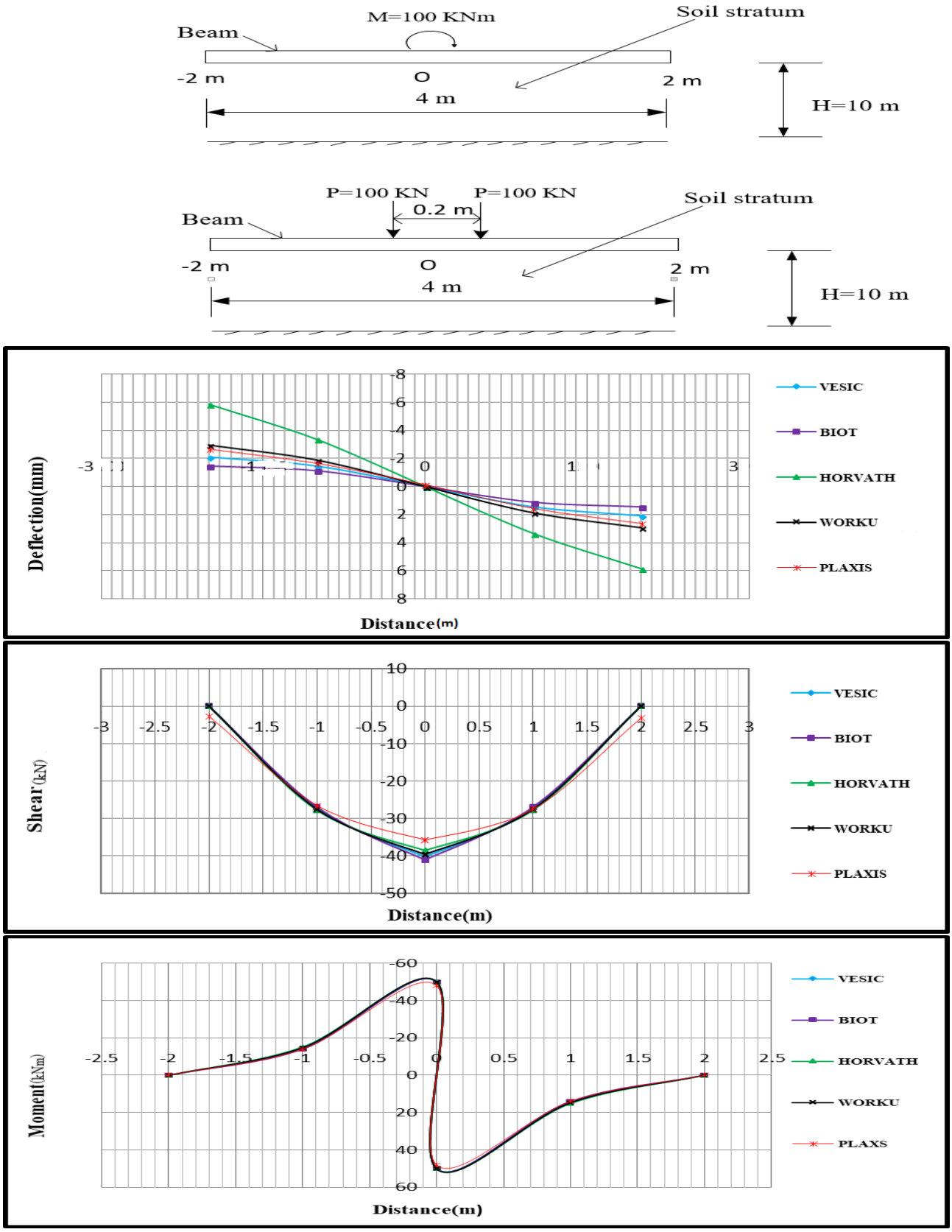

Figure 3.51: Finite beam resting on soft/loose soil subjected to a concentrated moment on a single-parameter subgrade model

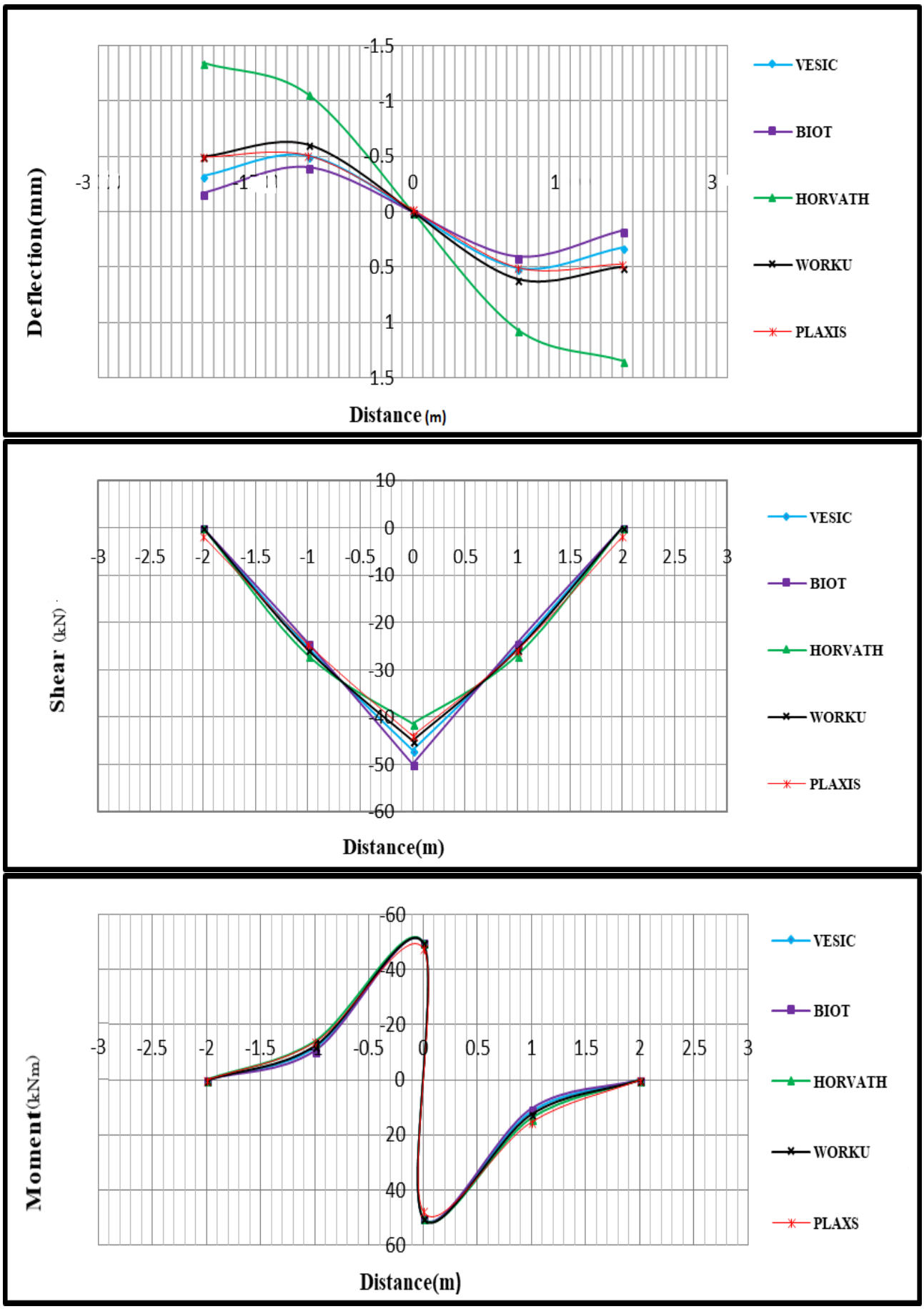

Figure 3.52: Finite beam resting on hard/dense soil subjected to a concentrated moment on a single-parameter subgrade model

A review of the curves reveals a number of significant observations:

- The deflection obtained by Worku model is in a very good agreement with the FE based Plaxis 2D model throughout the beam span.
- Horvath subgrade model gives the highest deflection and moment compared to the other models.
- Shear and moment are not affected in comparison to the deflection.

Finite beam subjected to a Concentrated moment on a two-parameter subgrade model

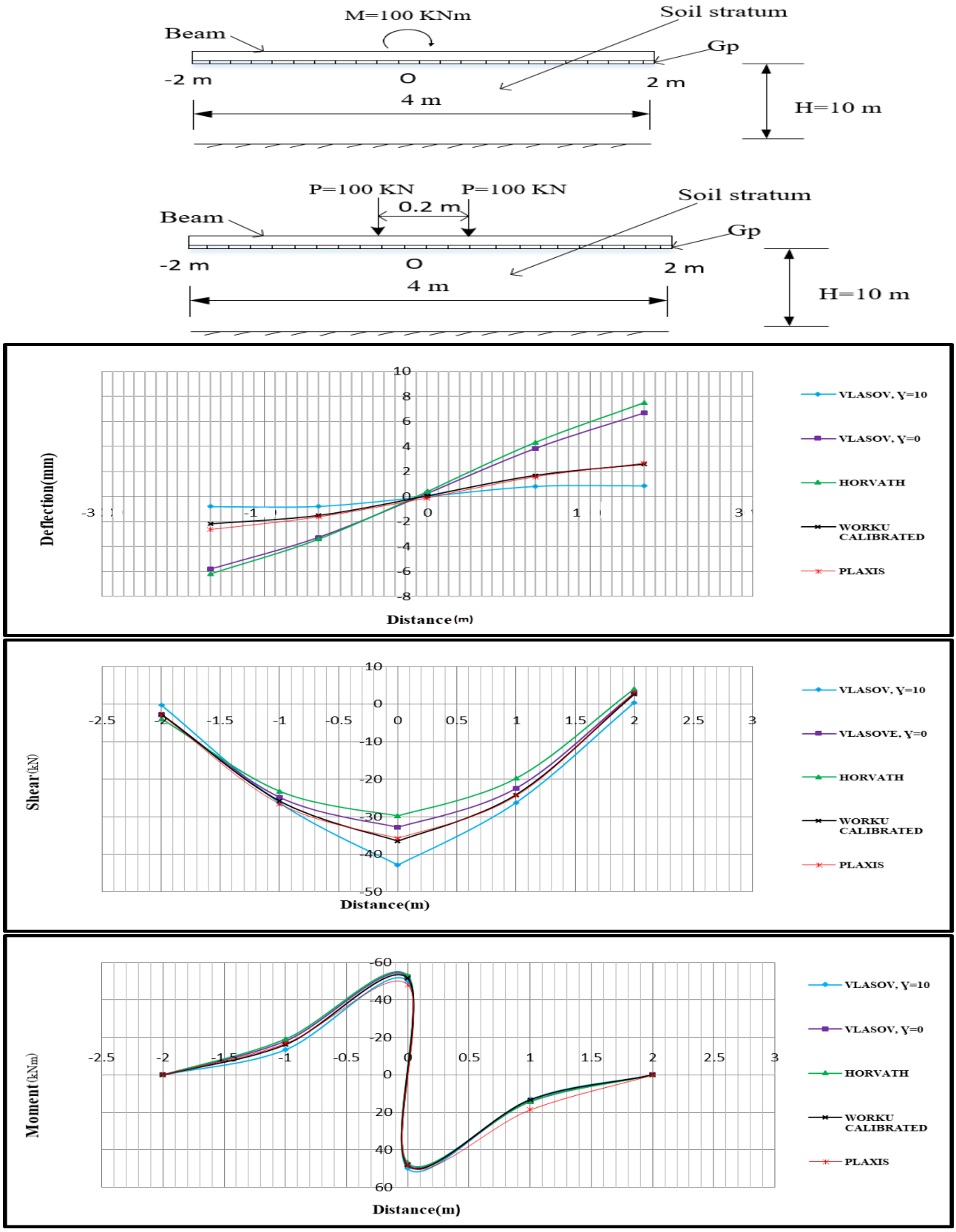

Figure 3.53: Finite beam resting on soft/loose soil subjected to a concentrated moment on a two-parameter subgrade model

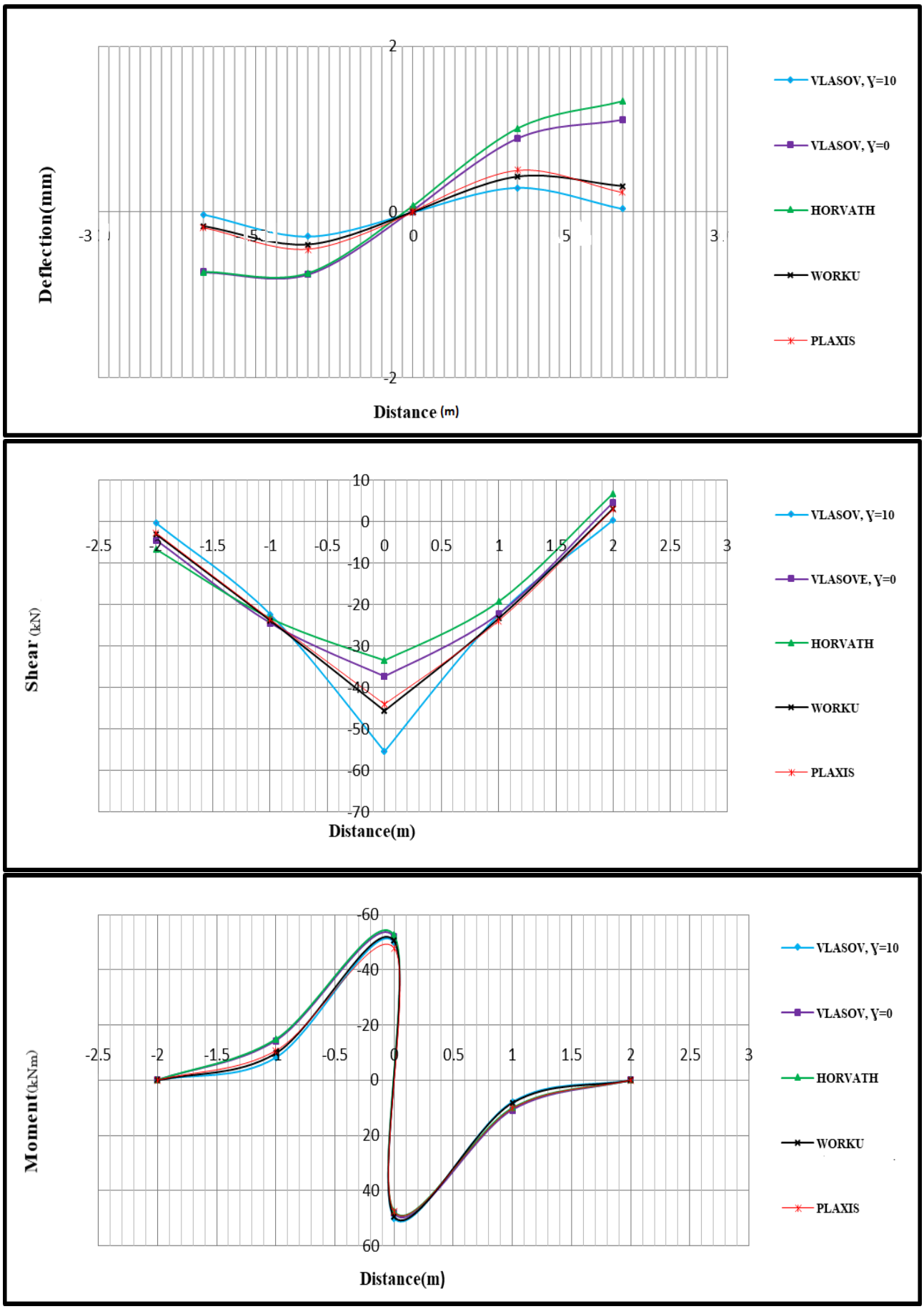

Figure 3.54: Finite beam resting on hard/dense soil subjected to a concentrated moment on a two-parameter subgrade model

A review of the curves reveals a number of significant observations:

- The deflection obtained by the calibrated model of Worku is once again in a good agreement with the FE based Plaxis 2D model throughout the beam span.
- Vlasov($\gamma = 0$) and Horvath subgrade models give the highest deflection compared to the other models.
- Moment is not affected in comparison to the deflection.
- Vlasov's model overlaps with the generalized Kerr-Equivalent Pasternak model of Worku when $\gamma = 5$ and $\gamma = 4$ for loose and hard soil, respectively.

Finite beam subjected to a Uniformly distributed load on a single-parameter subgrade model

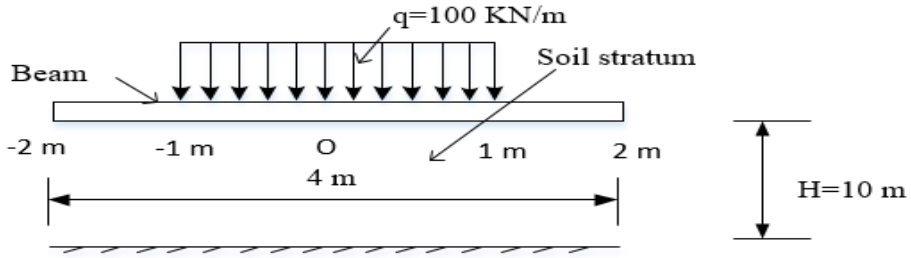

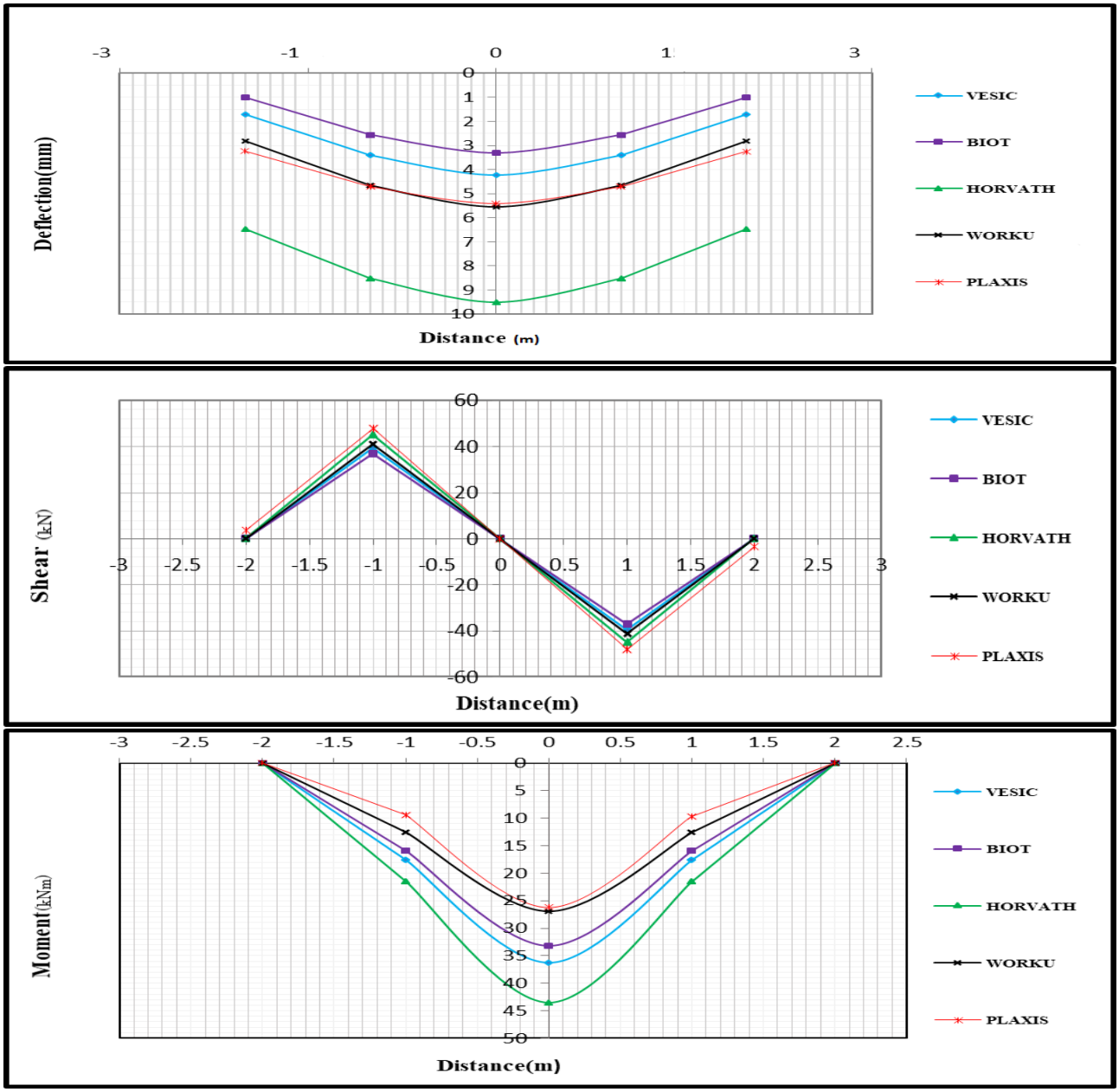

Figure 3.55: Finite beam resting on soft/loose soil subjected to a uniformly distributed load on a single-parameter subgrade model

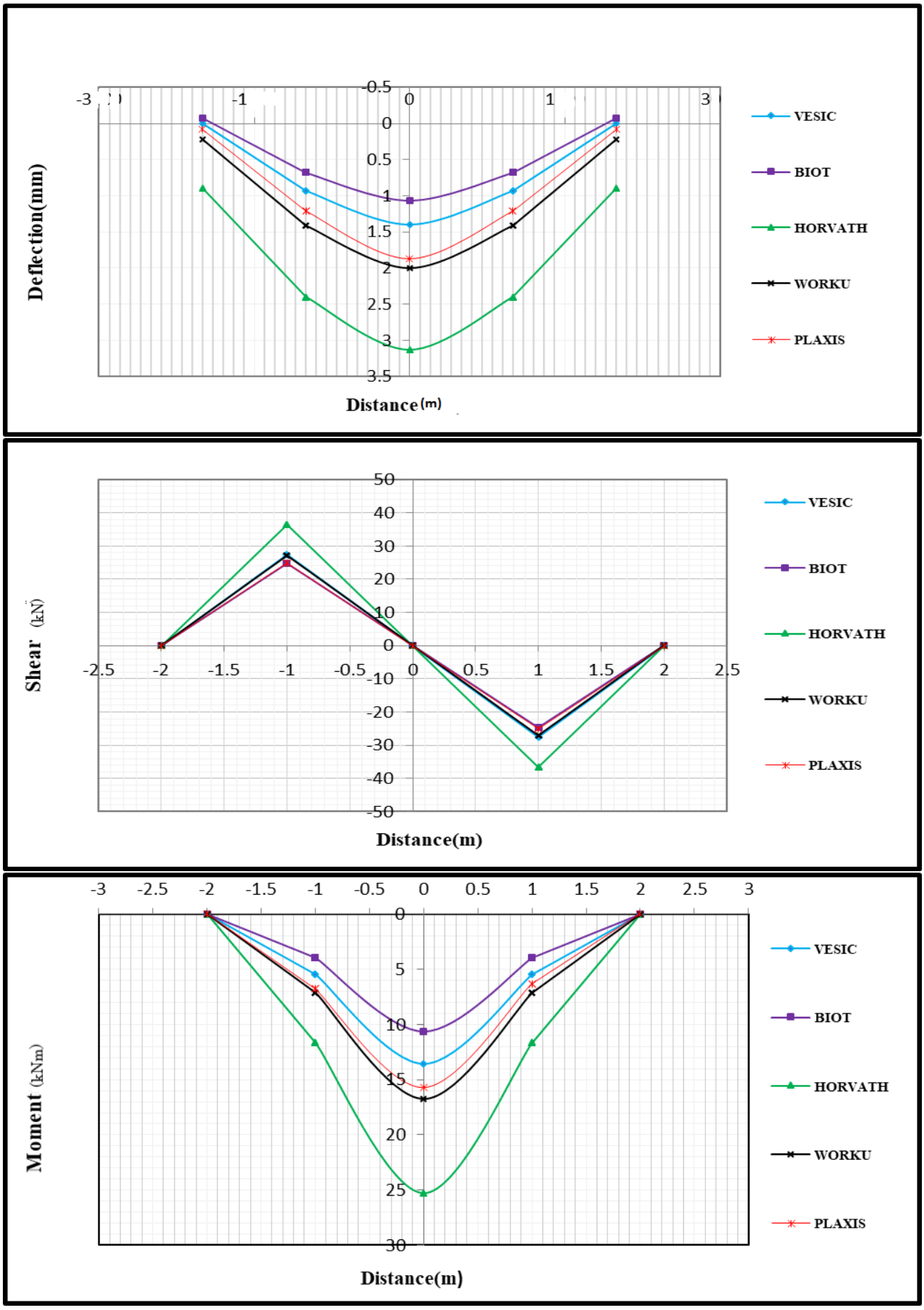

Figure 3.56: Finite beam resting on hard/dense soil subjected to a uniformly distributed load on a single-parameter subgrade model

A review of the curves reveals a number of significant observations:

- The deflection obtained by Worku model is in a very good agreement with the FE based Plaxis 2D model throughout the beam span.
- Horvath subgrade model gives the highest deflection and moment compared to the other models.
- Shear is not affected in comparison to the deflection and moment.

Finite beam subjected to a Uniformly distributed load on a two-parameter subgrade model

case(a) Loaded region=2m

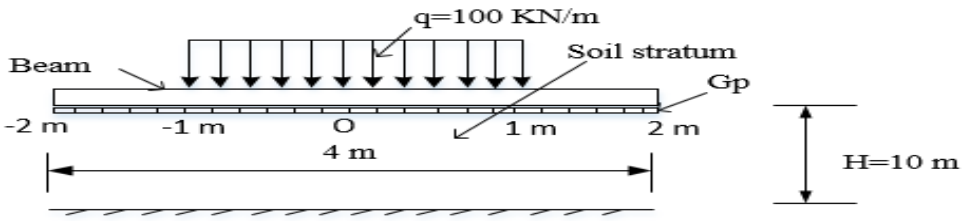

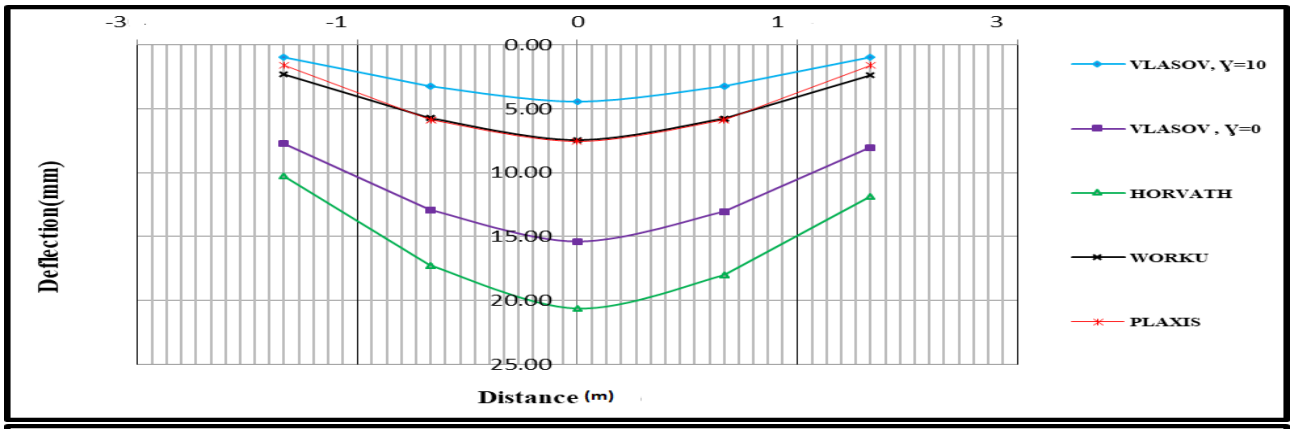

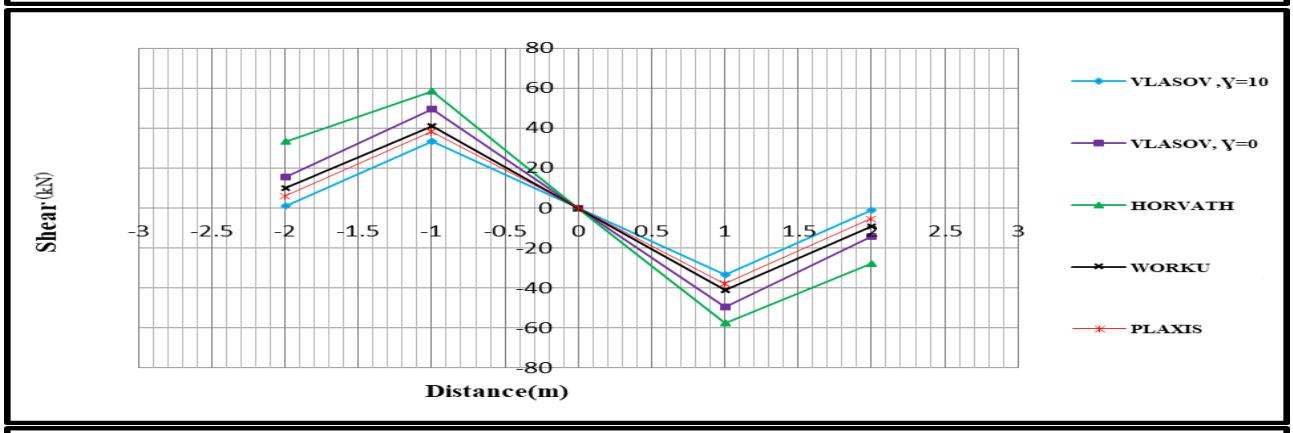

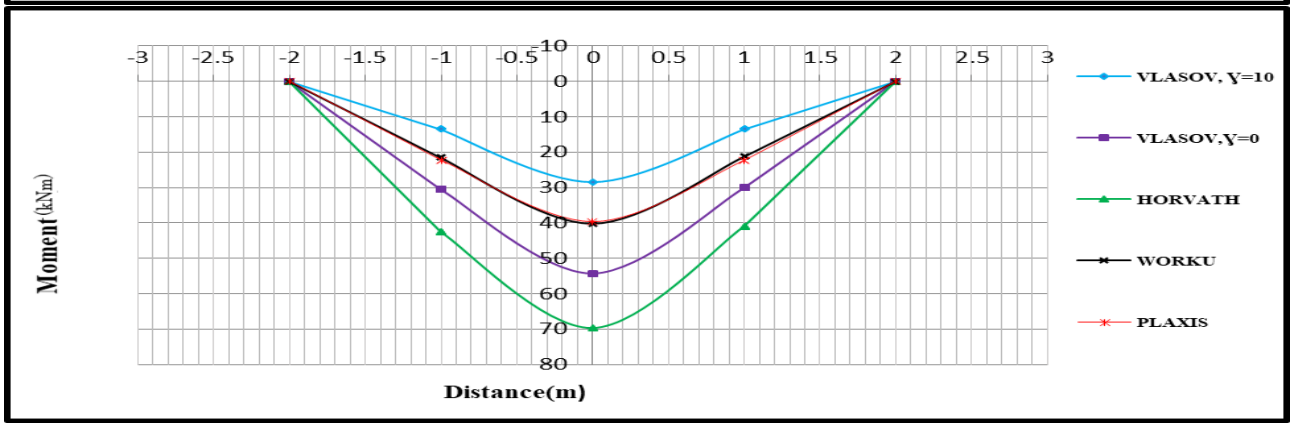

Figure 3.57: Finite beam resting on soft/loose soil subjected to a uniformly distributed load on a two-parameter subgrade model

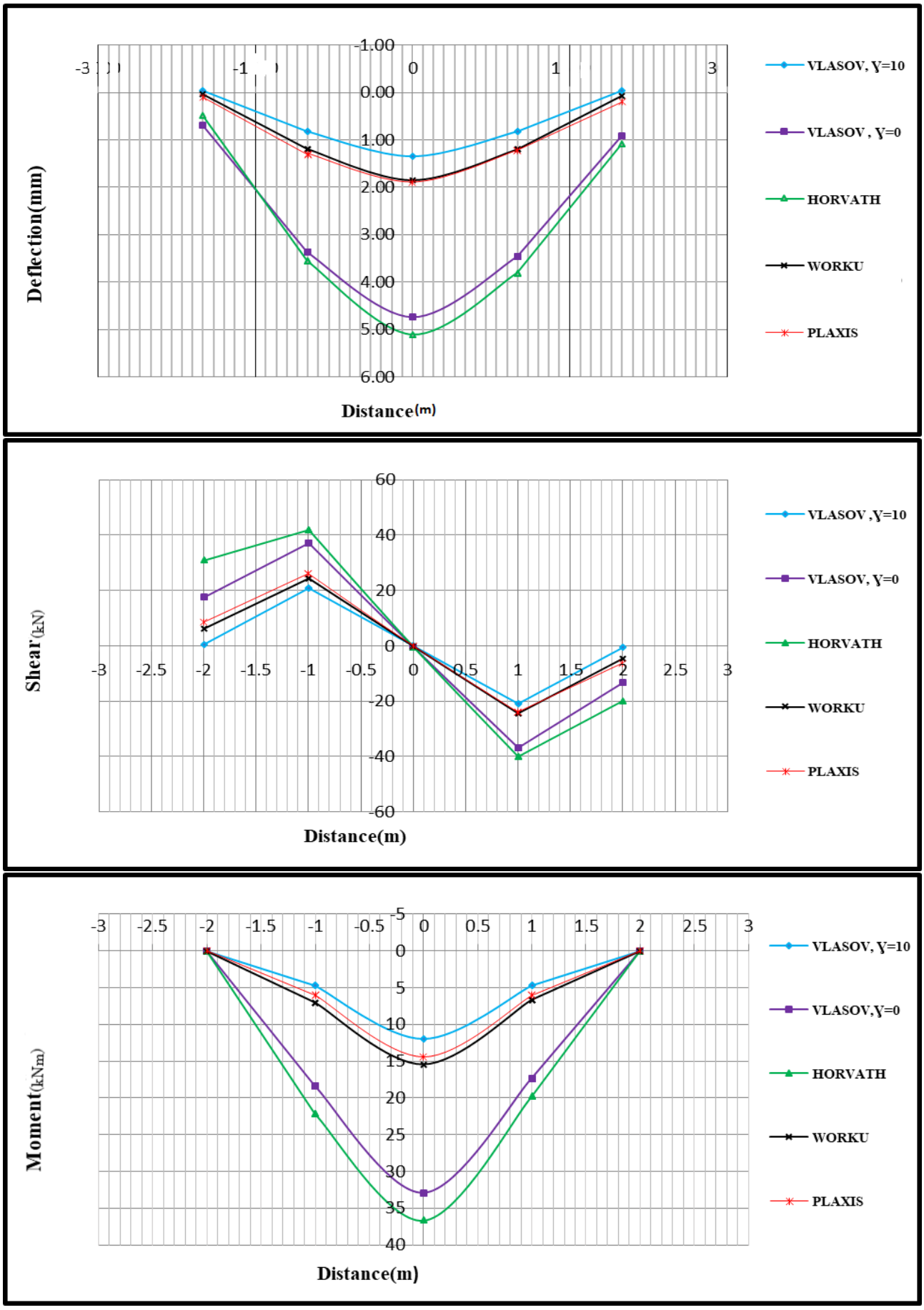

Figure 3.58: Finite beam resting on hard/dense soil subjected to a uniformly distributed load on a two-parameter subgrade model

A review of the curves reveals a number of significant observations:

- The deflection obtained by the calibrated model of Worku is in a very good agreement with the FE based Plaxis 2D model throughout the beam span.
- Horvath subgrade model gives the highest deflection and moment compared to the other models.
- Vlasov subgrade model underestimates the deflection when $\gamma = 10$,compared to the other models.
- Vlasov's model overlaps with the generalized Kerr-Equivalent Pasternak model of Worku when $\gamma = 6.5$ and $\gamma = 5$ for loose and hard soil, respectively.

case(b) Fully Loaded

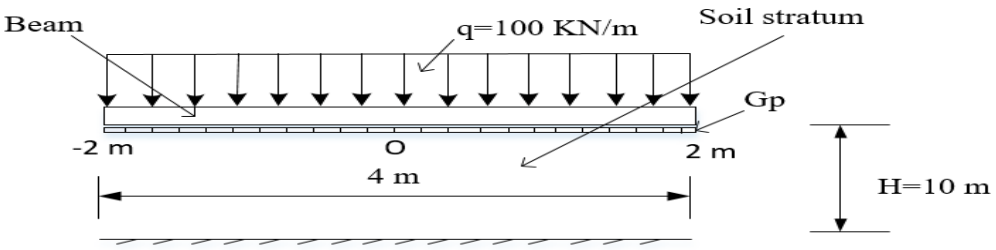

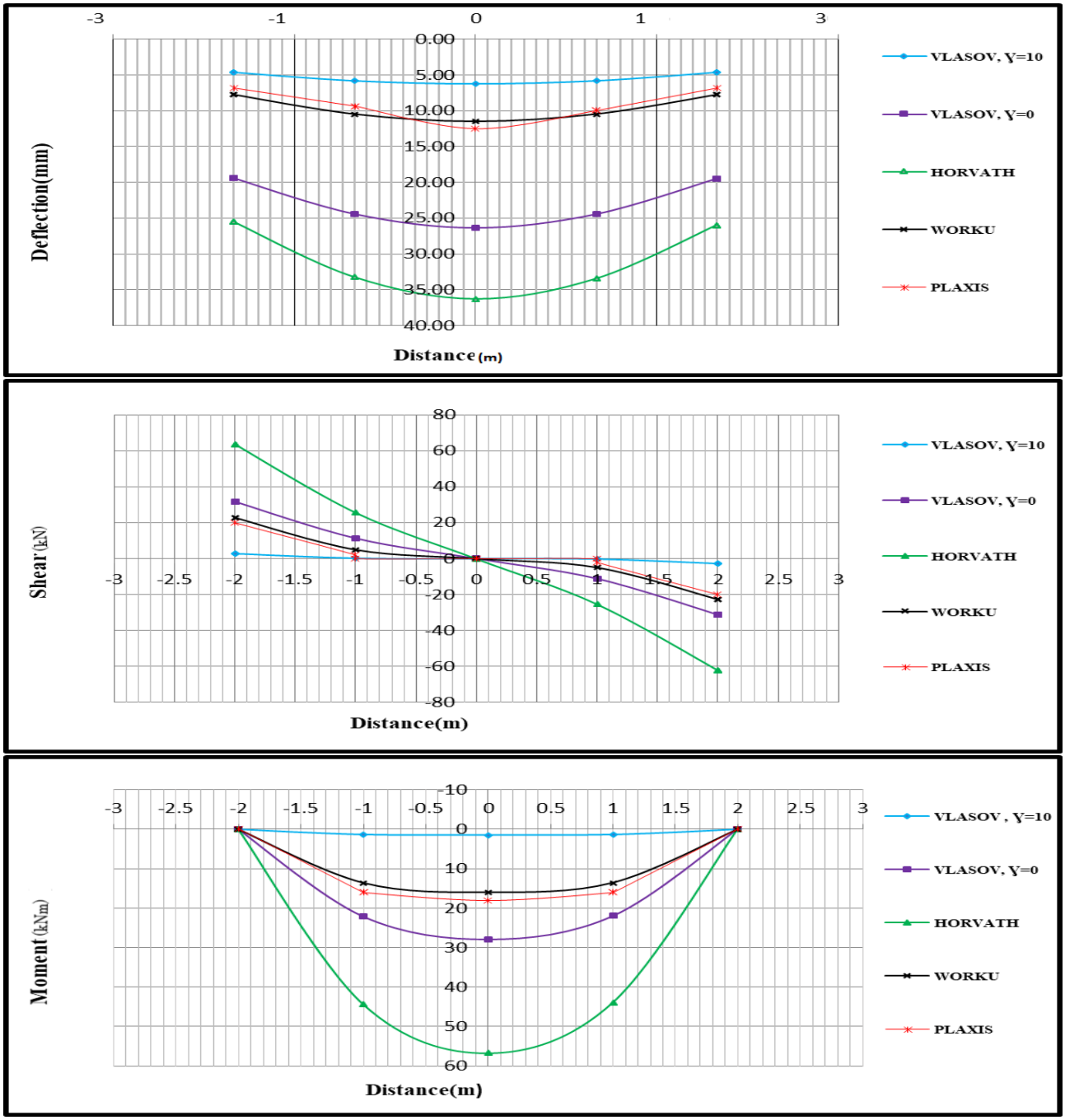

Figure 3.59: Finite beam resting on soft/loose soil subjected to a uniformly distributed load on a two-parameter subgrade model

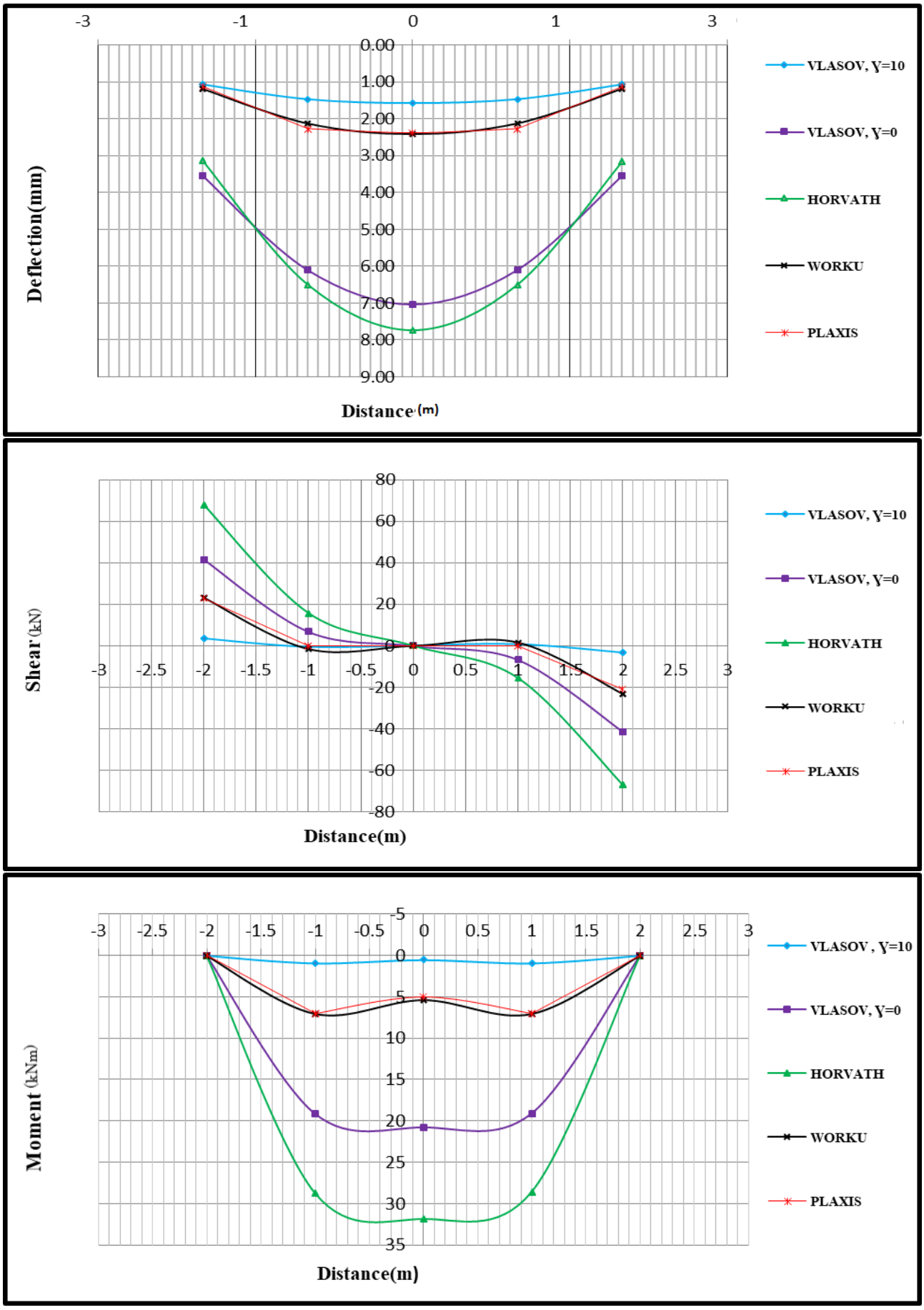

Figure 3.60: Finite beam resting on hard/dense soil subjected to a uniformly distributed load on a two-parameter subgrade model

A review of the curves reveals a number of significant observations.

- The deflection obtained by Worku model is in a good agreement with the FE based Plaxis 2D model throughout the beam span.
- Horvath subgrade model gives the highest deflection and moment compared to the other models.
- Vlasov subgrade model underestimates the deflection when $\gamma = 10$, compared to the other models.
- Vlasov's model overlaps with the generalized Kerr-Equivalent Pasternak model of Worku when $\gamma = 6$ and $\gamma = 5$ for loose and hard soil, respectively.

Comparison of case(a) with case(b) shows that Calibrated Kerr-Equivalent Pasternak model of Worku is in a good agreement with the FE based Plaxis 2D for both cases.

The maximum deflection obtained by the two models of Worku is in a very good agreement with the FE based Plaxis 2D model. Unlike single parameter models, Two-parameter models give a non-zero shear at the end of the beam. This is due to the shear continuity. Vlasov's model underestimates the short beam deflection for the entire range of γ in concentrated force case. Vlasov's model capacity to predict the soil-foundation response depends on values of γ employed. Vlasov's model underestimates the short beam deflection for the entire range of γ.

Table 3.6: γ values for finite beam where Vlasov's model gives the closest result to Plaxis 2D output

Load type	γ	
	Loose soil	Hard soil
Concentrated force		
$\lambda l = 6$	3.5	2
$\lambda l < 6$	0^*	0^*
Concentrated moment	6	4
Uniformly distributed load		
Fully loaded	6.5	5
Partially loaded	6	5

:- 0^* mean that Vlasov's model gives the closer result to Plaxis 2D and Worku's model when $\gamma = 0$ but steal-underestimate the deflection. The more increase the value of γ cause deflection more underestimated.
Comparison of Vlasov's model γ value given in Tables 3.5-3.6 to Worku's subgrade model

calibration factor given in Tables 3.3-3.4 show that the Worku's models calibration factor found in a small range.

3.6 Overall Comparison of Single and Two Parameter Subgrade Models

In this section cross comparison between both single and two parameter Worku's models, Vesic, Vlasov's model, and Plaxis 2D are made. Vlasov's model calibrated using different values of γ for a given loading case as presented in Tables 3.5-3.6. Vesic's model gives the closest results to Plaxis 2D and Worku's models, though it consistently yields smaller estimates of the deflection.

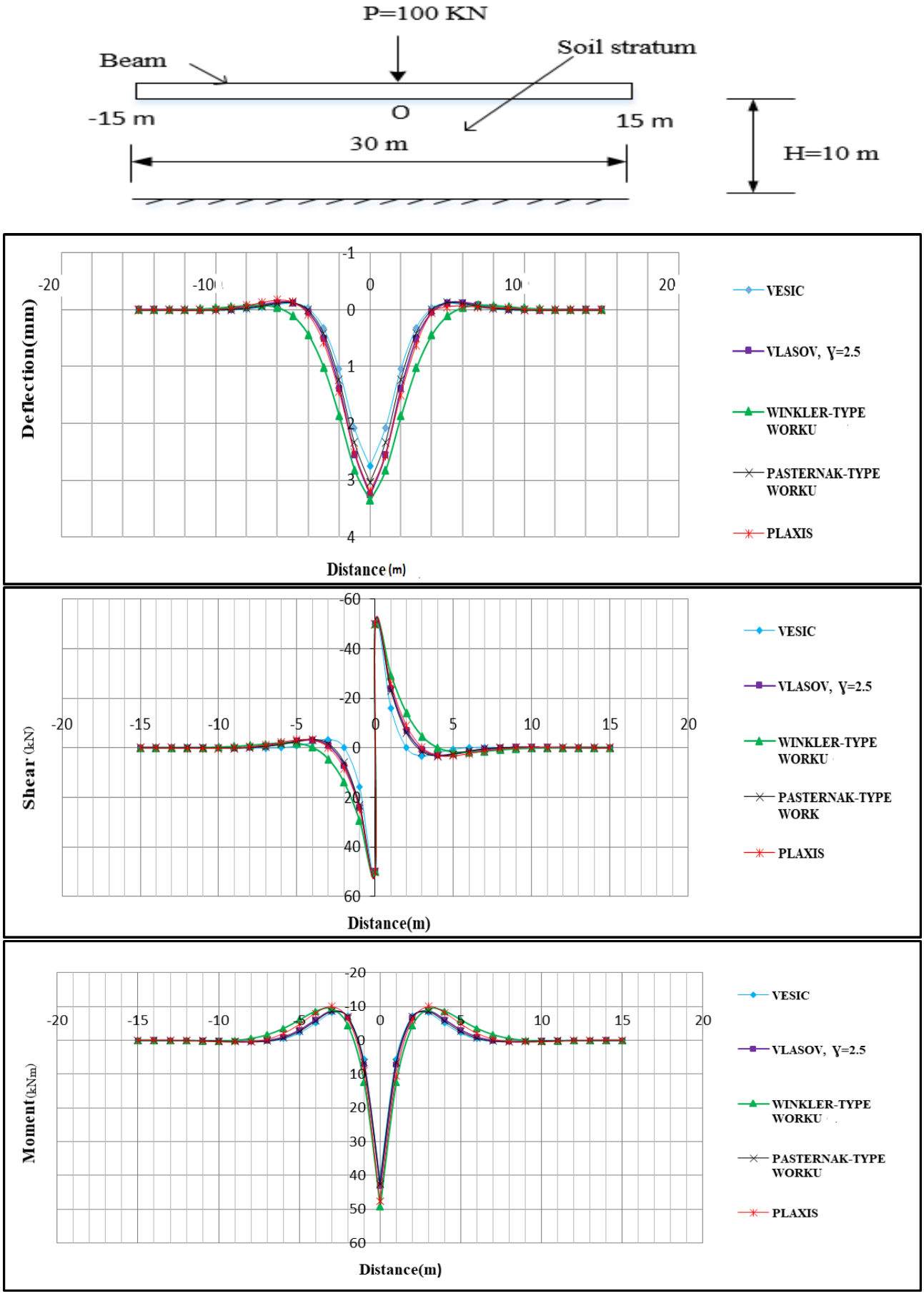

Figure 3.61: Infinite beam resting on soft/loose soil subjected to a vertical concentrated force

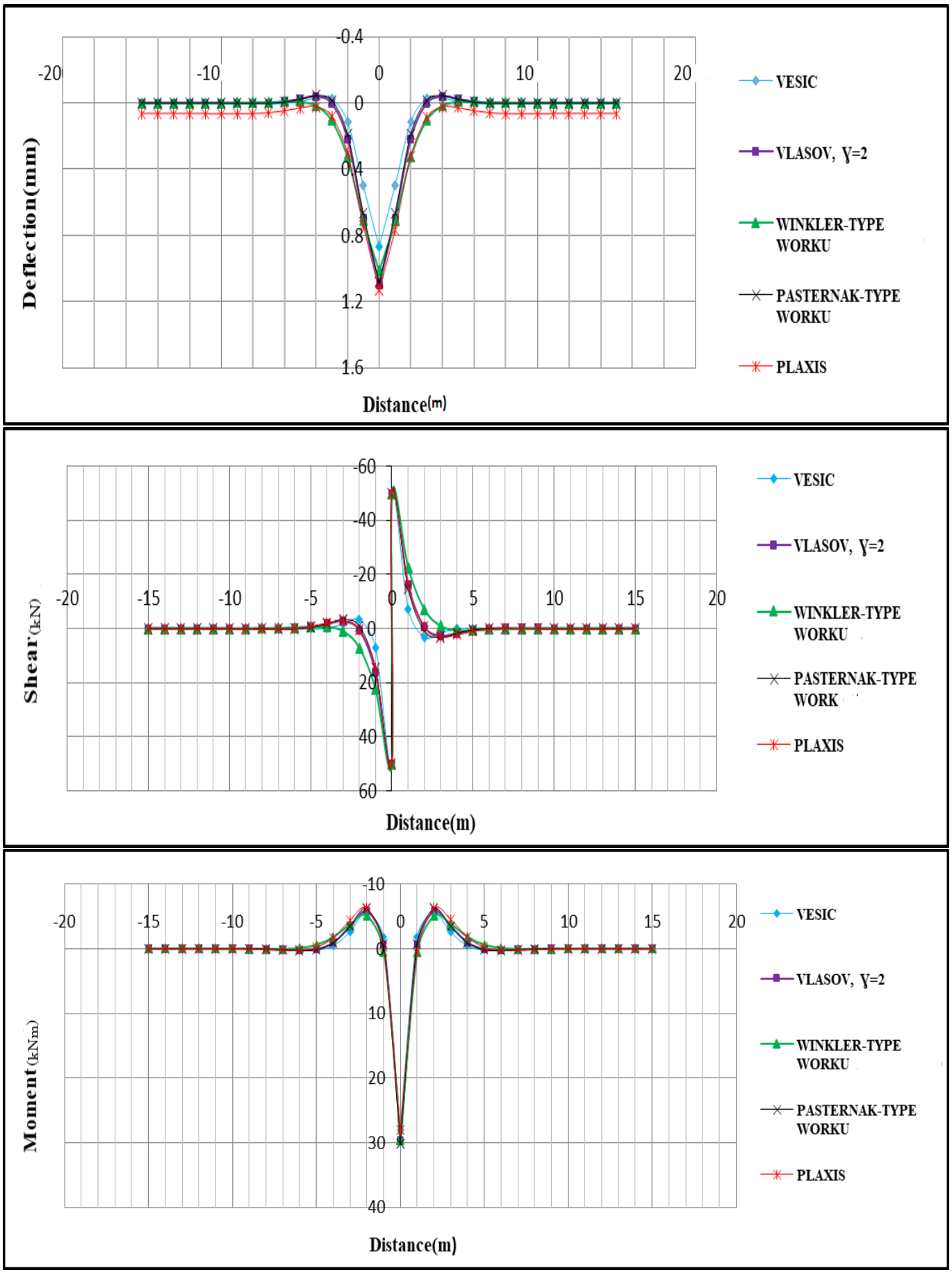

Figure 3.62: Infinite beam resting on hard/dense soil subjected to a vertical concentrated force

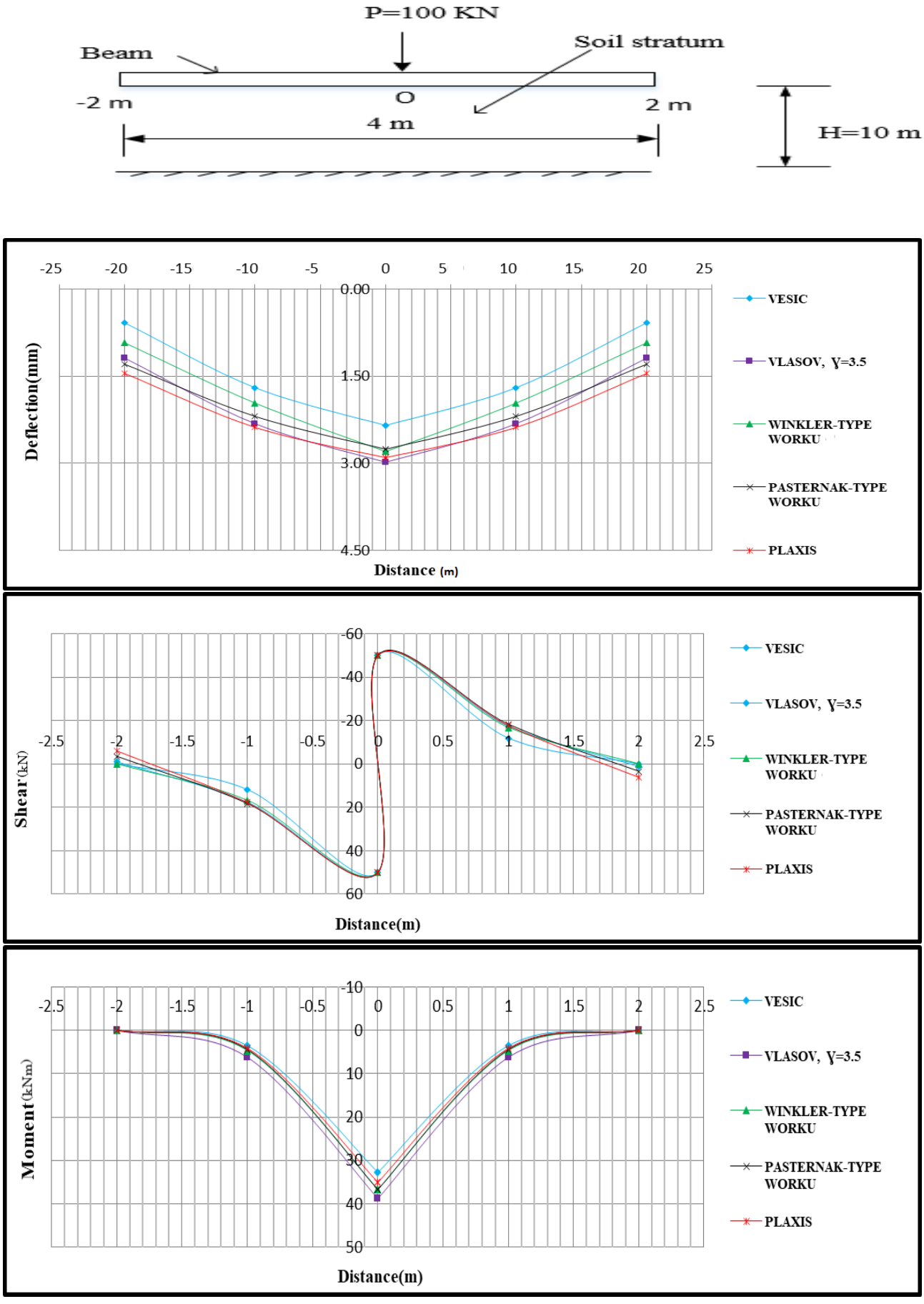

Figure 3.63: Finite beam resting on soft/loose soil subjected to a vertical concentrated force

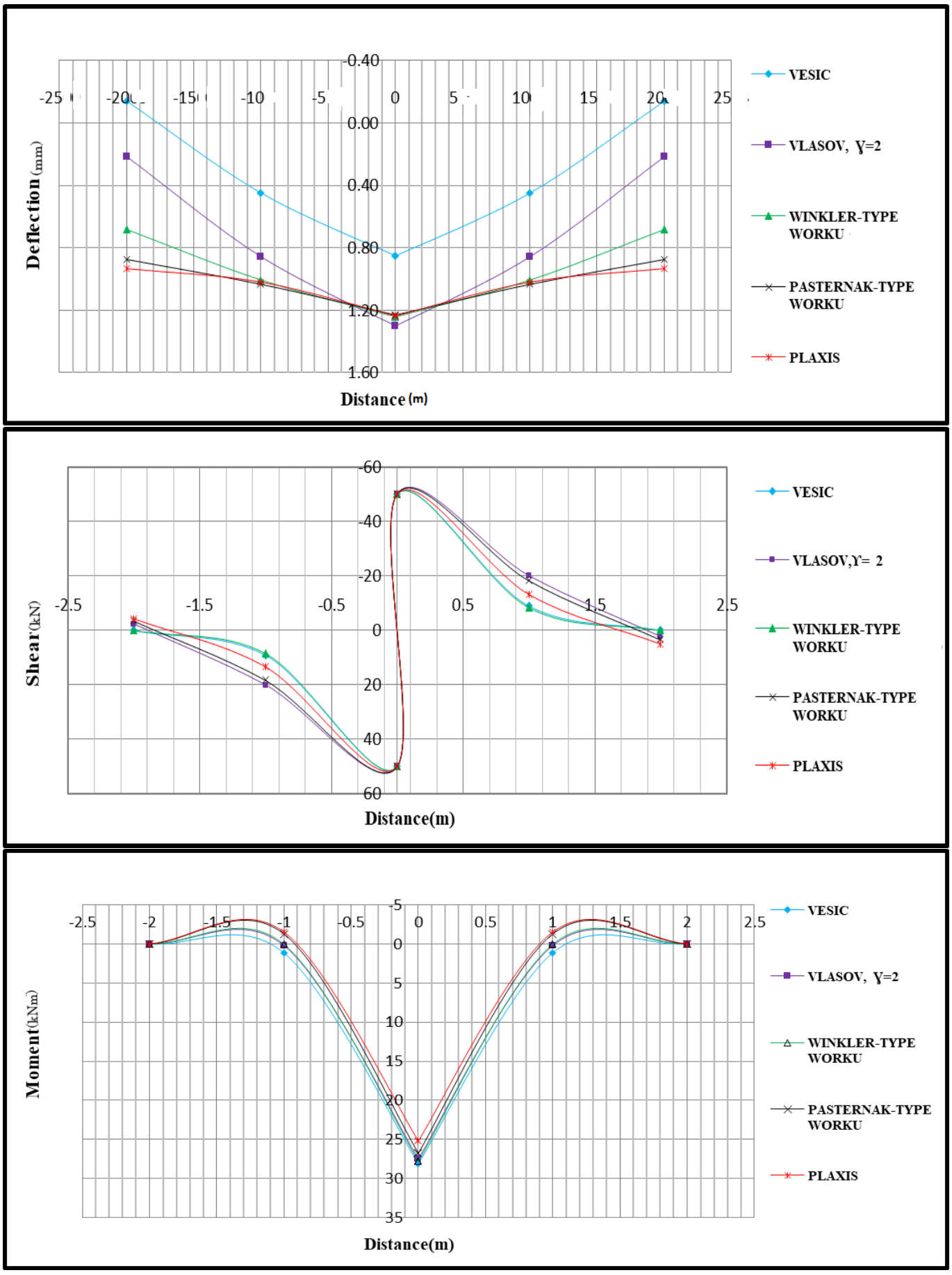

Figure 3.64: Finite beam resting on hard/dense soil subjected to a vertical concentrated force

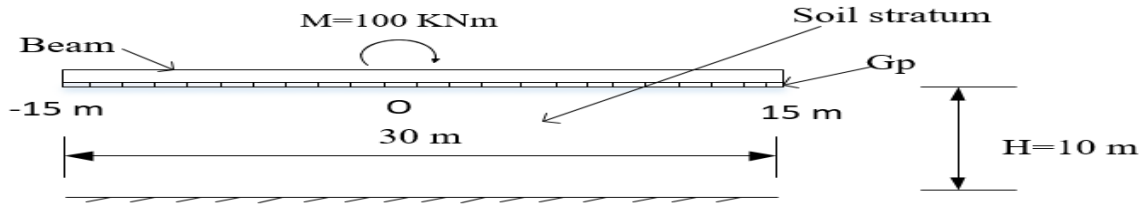

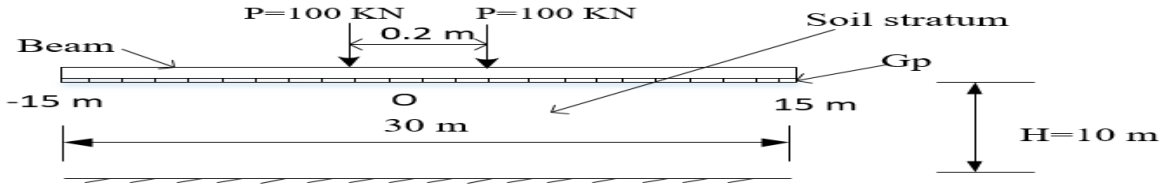

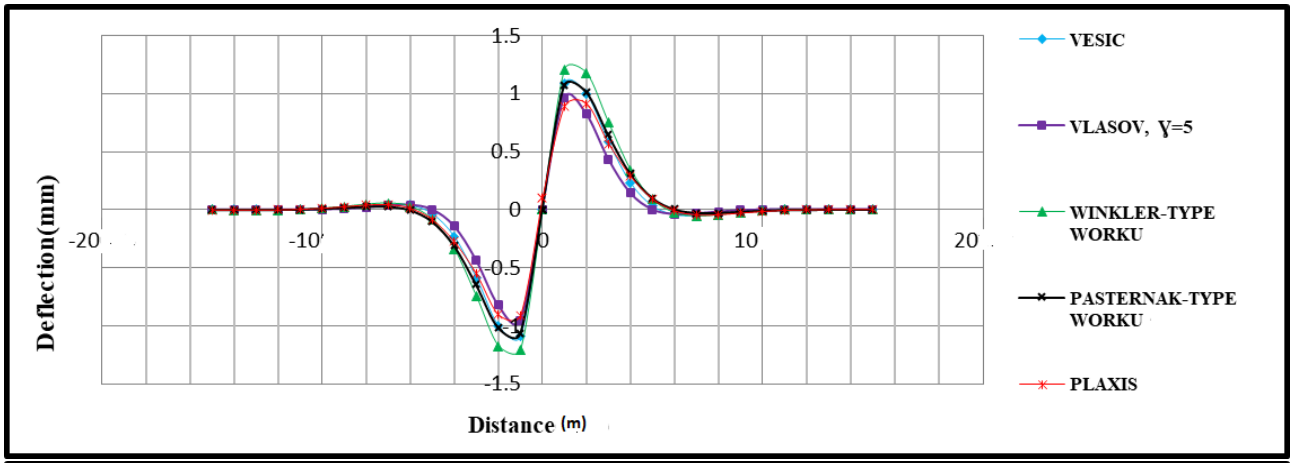

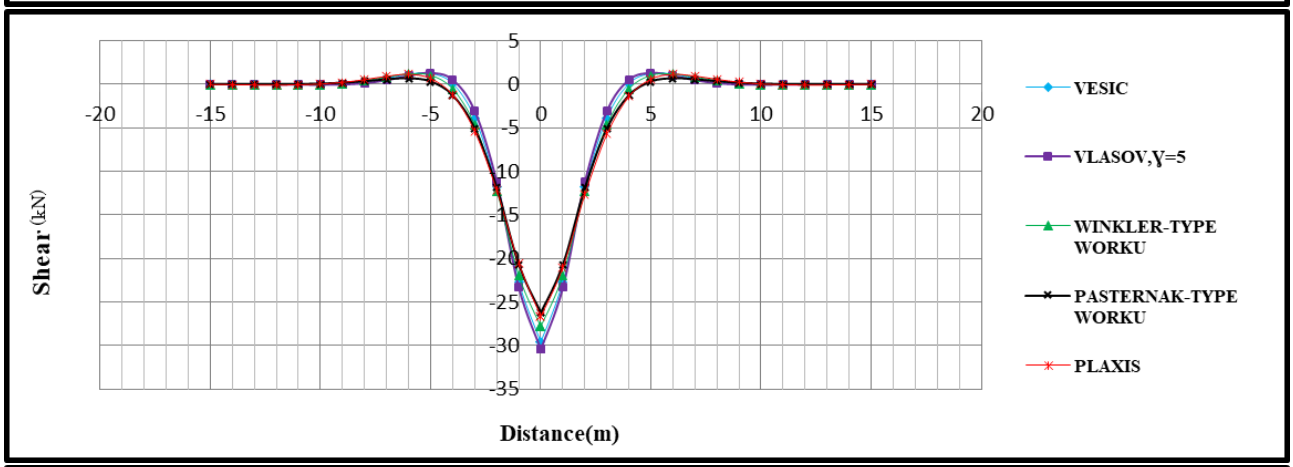

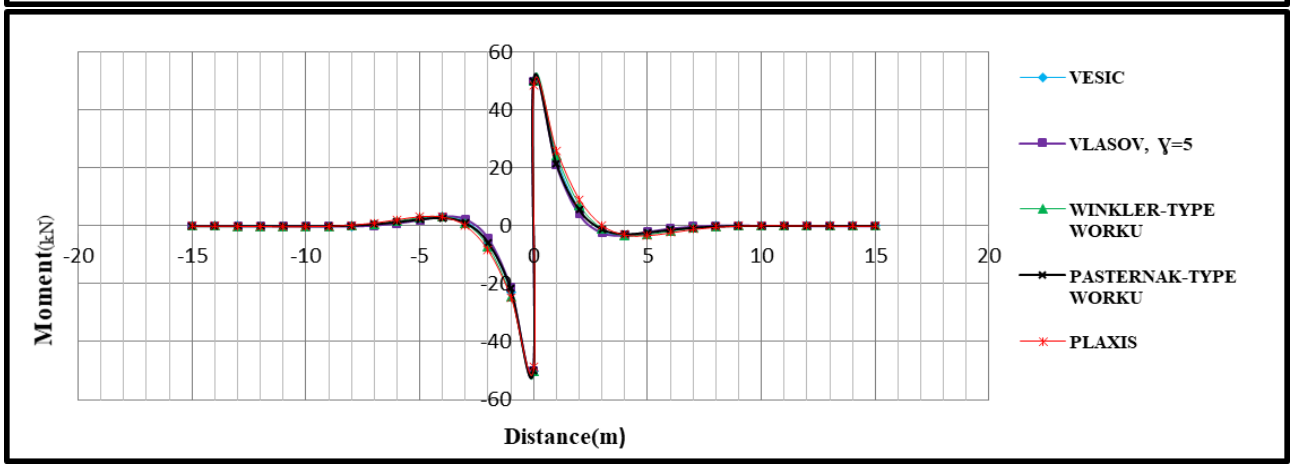

Figure 3.65: Infinite beam resting on soft/loose soil subjected to a concentrated moment

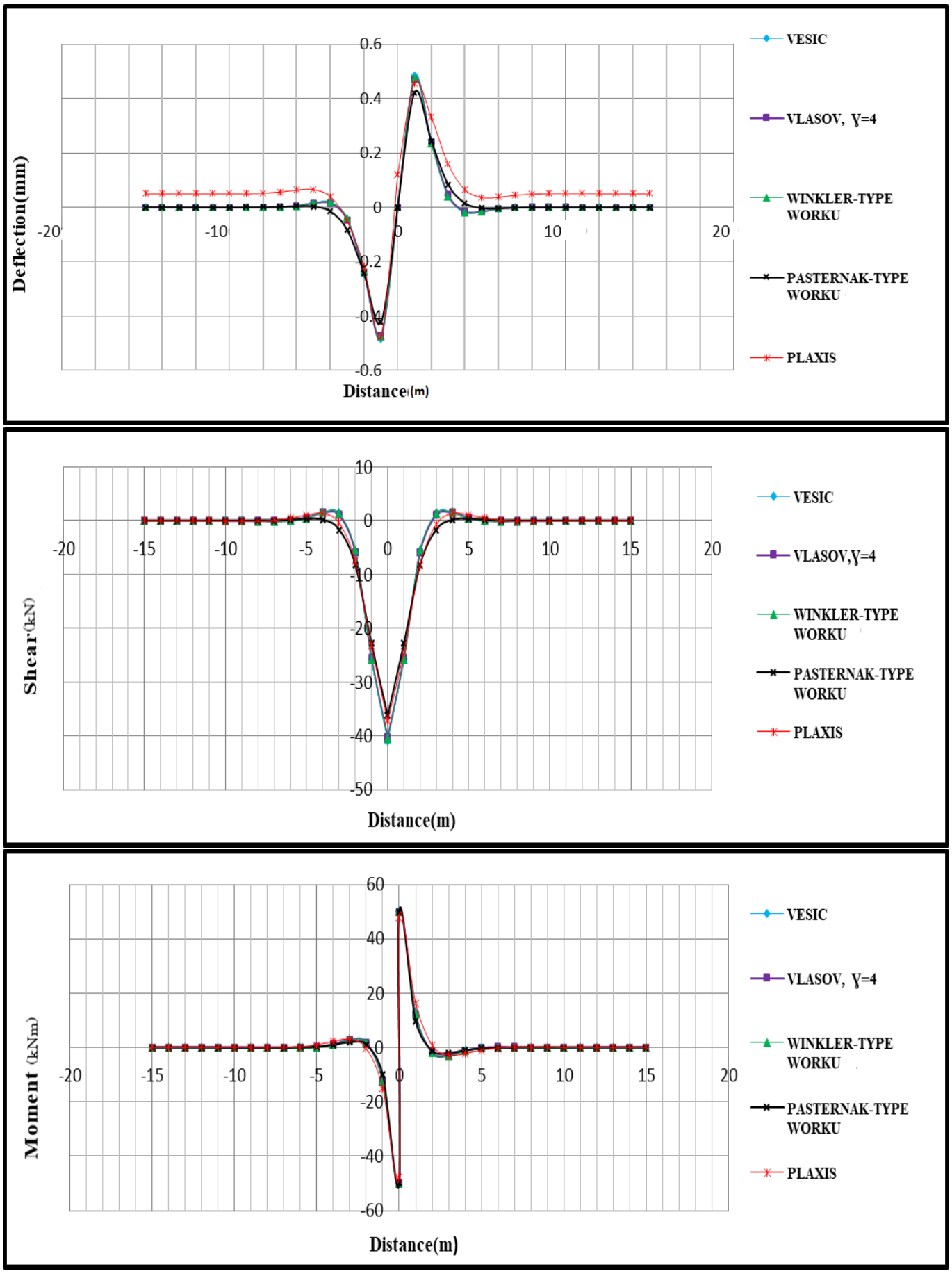

Figure 3.66: Infinite beam resting on hard/dense soil subjected to a concentrated moment

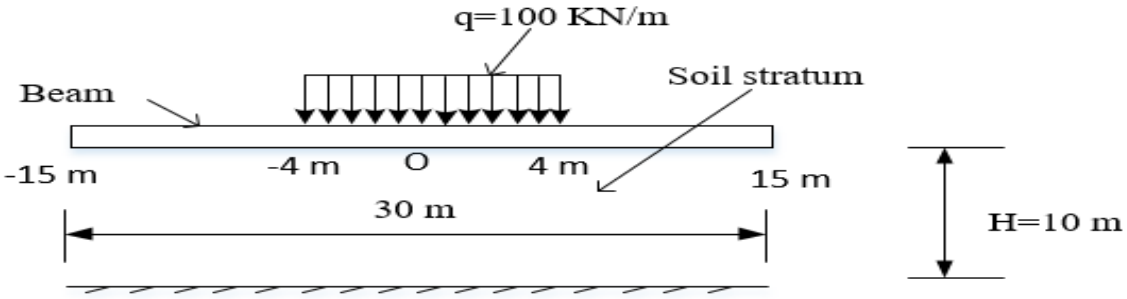

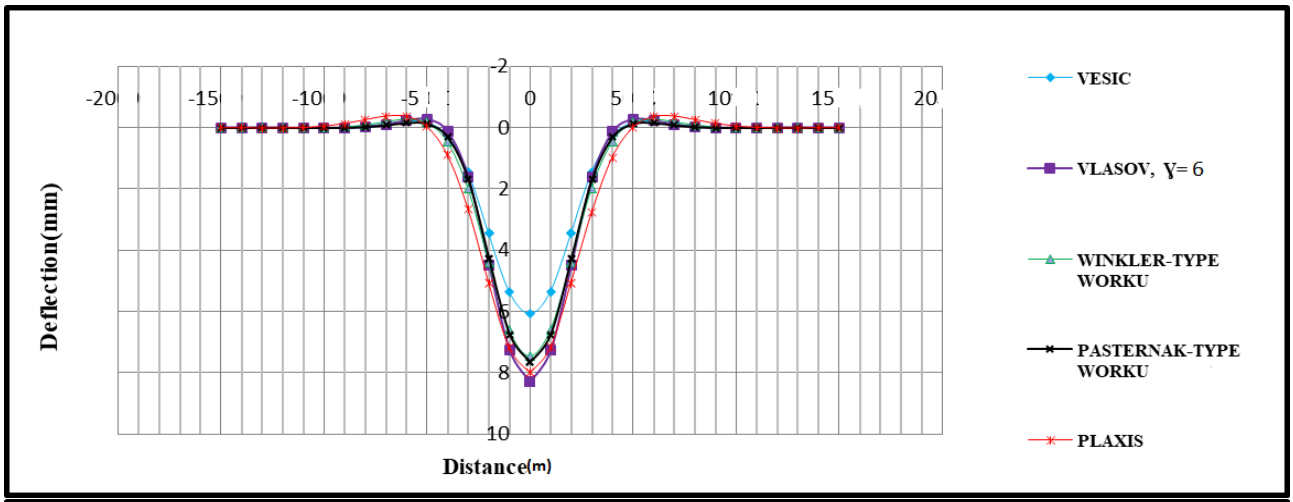

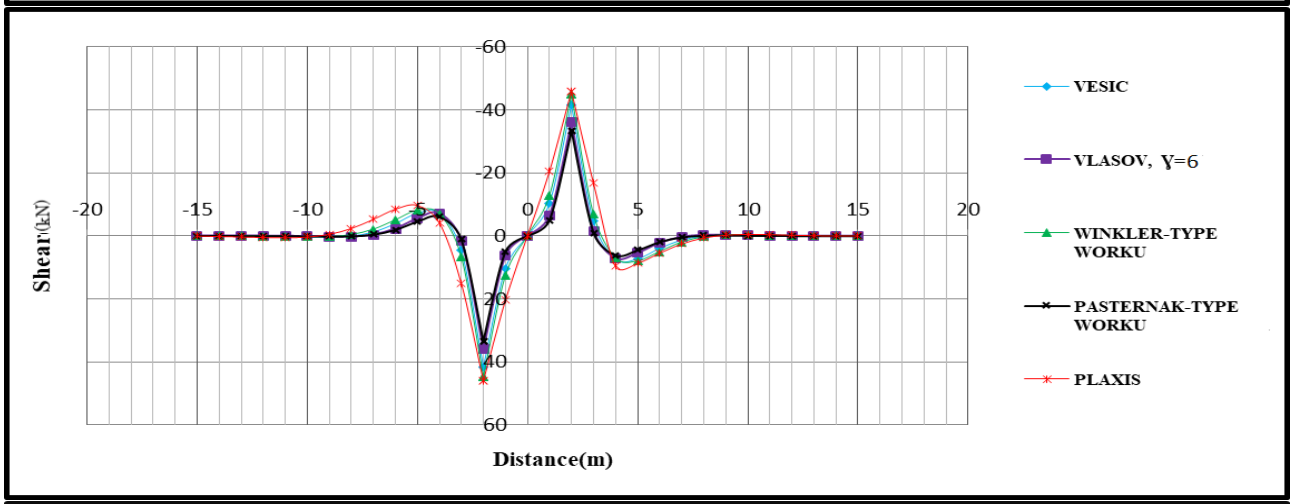

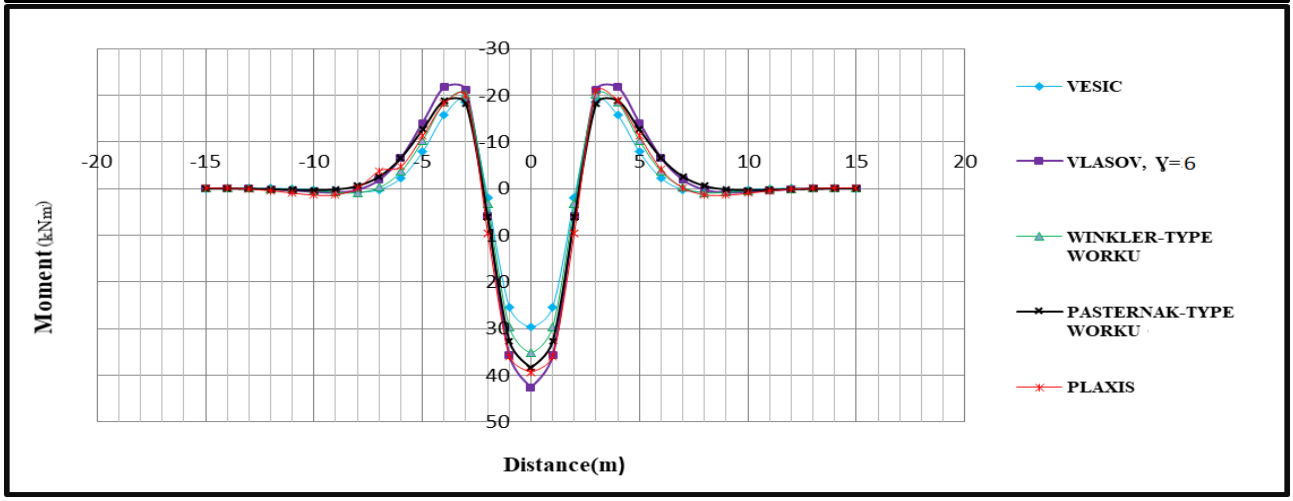

Figure 3.67: Infinite beam resting on loose/soft soil subjected to a uniformly distributed load

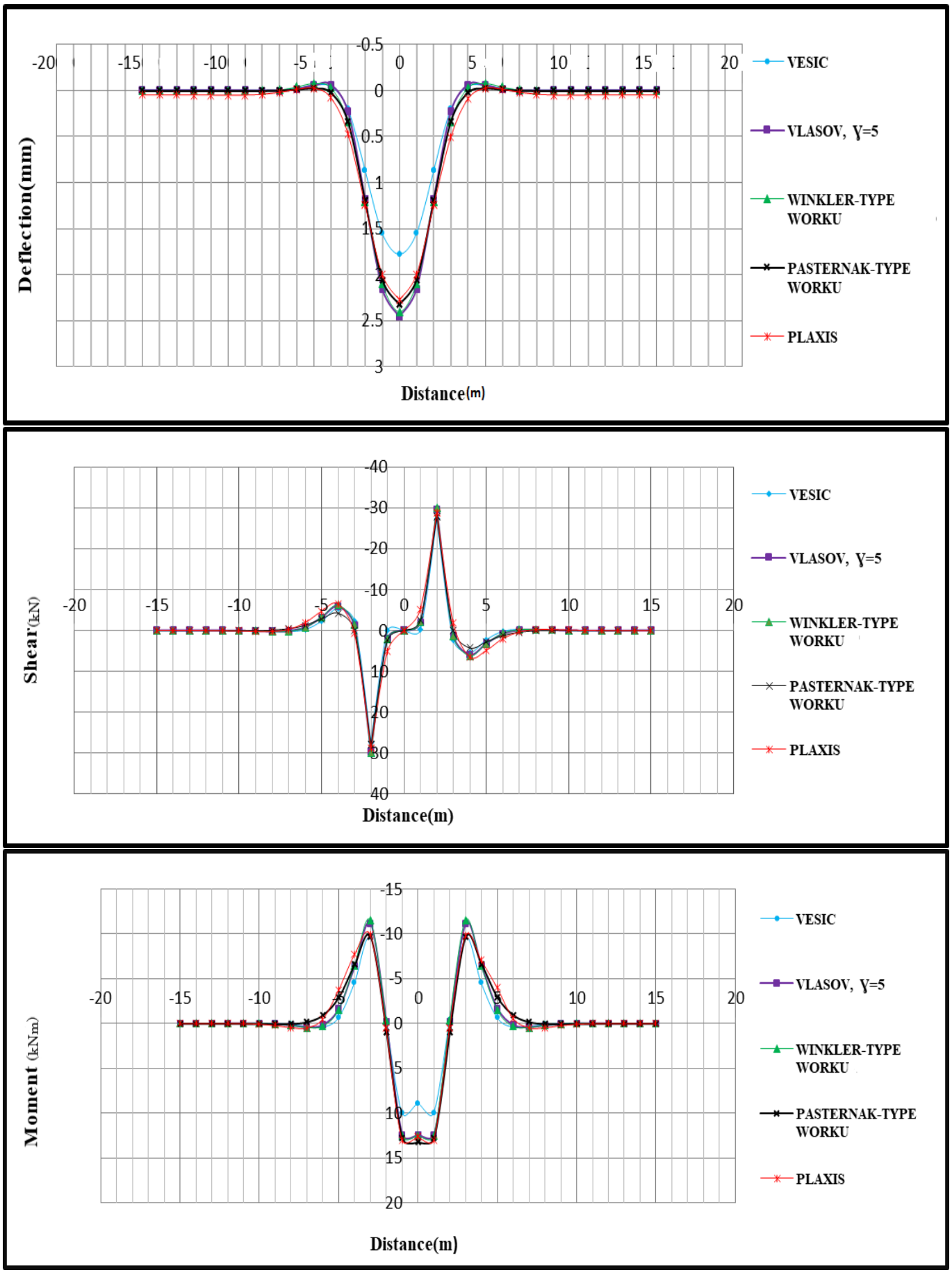

Figure 3.68: Infinite beam resting on loose/soft soil subjected to a uniformly distributed load

In general, the two-parameter Worku Kerr Equivalent Pasternak-type model gives more compatible results to the Plaxis 2D output for the considered mesh size (Figure 3.19) and loading cases. The Winkler-type model of Worku has also performed quite well in many cases. Thus, this models can be proposed as an efficient means to analyze the finite and infinite beam on elastic foundation.

Chapter 4

Conclusions and Recommendations

4.1 Conclusions

The major part of this study has been centered around the comparison of subgrade models of special interest in the application of single-parameter and two-parameter generalized continuum models developed by Worku for the analysis of finite and infinite beams. A spreadsheet program is developed to compute the internal actions for selected loading conditions. In the process, generalized continuum model developed by Worku has been calibrated to obtain the adjusted formulas for the model parameters. The results obtained by classical models are compared with Finite–Element based Plaxis 2D model results and with Worku's models. From the foregoing analysis, the following conclusions are drawn:

- Thickness of the stratum obtained for Worku's model which is 2.9-3 times the width of the foundation is in agreement with the range of depth of stress influence commonly known.
- Among the different solution cases that ascended in the determination of closed form solutions for beams on a two-parameter subgrade model, case III (i.e.D$<$1) is almost exclusively the case of practical significance.
- For finite beams, the discrepancies in deflection are slightly higher in Winkler's model, especially at the locations further away from the midspan. These differences are attributed to the end conditions and due to the fact that the model does not include shear interaction behavior of the soil. Another reason is that, the calibration factor is obtained based only on the maximum deflection.
- Considering the internal actions of both finite and infinite beams, the discrepancies in shear and moment are much smaller than observed in the deflection.
- Of the two-parameter subgrade models, Vlasov's model shows significant variation. This is due to the arbitrary assumption of negligible horizontal deformation components, u and v and also, the performance of the model depends on the value of γ it employs.

In general, the two-parameter Worku Kerr Equivalent Pasternak-type model gives more compatible results to the Plaxis 2D output than the Winkler-type model in all loading cases. The Winkler- type model of Worku has also performed quite well in many cases.

4.2 Recommendations

The Kerr-Equivalent Pasternak type model better represents the real physical problem than the Winkler model. Because it directly accounts for shear interaction from the outset.
The following recommendations are put forth for further studies:

- The generalized subgrade model is also applicable for beams subjected to unsymmetrical loadings, which is done by the method of superposition. Further works dealing with this is recommended.
- Further study needs to be conducted on non-homogenous soil strata which is an important case.

REFERENCES

Bowles, J.E. (1979). "*Foundation Analysis and Design*," Fifth Edition, New York.

Briaud, J. (2013). "*Introduction to Geotechnical Engineering: Unsaturated and Saturated Soils*," New Jersey, Canada.

Degu, Y. (2008). "Analysis of Beams on Elastic Foundations Using Newly Developed Generalized Continuum Based Sub-Grade Model," Department of Civil and Environmental Engineering, Addis Ababa Institute of Technology.

Gowthaman, S. (2017). "Numerical Study and Comparison of the Settlement Behaviors of Ax ially Loaded Piles using Different Material Models," Institution of Engineers,Sri Lanka, Vol.L, No. 02, pp.01-10.

Edward, T. (2013)." Analysis of Structures on Elastic Foundations,"Vol. 65, No. 2, pp.213-224.

Hetenyi. M. (1946). "*Beams on Elastic Foundation*," University of Michigan Press,Ann Arbor, Michigan.

Horvath, J.S. (1979). "A Study of Analytical Methods for Determining the Response of Mat Foundations to Static Loads," Thesis presented to the Poly-technic Institute of New York at Brooklyn, New York.

Horvath J.S. (1983). "Modulus of Subgrade Reaction: New Perspective," Journal of Geotechnical Engineering, Vol. 109, No. 12, pp.1591-1596.

Horvath J.S. (2011). "A Practical Subgrade Model for Improved Soil-Structure Interaction Analysis: Parameter Assessment," Manhattan College School of Engineering Civil and Environmental Engineering Department Bronx, New York, U.S.A.

Kerr A.D. (1964). "Elastic and Viscoelastic Foundation Models," Journal of Applied Mechanics, Vol. 31.

Kerr A.D. (1985). "Determination of Foundation Model Parameters," Journal of Geotechnical Engineering, Vol. l, No. 11.

"PLAXIS 2D", Material Models Manual, 2002.

"PLAXIS 3D", Material Models Manual, 2006.

Poulos, H. (2018). "Rational Assessment of Modulus of Subgrade Reaction," Journal of the SEAGS & AGSSEA, Vol. 49, No. 1, pp.453-460.

Selvadurai, A.P.S. (1979). "Elastic Analysis of Soil-Foundation Interaction," Department of Civil Engineering, New York.

Straughan, W.T. (1990). "*Analysis of Plates on Elastic Foundation*," Texas Tech University.

Tanahashi, H. (2004). "Formulas for Infinitely Long Bernoulli-Euler Beam on the Pasternak Model," Japanese Geotechnical Society, Tokyo, Japan, Vol.44, No. 5, pp. 109-118.

Timoshenko, S. and Goodier, J.N. (1951). "*Theory of Elasticity*," Engineering Societies library, New York.

Vlasov, V. Z., and Leont'ev, U. N. (1966). "Beams, plates and shells on elastic foundations, "Transaction of IPFST, p.357.

Worku, A. (2010). "Part I: A Generalized Formulation of Continuum Models for Elastic Foundations. Advances in Analysis, Modeling & Design, GeoFlorida.

Worku, A. and Degu Y. (2010). "Part II: Application of Newly Derived and Calibrated Subgrade Models in the Analysis of Beams on Elastic Foundations,"American Society of Civil-Engineers, GeoFlorida.

Worku, A. (2013). "Calibrated Analytical Formulas for Foundation Model Parameters,"International Journal of Geomechanics, Vol. 13,No,4.

Worku, A. (2014). "Development of a Calibrated Pasternak Foundation Model for Practical Use," International Journal of Geotechnical Engineering, Vol. 8, No. 1.

Appendix A

Solution of Beam On Two Parameter Subgrade Model

For infinitely long beam on Pasternak foundation model the solution of ODE is derived by combing differential equation of the beam from classical beam theory to the model. The ODE for homogenous case is given by

$$EI\frac{d^4w}{dx^4} + k_s w - G_p\frac{d^2w}{dx^2} = 0 \tag{A.1}$$

$$\frac{d^4w}{dx^4} + \frac{k_s}{EI} - \frac{G_p}{EI}\frac{d^2w}{dx^2} = 0 \tag{A.2}$$

Equation (A.2) is an ODE with constant coefficients which have the solution of the form $w = Ce^{mx}$. Substitute it into Equation (A.1) gives;

$$m^4 + \frac{k_s}{EI} - \frac{G_p}{EI}m^2 = 0 \tag{A.3}$$

Let $m^2 = n$ into Equation (A.3) gives

$$n^2 - \frac{G}{EI}m + \frac{k_s}{EI} = 0 \tag{A.4}$$

Then the roots of the quadratic equation become

$$n_{1,2} = \frac{G}{2EI} \pm \sqrt{\left(\frac{G}{2EI}\right)^2 - \frac{k_s}{EI}} \tag{A.5}$$

The roots of Equation(A.3) become

$$m_{1,2,3,4} = \pm\sqrt{n_i} = \pm\sqrt{\frac{G}{2EI} \pm \sqrt{\left(\frac{G}{2EI}\right)^2 - \frac{k_s}{EI}}} \tag{A.6}$$

Let,$D = \frac{G}{2\sqrt{EIk_s}}$

There are three possible cases of the general solution of Equation (A.2) depending on whether,$D <$ $1, D = 1$ or $D > 1$.

Case I ($D < 1$) In this case the root is the complex number then Equation(A.6) re-written as;

$$m_{1,2,3,4} = \pm\sqrt{\frac{G}{2EI} \pm i\sqrt{\frac{k_s}{EI} - \left(\frac{G}{2EI}\right)^2}} \tag{A.7}$$

From the algebra of complex numbers, the following relation is known(Tanahashi, 2004).

$$\sqrt{y \pm iz} = \pm\left[\sqrt{\frac{1}{2}(r+y)} + (sign(z))i\sqrt{\frac{1}{2}(r-y)}\right] \tag{A.8}$$

Where,$r = \sqrt{y^2 + z^2}$ Applying the relationship to Equation(A.7) gives

$$m_{1,2,3,4} = \pm\left[\sqrt{\sqrt{\frac{k_s}{4EI}} + \frac{G}{4EI}}\right] \pm i\left[\sqrt{\sqrt{\frac{k_s}{4EI}} - \frac{G}{4EI}}\right] \tag{A.9}$$

$$m_{1,2,3,4} = \pm\left[\sqrt{\lambda^2 + \frac{G}{4EI}}\right] \pm i\left[\sqrt{\lambda^2 - \frac{G}{4EI}}\right] \tag{A.10}$$

Where,$\lambda^2 = \sqrt{\frac{k_S}{4EI}}$

$$m_{1,2,3,4} = \pm(\alpha \pm i\beta) \tag{A.11}$$

Where

$$\begin{aligned} \alpha &= \sqrt{\lambda^2 + \frac{G}{4EI}} \\ \beta &= \sqrt{\lambda^2 - \frac{G}{4EI}} \end{aligned} \tag{A.12}$$

Substituting Equation (A.12) into $w = Ce^{mx}$

$$w(x) = \sum_{i=1}^{4} C_i e^{mix} \tag{A.13}$$

$$w(x) = C_1 e^{(\alpha+i\beta)x} + C_2 e^{(-\alpha-i\beta)x} + C_3 e^{(-\alpha+i\beta)x} + C_4 e^{(\alpha-i\beta)x} \tag{A.14}$$

$$\begin{aligned} w(x) = C_1 e^{\alpha x}(\cos\beta x + i\sin\beta x) + C_2 e^{-\alpha x}(\cos\beta x - i\sin\beta x) + \\ C_3 e^{-\alpha x}(\cos\beta x + i\sin\beta x) + C_4 e^{\alpha x}(\cos\beta x - i\sin\beta x) \end{aligned} \tag{A.15}$$

$$w(x) = (C_1 e^{\alpha x} + C_2 e^{-\alpha x}) \cos \beta x + (C_3 e^{\alpha x} + C_4 e^{-\alpha x}) \sin \beta x \tag{A.16}$$

Where, C_1, C_2, C_3, C_4 are open constants.

Case II $(D = 1)$

$$m_{1,2,3,4} = \pm \sqrt{\frac{G}{2EI}} \tag{A.17}$$

$$\alpha = \sqrt{\frac{G}{2EI}} \tag{A.18}$$

$$w(x) = \sum_{i=1}^{4} C_i e^{mix} \tag{A.19}$$

$$w(x) = C_1 e^{\alpha x} + C_2 x e^{\alpha x} + C_3 e^{-\alpha x} + C_4 x e^{-\alpha x} \tag{A.20}$$

$$w(x) = (C_1 e^{\alpha x} + C_2 e^{-\alpha x}) \cos \beta x + (C_3 e^{\alpha x} + C_4 e^{-\alpha x}) \sin \beta x \tag{A.21}$$

Where, C_1, C_2, C_3, C_4 are open constants.

Case III $(D > 1)$ In this case the root is the real number then

$$m_{1,2,3,4} = \pm \sqrt{\frac{G}{2EI} \pm \sqrt{\left(\frac{G}{2EI}\right)^2 - \frac{K_s}{EI}}} \tag{A.22}$$

All are real roots;the following relation is known(Tanahashi, 2004).

$$\sqrt{y + z} = \pm \left[\sqrt{\frac{1}{2}(r + y} + \sqrt{\frac{1}{2}(y - r)} \right] \tag{A.23}$$

Where,$r = \sqrt{y^2 + z^2}$

Applying the relationship to Equation(A.22) gives

$$m_{1,2,3,4} = \pm \left[\sqrt{\sqrt{\frac{K_s}{4EI} + \frac{G}{4EI}}} \right] \pm \left[\sqrt{\sqrt{\frac{G}{4EI} - \frac{K_s}{4EI}}} \right] \tag{A.24}$$

$$m_{1,2,3,4} = \pm \left[\sqrt{\lambda^2 + \frac{G}{4EI}}\right] \pm \left[\sqrt{\frac{G}{4EI} - \lambda^2}\right] \tag{A.25}$$

Where,$\lambda^2 = \sqrt{\frac{K_S}{4EI}}$

$$m_{1,2,3,4} = \pm(\alpha \pm \beta) \tag{A.26}$$

Substituting Equation (A.26) into $w = Ce^{mx}$

$$w(x) = \sum_{i=1}^{4} C_i e^{mix} \tag{A.27}$$

$$w(x) = C_1 e^{(\alpha+\beta)x} + C_2 e^{(\alpha-\beta)x} + C_3 e^{(-\alpha+\beta)x} + C_4 e^{(-\alpha-\beta)x} \tag{A.28}$$

$$\begin{aligned} e^{x} &= \cosh x + \sinh x \\ e^{-x} &= \cosh x - \sinh x \end{aligned} \tag{A.29}$$

Substitute into Equation(A.28)

$$\begin{aligned} w(x) = C_1 e^{\alpha x}(\cosh \beta x + \sinh \beta x) + C_2 e^{-\alpha x}(\cosh \beta x - \sinh \beta x) + \\ C_3 e^{-\alpha x}(\cosh \beta x + \sinh \beta x) + C_4 e^{\alpha x}(\cosh \beta x - \sinh \beta x) \end{aligned} \tag{A.30}$$

$$w(x) = (C_1 e^{\alpha x} + C_2 e^{-\alpha x}) \cosh \beta x + (C_3 e^{\alpha x} + C_4 e^{-\alpha x}) \sinh \beta x \tag{A.31}$$

Where, C_1, C_2, C_3, C_4 are open constants.

Appendix B

Infinite beam Plaxis 2D result samples

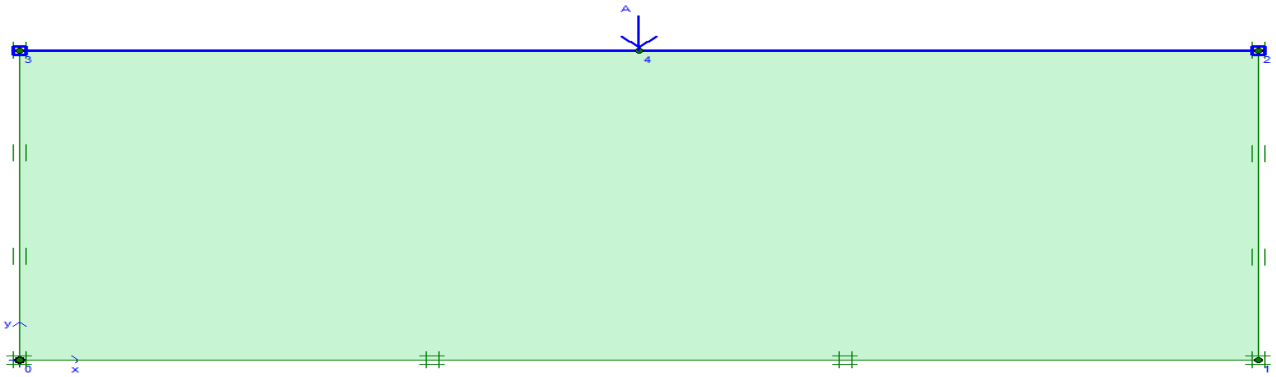

(a) Plaxis 2D model

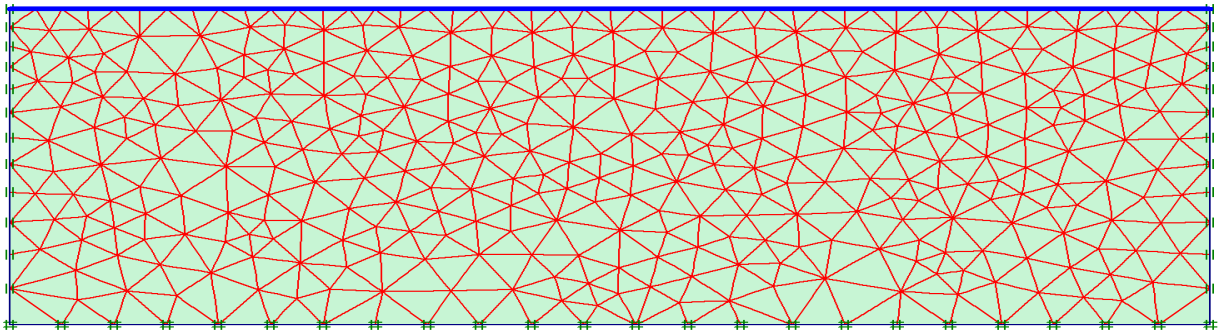

(b) Generated mesh

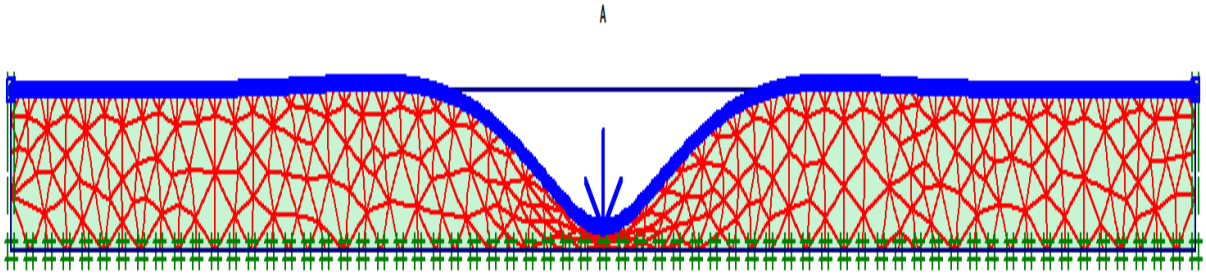

(c) Deformed mesh

Figure B1: Plaxis 2D model output of infinite beam subjected to concentrated Force

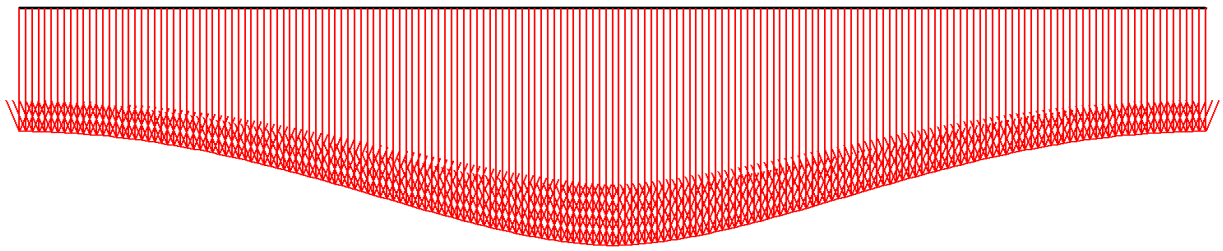

(a) Deformation

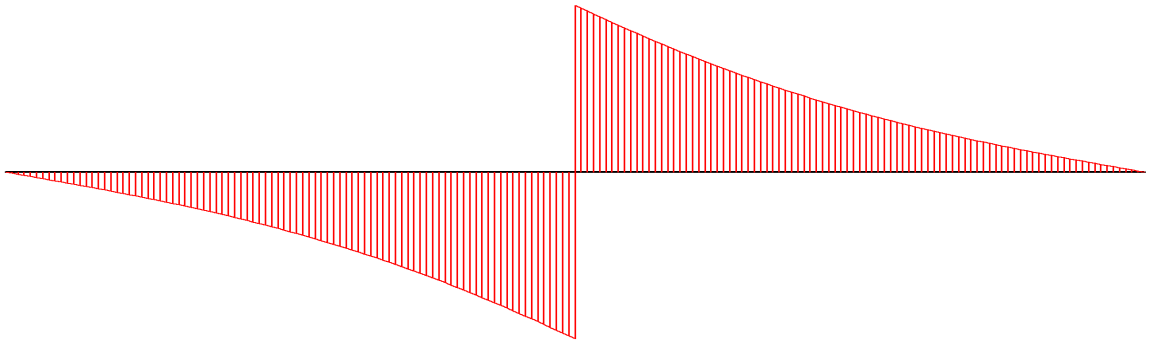

(b) Shear force

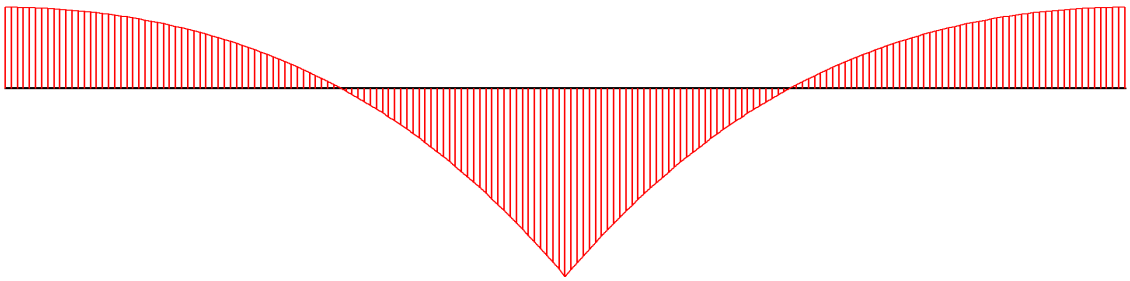

(c) Bending Moment

Figure B2: Cont'd....

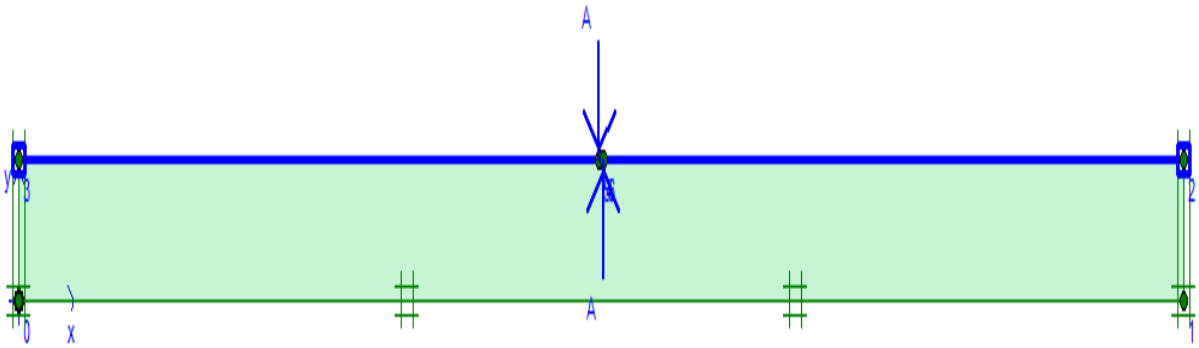

(a) Plaxis 2D model

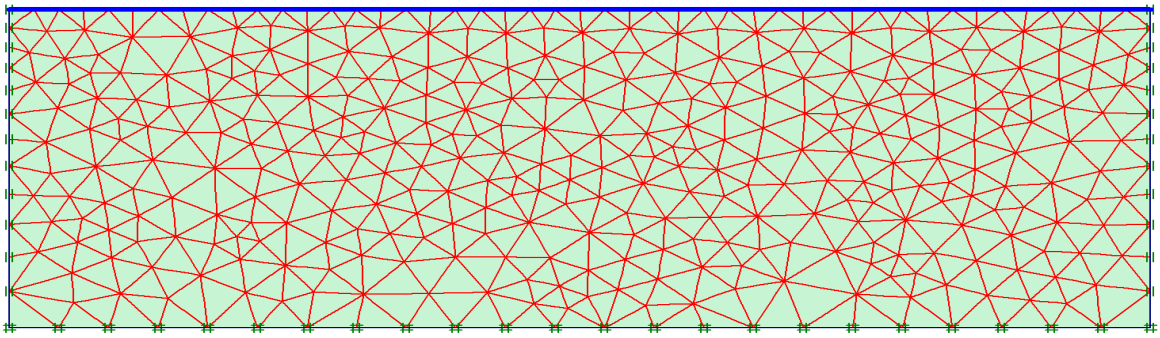

(b) Generated mesh

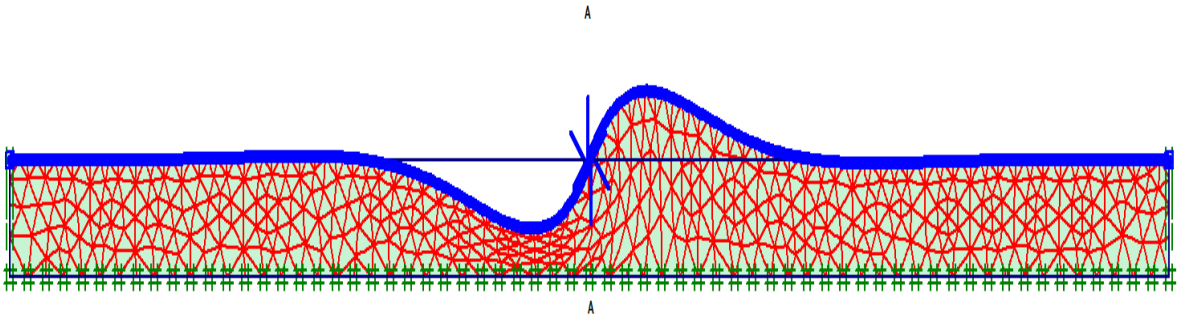

(c) Deformed mesh

Figure B3: Plaxis 2D model out put of infinite beam subjected to concentrated moment

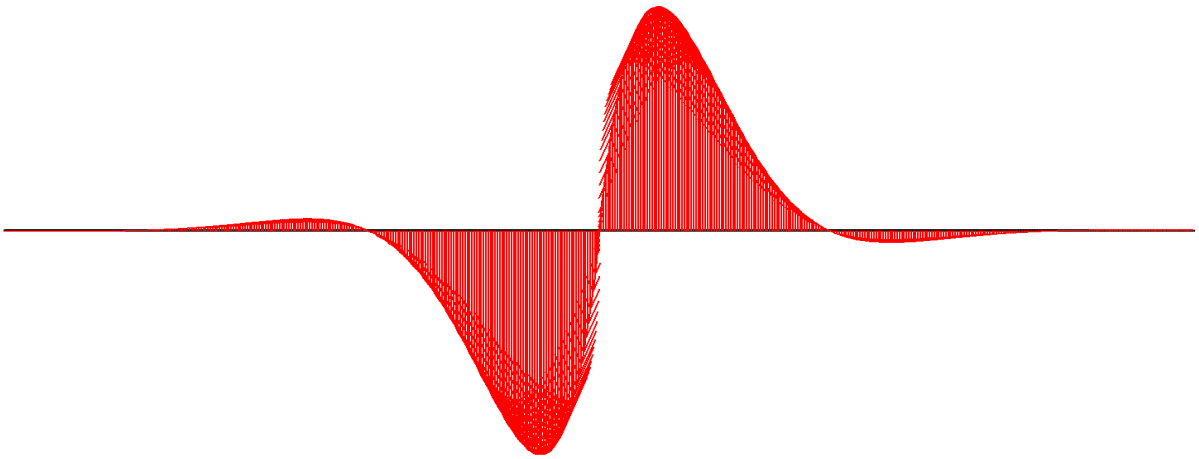

(a) Deformation

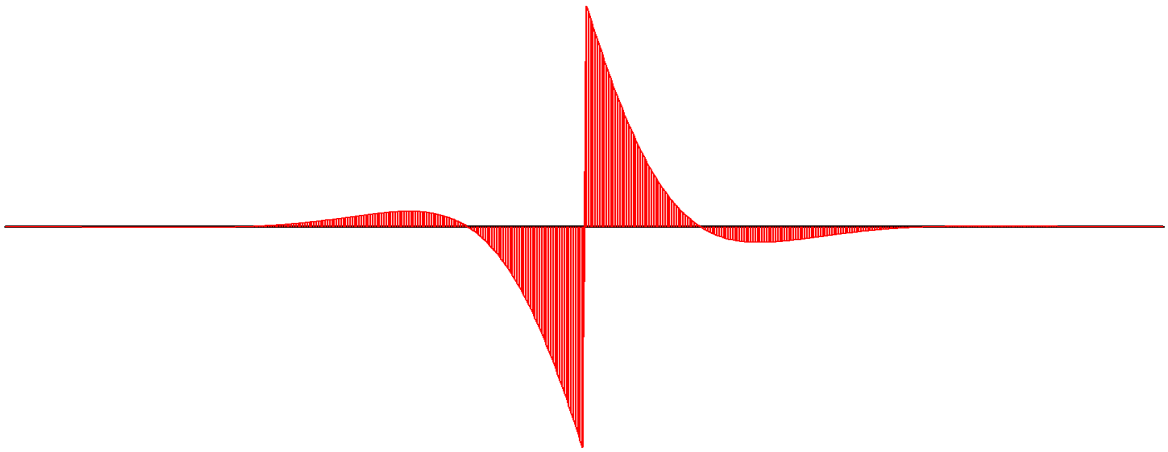

(b) Shear force

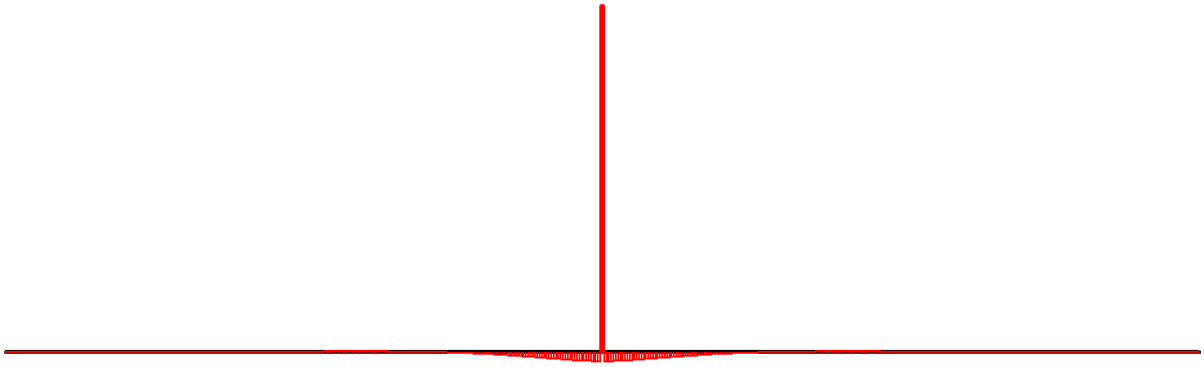

(c) Bending moment

Figure B4: Cont'd....

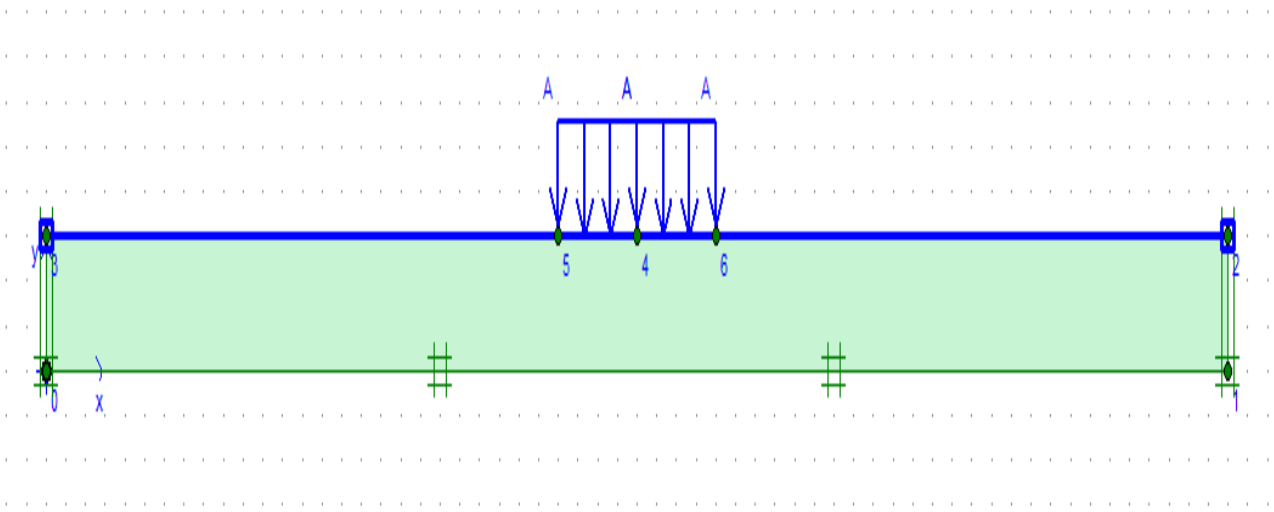

(a) Plaxis 2D model

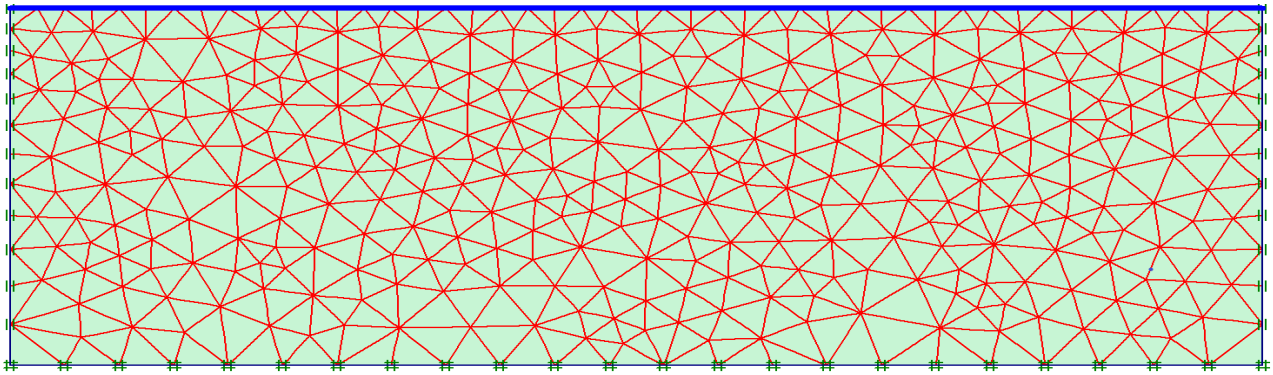

(b) Generated mesh

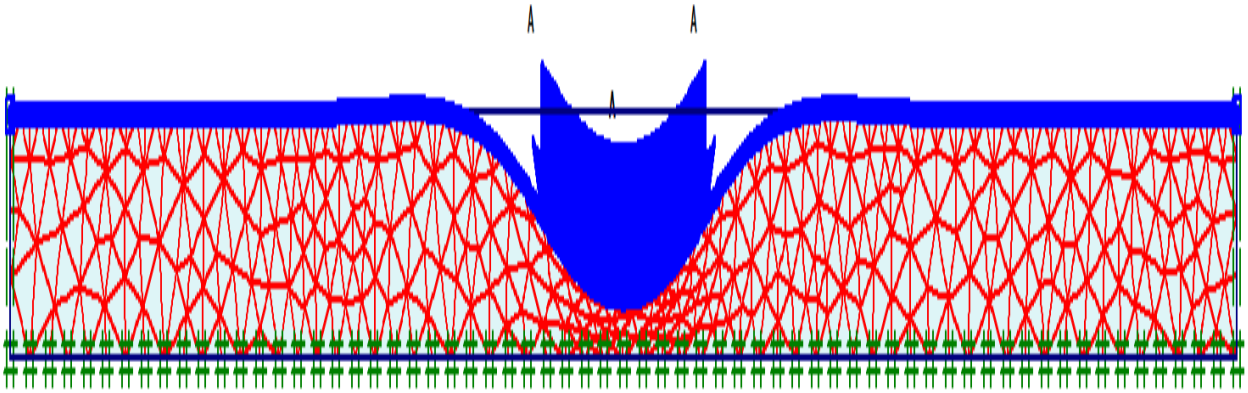

(c) Deformed mesh

Figure B5: Plaxis 2D model output of infinite beam subjected to uniformly distributed load

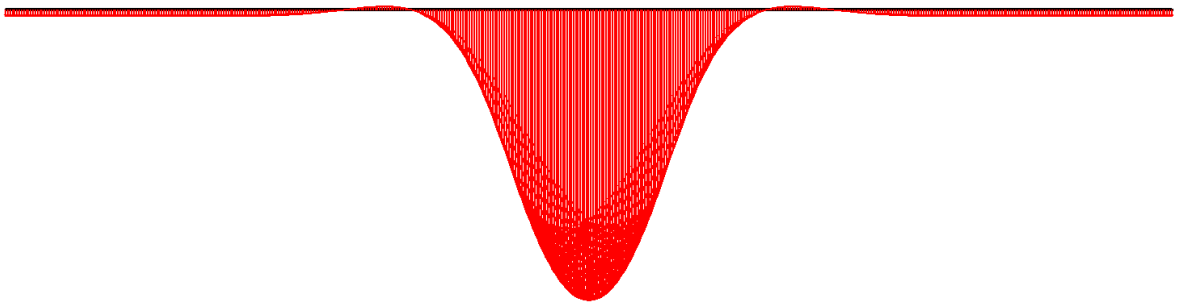

(a) Deformation

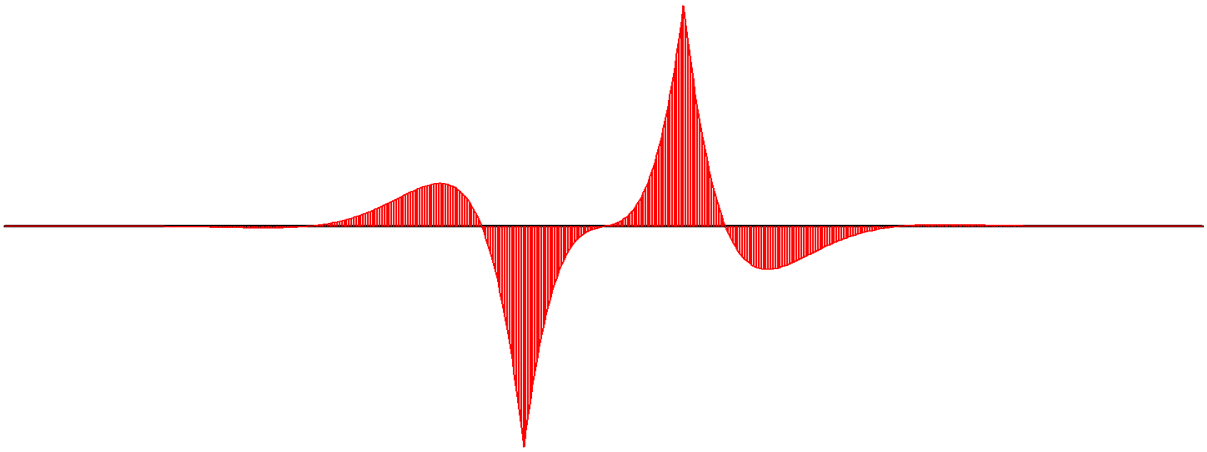

(b) Shear force

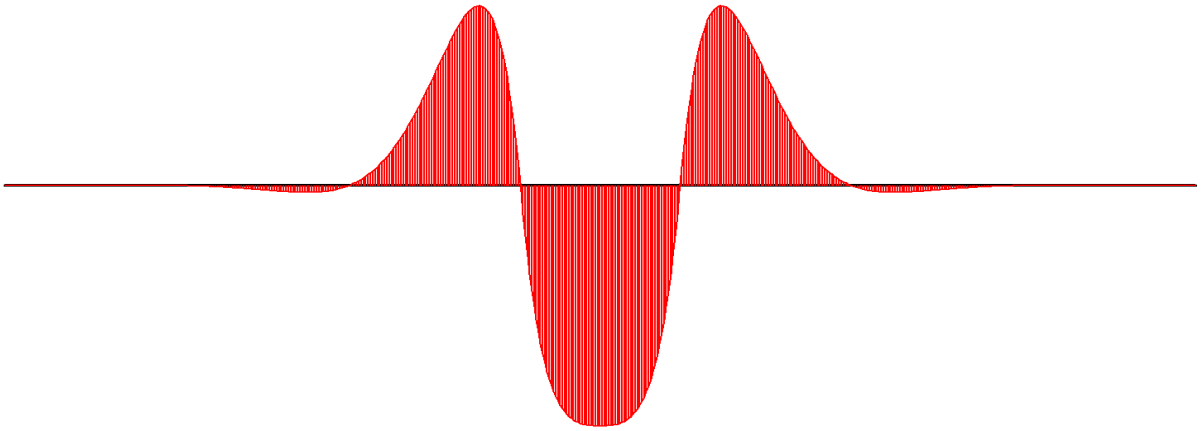

(c) Bending moment

Figure B6: Cont'd....

Appendix C

Finite beam Plaxis 2D result samples

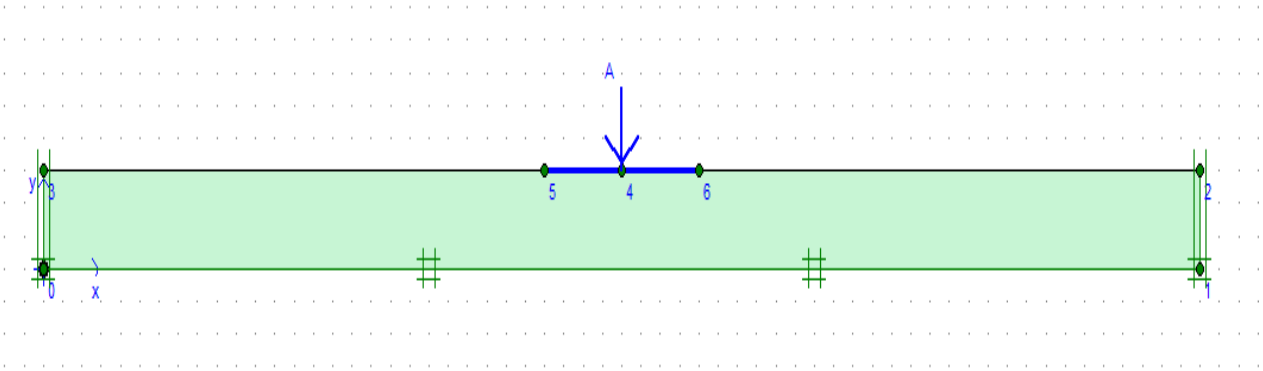

(a) Plaxis 2D model

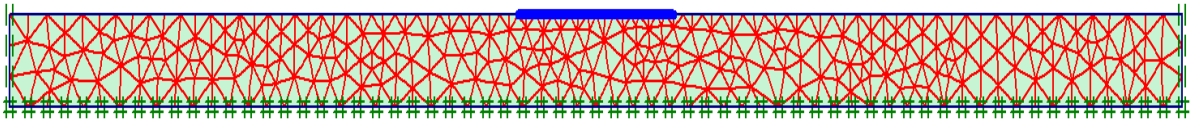

(b) Generated mesh

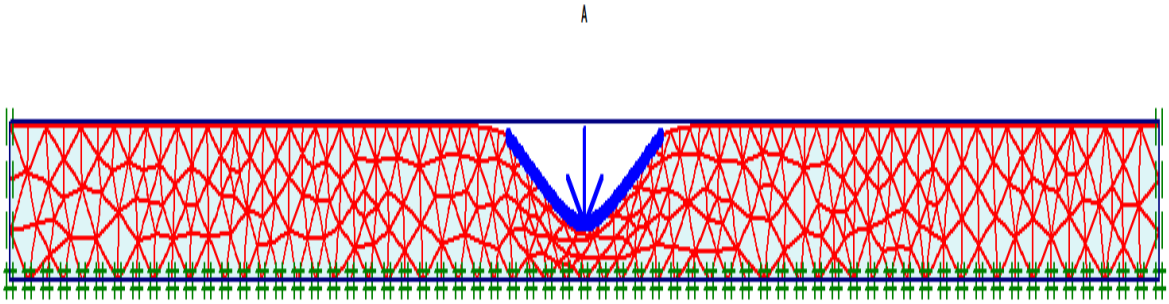

(c) Deformed mesh

Figure C1: Plaxis 2D out put of finite beam subjected to concentrated load

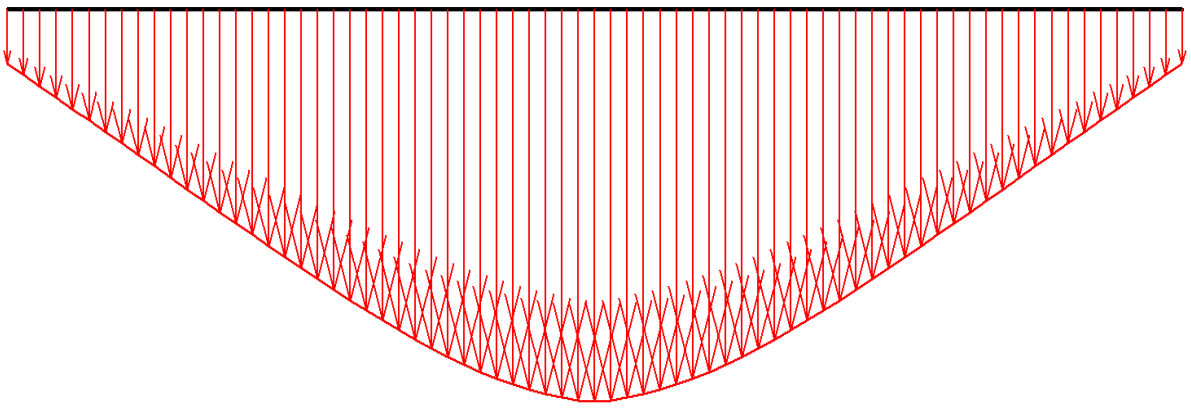

(a) Deformation

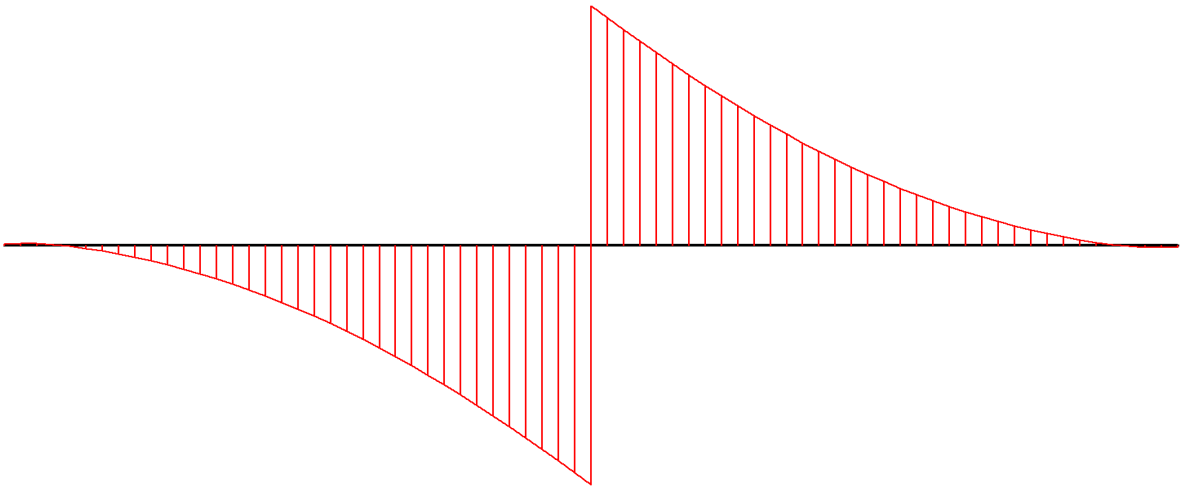

(b) Shear force

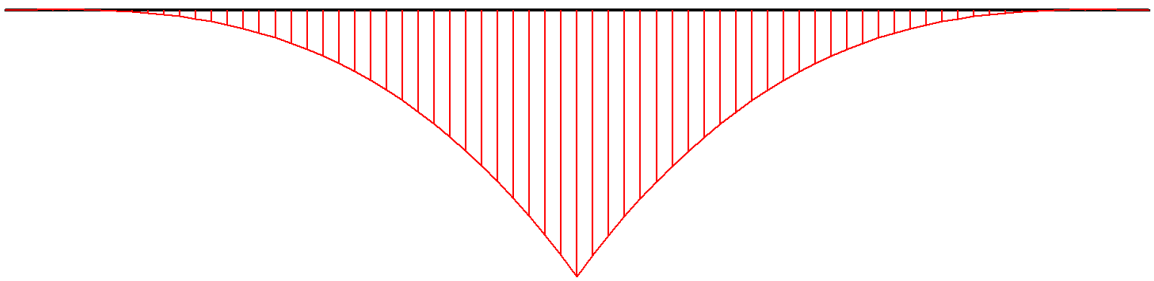

(c) Bending moment

Figure C2: Cont'd....

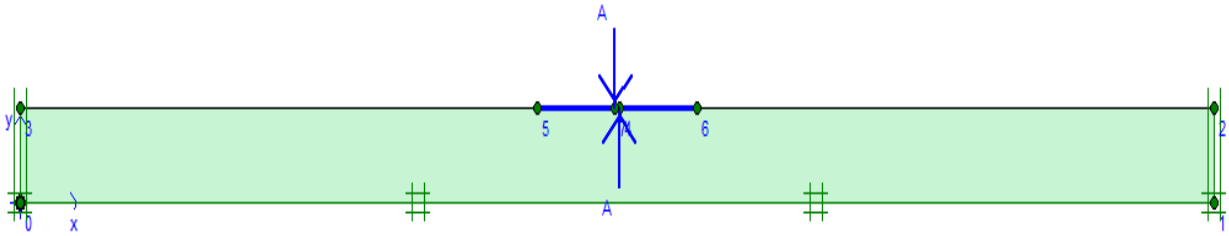

(a) Plaxis 2D model

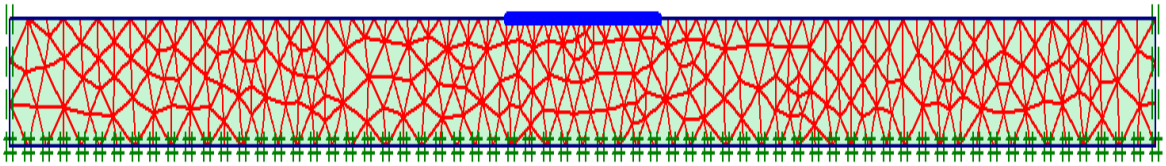

(b) Generated mesh

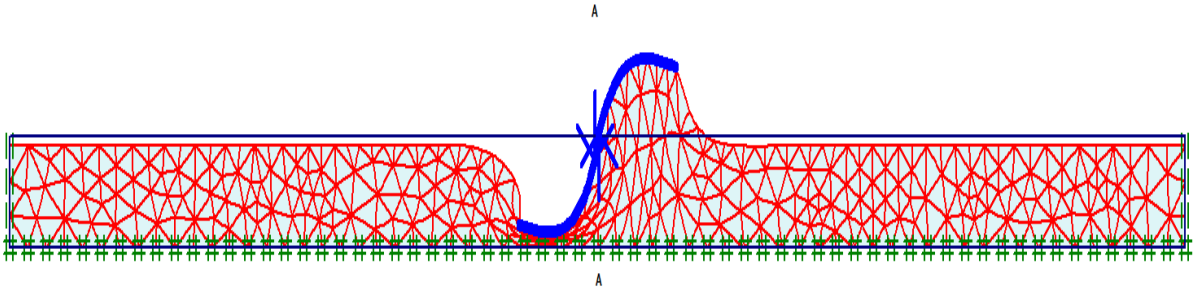

(c) Deformed mesh

Figure C3: Plaxis 2D out put of finite beam subjected to concentrated moment

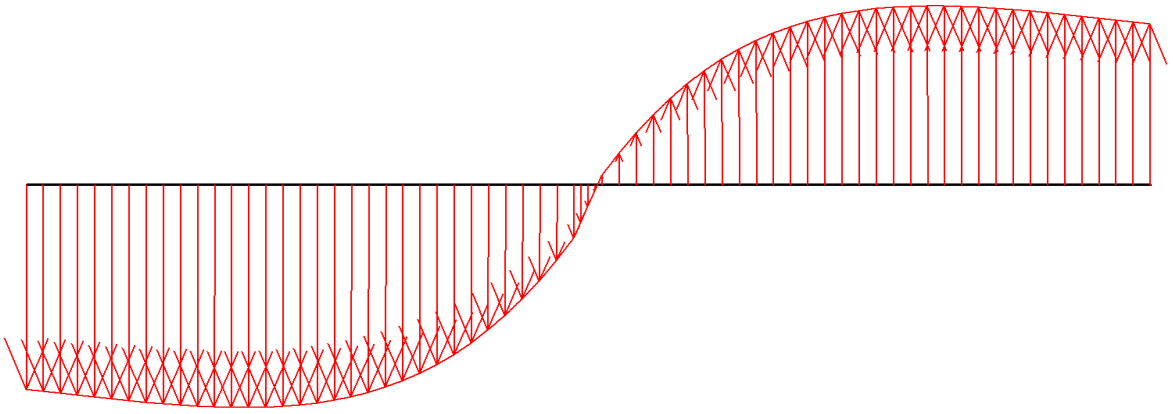

(a) Deformation

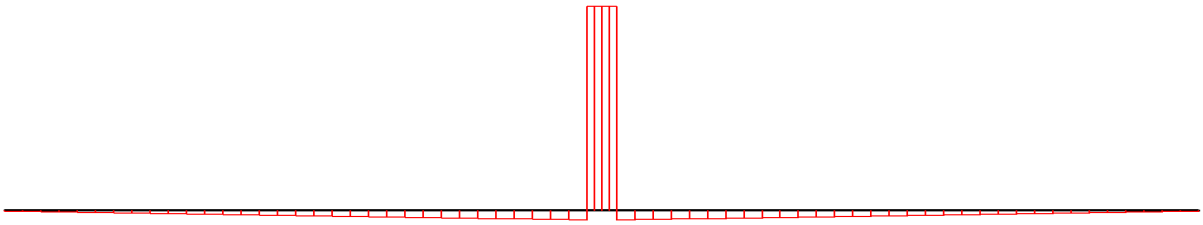

(b) Shear force

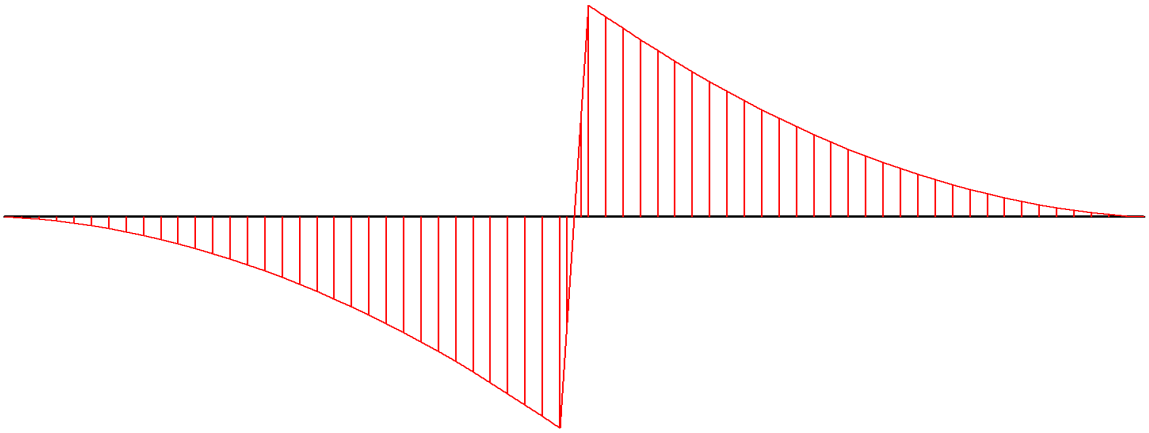

(c) Bending moment

Figure C4: Cont'd....

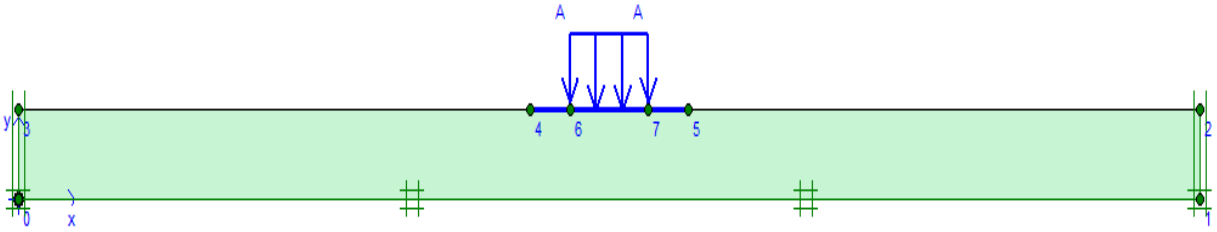

(a) Plaxis 2D model

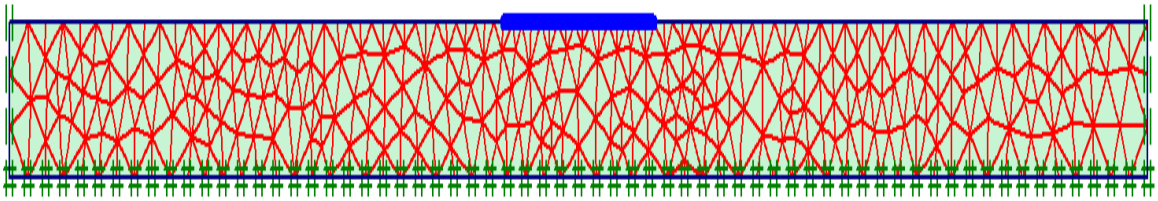

(b) Generated mesh

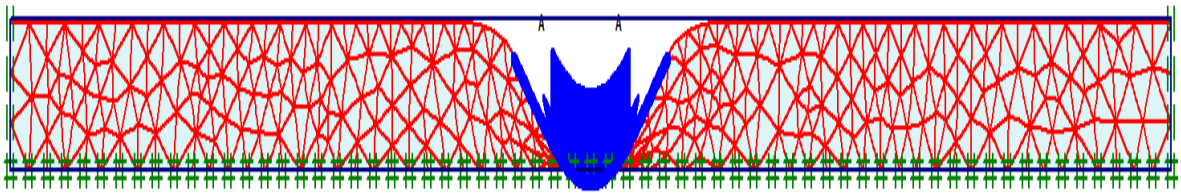

(c) Deformed mesh

Figure C5: Finite beam subjected to uniformly distributed load

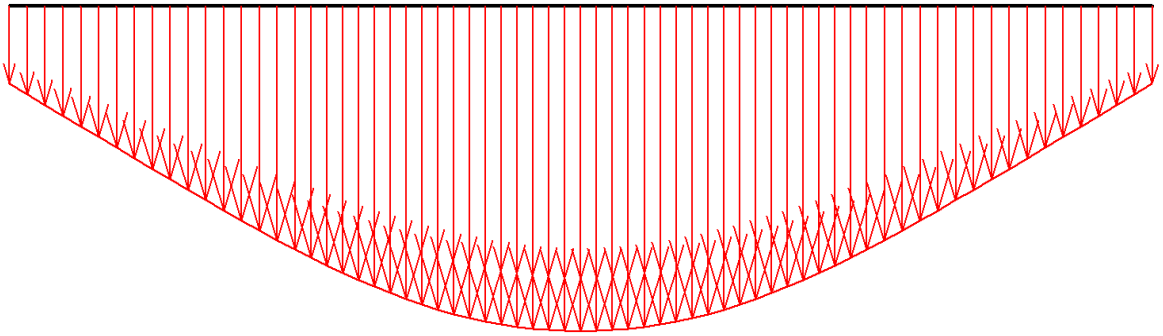

(a) Deformation

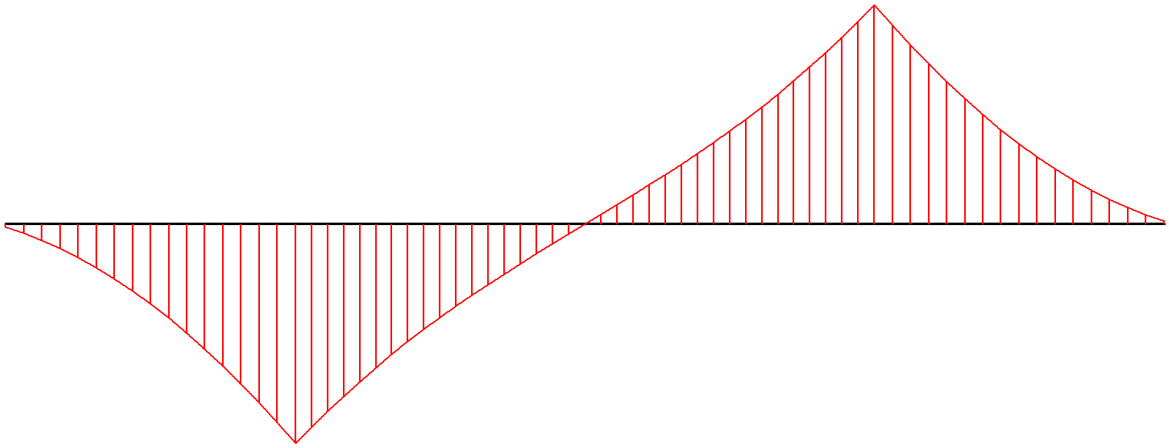

(b) Shear force

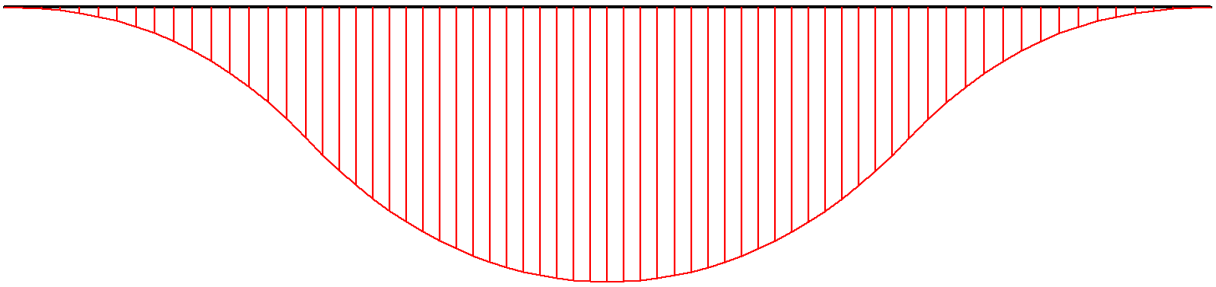

(c) Bending moment

Figure C6: Cont'd....